UNIVERSITÀ DI PARMA

UNIVERSITA' DEGLI STUDI DI PARMA

DOTTORATO DI RICERCA IN

BIOTECNOLOGIE E BIOSCIENZE

CICLO XXXIV

Composti Antibatterici Che Hanno Come Target L' Oloenzima DNA Polimerasi III

Coordinatore:

Chiar.mo Prof. Ventura Marco

Tutore:

Chiar.mo Prof. Montanini Barbara

Dottorando: Caputo Alessia

Anni Accademici 2018 /2019 – 2020/2021

UNIVERSITÀ DI PARMA

Università Degli Studi Di Parma

Ph. D. Program in

Biotechnology and Life Science

XXXIV cycle

Antibacterial Compounds targeting the DNA Polymerase III Holoenzyme

Coordinator:

Chiar.mo Prof. Ventura Marco

Tutor:

Chiar.mo Prof. Montanini Barbara

Ph. D. student: Caputo Alessia

2018/2019 – 2020/2021

Sommario

1. INTRODUCTION

- Drug Discovery

The discovery of molecules that could be used for drug development is one of the main activities contributing to the improvement of human and non-human health. The road to drug discovery is a long one and can sometimes prove to be tough and competitive. The process can be broadly divided into four main phases: (i) target selection and validation; (ii) compound screening and lead optimization; (iii) preclinical studies; and (iv) clinical studies[1].

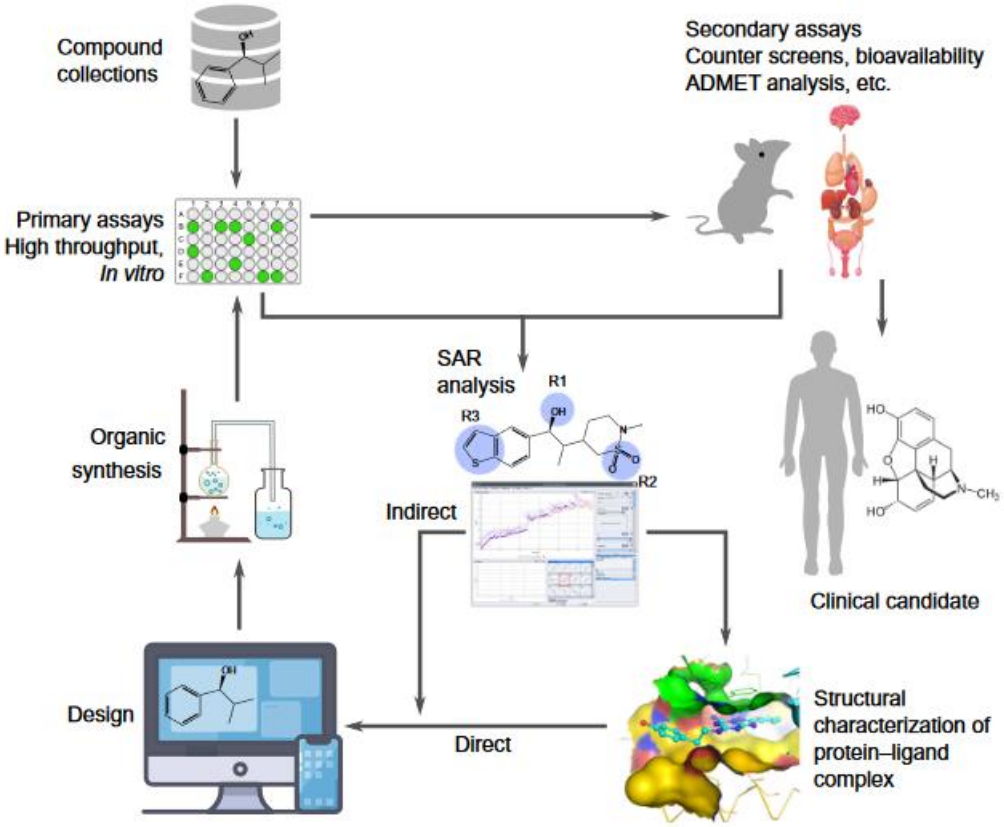

Figure 1. Graphical representation of the steps involved in drug discovery[1].

The first step is therefore to identify the target of a specific disease. Its validation is done using different types of analysis such as genomics and proteomics, aided by bioinformatic predictions, which have made a considerable improvement in the field of research in recent decades. Next comes the screening of molecules capable of binding to the target. Very often a virtual screening is performed, but there are now several molecular assays that allow high throughput screening of small molecules collected in libraries of chemical or natural compounds. Once a chemical class of molecules capable of binding to the chosen target has been identified, structure-activity and *in silico* studies in combination with cellular functional assays allow to improve the activity of the compound. This may be possible, for example, by making chemical modifications to certain groups identified in the structure of the compound. These 'new molecules' must be validated by molecular assays and are then tested in *in vivo* studies in animal models. This step is extremely important as pharmacokinetic investigations and toxicity tests are carried out. Finally, the drug candidate, which successfully passed all preclinical tests, moves on to clinical trials.

The clinical study involves three phases: Phase I, safety testing of the drug with a small number of human subjects[1]; Phase II, efficacy testing of the drug with a small number of people with the target disease[1]; and

Phase III, efficacy studies with a larger number of patients[1]. If the drug passes all three phases, it is reviewed by agencies such as FDA and EMA for approval and marketing.

From the above, it may seem that drug discovery is a 'modern' science or activity, which has taken off thanks to modern molecular biology techniques. Actually, these have only helped to improve the search for candidate molecules for drug development. In fact, in the last 100 years, many drugs have been discovered that have radically changed the practice of medicine and impacted many aspects of our culture, and their discovery was achieved with a target- and mechanism-agnostic approach that relied on ethnobotanical knowledge, often fuelled by serendipity[2]. Since the 19th century, experimental biological and medical research by Claude Bernard, Louis Pasteur, Robert Koch, Paul Ehrlich, and Joseph Lister, and advances in organic chemistry, have advanced the modern discovery of drugs, many of which are now well-known and act by a variety of mechanisms. These drugs are currently used in the treatment of diseases ranging from bacterial infections to psychiatric illnesses and various types of cancer. In addition, they have enabled many surgical procedures, such as cell and solid organ transplantation[2]. The first 100 years of modern drug discovery were driven by chemocentric approaches, i.e., approaches based on a specific compound or class of compounds that served as a starting point for further optimization. These chemotypes were discovered through ethnobotanical knowledge or derived from ligands and natural substances[2]. Examples are aspirin, ergotamine, penicillin, and steroid hormones. In the case of aspirin, for example, Johann Andreas Buchner extracted salicin from the bark extract of the white willow tree (*Salix alba*) in 1828. However, its effects were already well known in Europe and North America for relieving pain, treating inflammation and fever. It was Felix Hoffman, a chemist at Bayer in Germany, who, through his systematic search for derivatives of salicylic acid in 1897, succeeded in synthesizing acetylsalicylic acid, known since 1899 as Aspirin®[3].

Currently, drug discovery uses a spectrum of generation/optimization approaches ranging from hypothesis-driven strategies that associate specific molecular targets with disease states (target-based drug discovery, or TDD) to biological/compound-driven approaches that are mechanism-agnostic and based on empirical observations (phenotypic drug discovery, or PDD)[4]. In recent years, there has been a shift in the use of various approaches.
While for the past three decades, target-based drug discovery (TDD) - in which the starting point is a defined molecular target that is hypothesized to play an important role in disease - has been the dominant approach for drug discovery in the pharmaceutical industry, in recent years, there has been a resurgence of interest in phenotypic drug discovery (PDD) approaches, which do not rely on knowledge of the identity of a specific drug target or a hypothesis about its role in disease[5].
The breakthrough came in 2011, when a paper published by David Swinney[6] highlighted how most first-in-class small molecule drugs (FICs) were discovered empirically through phenotypic drug discovery (PDD), while most followers were discovered using target-based drug discovery (TDD).
The power of this approach is due to rapid advances in various technologies for cell-based phenotypic screening in recent years, including the development of induced pluripotent stem cell (iPS) technologies[7], gene-editing tools such as CRISPR-Cas[8], organoids, and imaging assay technologies[5].

Despite the many technologies developed and used for drug discovery, it is striking how the rate of drug development against new target families is significantly lower. This is why over the years several studies have focused on trying to establish with confidence the number, characteristics, and biological diversity of approved drug targets[9].
John P. Overington, Bissan Al-Lazikani, and Andrew L. Hopkins, in their work, propose a consensus number of 324 drug targets for all classes of approved therapeutic drugs, reconciling previous reports into a current and comprehensive survey[9]. Their work grouped the targets in detail, including target names, target class,

cellular location, and United States Adopted Names (USAN) or launch dates. Of these, 266 are proteins derived from the human genome, and the rest are bacterial, viral, fungal, or other pathogenic targets. Small molecule drugs modulate 248 proteins, of which 207 are targets encoded by the human genome [9]. A very interesting factor that emerged from this detailed study, but also from previous literature, is that many drugs are referred to as 'dirty drugs', meaning that they have a clinically relevant polypharmacology. This characteristic can be explained by similarities either in the key pharmacophores at the binding sites of proteins from different families [10] or in the physicochemistry of the equivalent residues lining the binding site.

Using databases such as SCOP19 and PFAM20, the authors were also able to identify family relationships between all drug targets by analyzing the presence of specific domains. As we can see from the image below, analysis of the gene-family distribution of drug targets for both small molecules and biologics reveals that more than 50% of drugs target only four key gene families: class I GPCRs, nuclear receptors, ligand-gated ion channels, and voltage-gated ion channels[9].

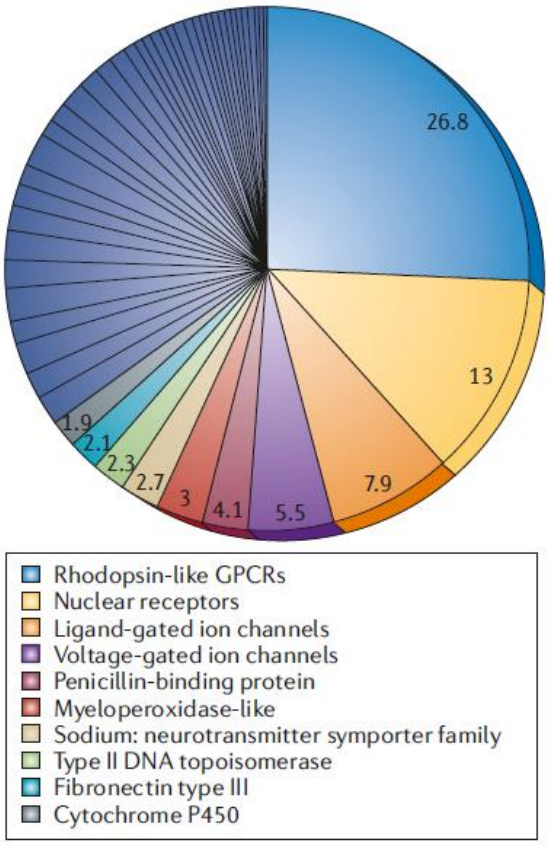

Figure 2. Gene-family distribution of current drug substances[9].

The targets with the largest number of approved drugs are the glucocorticoid receptor and the histamine receptor H1[9]. The protein kinase family has become one of the most important drug targets of the 21st because dysregulation of their activity is linked to numerous diseases, including cancer. For this reason, there are currently 68 FDA-approved therapeutic agents targeting around two dozen different protein kinases, and six of these drugs were approved in 2021[11]. A noteworthy feature shared by many targets is their location, meaning that 60% of drug targets are located on the cell surface, although being ~22% of all proteins in the human genome[9]. A study by the National Institute for Health Care Management Research and Educational Foundation (NIHCM Foundation)[12] found that, of 361 new molecular entities (NMEs) approved by the FDA between 1989 and 2000, 76% targeted a previously drugged domain and only 6% targeted a previously

undrugged domain; the remainder has unknown targets (4%) or is believed to have no distinct molecular target underlying its action (17%)[9].

Currently, the identification of new drug candidates in a target-agnostic manner includes high-throughput screening of different chemical libraries, fragment-based screening, rational drug design, use of target family knowledge, and *in silico* drug discovery methods.

- Protein-Protein Interactions (PPIs)

Protein-protein interactions (PPIs) are of great importance because they mediate numerous biological functions, involved in virtually all cellular processes, including metabolic cycles, DNA transcription and replication, enzymatic activity, signaling cascades, apoptosis, and other processes. It is estimated that there are between 130,000 and 650,000 types of PPIs in the human interactome[13,14]. PPIs play a key role in both physiological and pathological conditions and represent a potential source of therapeutic targets, as a disturbance in the dynamic balance of proteins often leads to a dysfunction that, at a systemic level, signifies pathology.

Modulation of PPIs by peptides is a technique already 'tried and tested' in nature. Many organisms use naturally occurring peptides to inhibit, compete and regulate interactions. Examples include the peptide Extracellular Death Factor (EDF), which interposes itself between the binding of the anti-toxin MazE to the toxin MazF[15], thus activating this enzyme that triggers the cell death process. Alternatively, BH3 domain peptides in anti-apoptotic proteins compete with the internal interactions of a helix with the same binding groove in apoptotic proteins such as Bcl-xL, thus preventing apoptosis[16,17].

Nowadays, however, the possibility of inhibiting the interaction between two proteins is not just limited to the human interactome, but the concept is growing and expanding to include viral and bacterial organisms. It is important to define from the outset what kind of PPI we are dealing with:

- PPIs can occur between identical or non-identical chains[18]. Oligomers of identical or homologous protein units can be organized in an isologous or heterologous manner[19] with structural symmetry[18,20]. An association is defined as isologous when the same surface on both monomers is involved in the interaction, whereas it is defined as heterologous when different interfaces are involved[18].
- PPIs can be either an obligate or non-obligate complex. In the former case, protomers are not found as stable structures on their own *in vivo* (e.g., the dimer of the Arc repressor is essential for DNA binding), whereas in non-obligate interactions protomers exist independently (e.g., antibody-antigen complexes). Obligate interactions are usually permanent, whereas non-obligate interactions may be transient or permanent[18].
- PPIs may be permanent, i.e., they are very stable interactions, and the proteins tend to exist only in the complexed form; or they may be transient, where *in vivo* association/dissociation dynamics are observed. Within this classification, we can distinguish subcategories of PPIs. There are weak transient interactions with dynamic oligomeric equilibrium in solution (the interaction breaks down and forms continuously), and strong transient interactions that require a molecular trigger to shift the oligomeric equilibrium[18].

However, it is important to emphasize that it is not possible to draw up a table in which the different PPIs are divided and listed. There is, therefore, no clear-cut classification, as everything depends on the surrounding cellular environment at a given time. What we see is therefore a continuum between obligatory and non-obligatory interactions.

PPIs can take place between two globular proteins with preformed surfaces (a), between two globular proteins with an induced binding surface (b), between a rigid globular protein and a peptide (c), between a flexible globular protein and a peptide (d), or ultimately between two peptides (e).

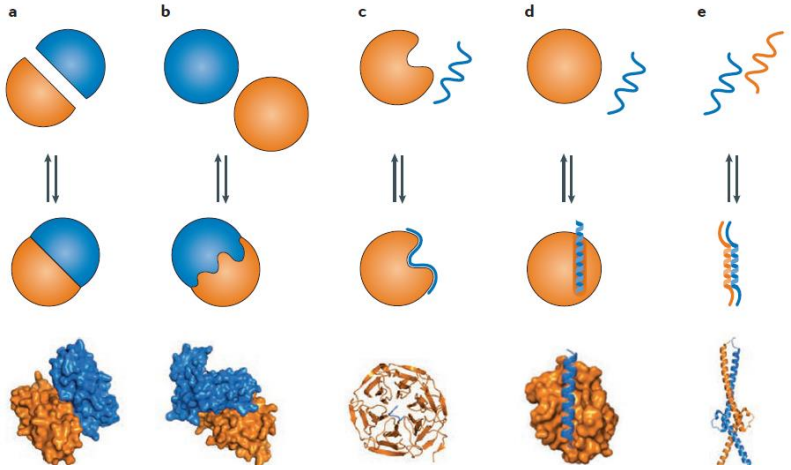

Figure 3. Structural classification of protein-protein interaction (modified by [21]).

The interaction between two proteins involves a surface area of between 1,000 - 6,000 Å^2. Generally, the interface consists of a central region and an edge region[22]. Another type of classification applies to PPI interfaces. These can be classified as follows: narrow (surface area < 2500 Å^2) / wide (surface area > 42500 Å^2) and tight (K_d < 200 nM) / loose (K_d > 4200 nM) based on their affinity[23,24]. The 'narrow and tight' interfaces are the most suitable for the design of small molecule inhibitors[24].

The concept of the 'hot spot' was first introduced by Clackson and Wells[25]. They identified at the interface of interaction between human growth hormone (hGH) and its bound receptor (hGHbp), a small set of residues critical for the interaction[24]. 'Hot spots' represent on average 9.5% of the residues at the interface and most of them are located in the central regions[26]. In PPIs, we often find "hot segments", which is an extension of the hot spot concept to a continuous binding epitope that dominates the interaction[27]. A characteristic feature of hot spots is the presence of particular amino acid residues. Systematic analyses have revealed a high presence of Tryptophan (21%), Arginine (13.3%), and Tyrosine (12.3%) residues[26]. To a lesser extent, polar residues such as Aspartic acid and Histidine are also fairly present[26]. The presence of these particular amino acids is related to the conformational change that enables them to accommodate small molecules[24]. In addition, these particular residues can form bonds with ligands driven by various forces, including hydrophobic, hydrogen bonding, π-π stacking, and electrostatic interactions[24].

There are several methods useful for studying the PPI interface. Most information is derived from conformational differences between unbound and bound proteins/structures[24]. However, sometimes this information is not available, so computational methods such as flexible molecular docking and molecular dynamics (MD) simulations are used[24]. Another type of analysis is scanning alanine mutagenesis[25,26,28] in combination with X-ray crystallography. This method makes it possible to identify PPI 'hot spots' by measuring the impact of each residue on the binding affinity to the partner protein by serially mutating each residue at the interface into alanine. However, this only highlights contributions due to the energy of mutual interaction within a protein-protein complex[24]. It is, therefore, necessary to make sure that those identified are indeed the binding sites for small molecules. The druggable sites of a protein have additional topological characteristics that are appropriate for binding a small ligand. The druggable site of a protein can be determined by finding consensus sites that are characterized by their ability to bind a variety of fragments or small organic "probes"[24]. Consensus sites can be identified using the MSCS[29] (Multiple Solvent Crystal Structure) approach and fragment screening techniques[30] (such as "SAR by NMR"[31]). By combining computational solvent mapping (finding energetically accessible hot spots) with conformational sampling

(considering flexibility to accommodate drug-sized molecules), Kozakov et al.[32] demonstrated that druggable sites tend to have a hydrophobic concave scaffold from which branch polar groups that can bind organic molecules. Metz et al.[33] managed to coordinate the aspects of energy and plasticity. With this approach they identify hot spots, transient pockets and determinants of small-molecule binding at the PPI interface.

The importance of PPIs, their extensive study, and the need to develop new drugs to combat various diseases have led to the growth of research on inhibitors of protein-protein interactions. Works in recent years has highlighted classes of PPIs that are particularly susceptible to inhibition by small molecules. An inhibitor that disrupts the interaction between a globular protein and a single peptide or peptide chain on the partner protein, for example, binds in pockets on the surface of the globular protein, leaving no room for the partner protein to make the bonds necessary for the native interaction.

Protein-protein interactions can be modulated mainly by orthosteric or allosteric mechanisms. An orthosteric or allosteric modulator can also differentiate into a disruptor or a stabiliser[34].

1. Orthosteric PPI Disruptors. The formation of the protein complex is inhibited by direct competition at the interface. Most of the PPI inhibitors currently in clinical trials belong to this class and act on therapeutic targets such as proteins of the IAP family[35], MDM2[36–39], and HIV integrase[40].

2. Allosteric PPI Disruptor, the formation of the protein complex is inhibited by a molecule bound to the protein at a remote site of the interface. One complex modulated by this mechanism is the interaction of the c-Myc-MAX heterodimer, a pleiotropic transcription factor involved in the regulation of proliferation and therefore an interesting anti-cancer target[34].

3. Orthosteric PPI stabilizer, the affinity of the interaction is increased through the binding of a small molecule to a newly formed binding site at the PP interface. Well-known examples of orthosteric stabilizers are the immunosuppressants rapamycin and FK506 isolated from Streptomycetaceae[41].

4. Allosteric PPI stabilizer, the affinity of the interaction increases through the binding of a small molecule to a remote site of the interface. One protein susceptible to allosteric stabilization is the E2 ubiquitin ligase Cdc34a[34].

Another mechanism to modulate protein-protein interaction is mediated by dynamic interfacial modulators, which in addition to modifying the affinity between the targeted interacting proteins, also act as allosteric modulators of the individual components of the protein complex by influencing their dynamics, which are crucial for protein function[42]. An example of dynamic interfacial modulators is a set of inhibitors of dihydropteroate synthase (DHPS), a dimeric bacterial enzyme that is targeted by sulphonamide antibiotics, which have many undesirable side effects such as allergies or brain damage[43].

Target-based drug discovery, using various assays to screen large chemical libraries, has struggled to find ligands that inhibit protein-protein interactions (PPIs)[44]. Several databases are currently available, such as TIMBAL[45], 2P2I[46], and iPPI-DB[47], which collect both structural data of the druggable sites of different PPIs, but also small molecules that are possible PPI inhibitors[17].
The development of a molecule capable of accessing several hot-spot pockets on the surface of a protein, while keeping the physicochemical properties within conventional limits for drug discovery projects, can be challenging[21]. As mentioned above, drug discovery is a very laborious path, as is the identification and design of small molecule inhibitors.

To analyse the binding mechanism and effect of PPI modulators, there are various screening methods, using many biochemical and biophysical assays, such as Thermal Shift (TS)[48], Surface plasmon resonance (SPR)[49], Ligand- or protein-based nuclear magnetic resonance (NMR)[50], X-ray crystallography[51], Isothermal titration calorimetry (ITC) [52], Förster Resonance Energy Transfer (FRET)[53], and Bioluminescence Resonance Energy Transfer (BRET)[54].

Several strategies can be used to identify compounds capable of disrupting specific PPIs:

- **High-throughput screening (HTS)** is a well-proven method for identifying hits against classical drug targets but has a relatively low success rate for PPIs. Most of the libraries used for screening are based on compounds that act primarily on conventional drug targets[24]. These are not able to occupy the chemical space required to inhibit the interaction between two proteins[24]. At the same time, however, HTS is useful for identifying starting points to target PPIs[24]. Large pharmaceutical companies such as Roche, Bristol-Myers Squibb, Pfizer, and Abbott, seeing the potential of HTS, are placing increasing emphasis on PPI targeting programmes[55]. Therefore, they are looking to expand their screening libraries by adding molecular diversity and complexity. There are two different types of libraries that can be used in HTS: random libraries of different drug-like structures, which are useful in cases where there is a new target where no lead is known and which can be derived from natural products from reptiles, marine organisms, microorganisms and plants; and focused libraries, which are based on the structural information provided by the input molecule (lead or natural ligand) and provide a richer base of information for the design of preferred structures[56]. Despite the limitations that HTS can present, this methodology has led to the identification of molecules that mimic a non-continuous epitope consisting of side chains on an α-helix, as in the successful screening against MDM2-p53[23,26,40,57–61], ZipA-FtsZ44[62] and human papillomavirus (HPV) E2-E1[63]. Most HTS hits are active at sub-micromolar or low-micromolar concentrations.

- **Fragment screening and Fragment-Based Drug Design (FBDD)** have proved to be good approaches for the search for PPI inhibitors. They are based on the construction of new lead structures from small molecular fragments taking the advantage of both random screening and structure-based drug design[64]. FBDD leads to weak to moderate (5 mM to 1 µM) binding of the desired target by screening libraries of fragments containing hundreds to thousands of small, low molecular weight fragments, typically less than 200 Da[24,65]. Compared to HTS, FBDD and fragment screening seem to be better approached to detect inhibitors of protein interactions. Successful approaches to fragment identification and optimization include structure-activity relationship (SAR) by NMR, X-ray crystallography, and tethering. SAR by NMR uses heteronuclear single quantum correlation (HSQC) 1H-15N NMR as a screening tool to identify fragments that bind to a site of interest on a protein[66,67]. The tethering method, on the other hand, exploits the formation of disulphide bonds. A cysteine mutation is placed near the small molecule binding site, and this mutant protein is interrogated with a mixture of disulphide-containing fragments. At equilibrium, those fragments that bind to the target and form a disulphide will be highly bound to the protein. Subsequent use of mass spectrometry easily reveals protein-fragment conjugates[68]. An important example of an inhibitor discovered with this strategy is the Bcl-xL inhibitor ABT-263 (Navitoclax, 1) as a novel anti-cancer agent[69,70]. Tethering has allowed the identification and improvement of modulators against interleukin-2 (IL-2). In particular, it allowed the identification of SP4026, a mimic of IL-2R receptor hotspot residues[71,72].

- **Rational design,** the rational design of PPI inhibitors has focused on efforts to mimic peptides using many different strategies[73]. Much work has been based on mimicking three main recognition motifs found to modulate PPIs: α-helices, β-row, and reversal[21]. Most of the binding energy comes from hydrophobic interactions. Of considerable interest to pharmaceutical industry are cyclic peptides and several companies have focused on the formulation of cyclic peptide libraries[74]. Libraries of synthetic cyclic peptides (or macrocycles) can be generated and screened by functional assays. One method to generate cyclic peptide libraries is the circular split-intein binding of peptides and proteins (SICLOPPS), which exploits intein splicing for the generation of cyclic peptide libraries in cells[74]. This strategy has the great advantage of being able to generate massive libraries composed of millions of different compounds.

- **Virtual screening** is a computational screening method whose approach can be either structure-based[75] or ligand-based[76]. Structure-based virtual screening uses docking and scoring to select molecules that have a good binding affinity to target proteins. The ligand-based approach prioritizes molecules according to their suitability for the pharmacophore or their chemical similarity. A very important feature is the low cost and high throughput of this type of screening. Virtual screening is an evolving type of screening. Many research groups are devising and launching software to analyse and detect PPI inhibitors. For example, Dr. PIAS[77] is software that identifies similarities in pocket structure from a database of known PPI inhibitors and targets. Meireless et al.[78] introduced the ANCHOR system to identify 'anchor' residues that are deeply buried at the time of binding. Virtual screening is also able to consider the binding dynamics of a protein. Using virtual screening, very important information can be learned, such as the greater propensity of druggable PPI sites to form surface pockets compared to non-PPI sites. In addition, predicting the ability of some PPI interfaces to accommodate small molecules through dynamic pocket formation could help in target selection.

- FÖRSTER RESONANCE ENERGY TRANSFER (FRET)

Förster Resonance Energy Transfer (FRET) was first described in the 1920s by Cario, Franck, and Perrin. In the late 1940s, Förster and Oppenheimer independently formulated a quantitative theory of energy transfer between a pair of point dipoles. The theory was verified by Stryer and Haugland in the late 1960s and they coined the term "spectroscopic ruler" for FRET. FRET provides accurate spatial measurements and detects molecular complexes over distances from ~10 Å to 100 Å[79] and enables the definition and detection of a variety of biological organizations and cellular events such as protein folding[80], substrate interactions[81], enzyme kinetics[82], and intercellular signalling[83].

FRET is a non-radiative energy transfer that occurs by dipole-dipole coupling from an excited state donor (D) fluorophore to a ground state acceptor (A; another fluorophore or a quencher) when appropriate spectral overlap and proximity requirements are satisfied[84]. Due to its inherent inverse-sixth-power distance dependence, FRET spectroscopy is useful for nanoscale proximity detection with a typical range of roughly 1–10 nm (and up to ~20 nm for some atypical FRET pairs)[84].

The energy transfer mechanism of FRET is similar to Near Field Communication (NFC): interactions between radio antennas or chromophores take place at a distance shorter than the wavelength of the emitted light. In the near-field region, the donor chromophore emits a photon that is immediately absorbed by the acceptor chromophore; this photon is unreliable because its existence violates the conservation of energy and momentum; for this reason, FRET is referred to as non-radiative transfer[85].

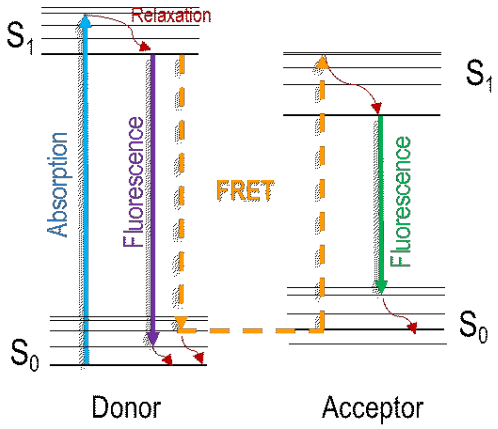

Figure 4. Jablonski diagram. Illustration of the coupled transitions involved between donor emission and acceptor absorbance in FRET (modified from[86]).

The efficiency of energy transfer (E) is a quantitative measure of the number of quanta that are transferred from *D* to *A*. E is essentially the 'quantum yield' of energy transfer, which is defined as follows:

$$E = \frac{the\ number\ of\ quanta\ transferred\ from\ D\ to\ A}{the\ number\ of\ quanta\ absorbed\ by\ D}$$

According to the theory of Förster, the rate (kT) and efficiency (E) of energy transfer can be written as:

$$E = \frac{K_T}{K_T + KF + KD}$$

Equation 1. The efficiency of energy transfer[86].

Where K_F is the rate constant of fluorescence emission of the donor, and K_D is the sum of the rate constants of all other deexcitation processes of the donor.

The distance between donor and acceptor greatly influences the efficiency of FRET, is:

$$E = \frac{1}{\left[1 + \left(\frac{r}{R_0}\right)^6\right]}$$

Equation 2. A distance lower than R_0 has an efficiency close to the maximum value, if instead is (much) higher than R_0, the efficiency is close to zero[85].

R_O is characteristic for each interaction and indicates the distance at which the efficiency is 50%. R_O depends both on the spectral superposition integral of the donor emission spectrum and the acceptor absorption spectrum, and on the relative orientation of the donor emission dipole moment and the acceptor absorption dipole moment (Figure 5)[85].

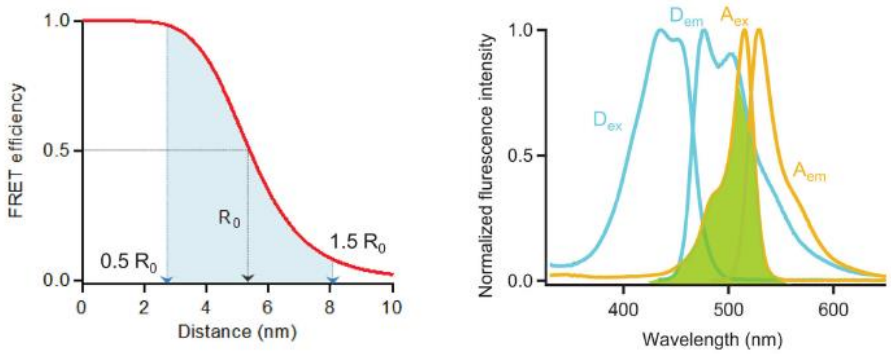

Figure 5. Left: FRET efficiency as a function of the distance between the donor and the acceptor fluorophores; notice the linearity of the FRET efficiency values at distances near R_0. Right: absorption and emission spectra of the donor (cyan) and acceptor (green). The overlap between donor emission spectrum and acceptor absorption spectrum is highlighted by green shade[87].

To quantify FRET one of the most widely used methods is fluorescence-lifetime imaging microscopy (FLIM), where the fluorescence lifetime of the donor alone (tD) or coupled with the acceptor (tDA) is measured[88].

$$E = 1 - \left(\frac{\tau_{DA}}{\tau_D}\right)$$

Equation 3. The efficiency of FLIM[87].

The application of FRET technology is very broad and is applied to analyse conformational changes[89] (static or real-time), interactions between membrane molecules[90], protein structure[91], PPIs[92], and nucleic acid-protein complexes[93].

The green fluorescent protein (GFP) of the jellyfish *Aequorea victoria* is widely used to study interactions in vivo[94], and mutations to its sequence have led to the development of new non-invasive fluorescent markers with different spectral properties[95,96]. Originally, the first chromophore pair was blue fluorescent protein (BFP) as donor and GFP as acceptor[96]. The BFP is a mutant of GFP (Try66His) and has an excitation peak in the ultraviolet (UV)[97,98] with the drawback of causing strong cellular autofluorescence noise and scattering. Therefore, attempts were made to create GFP mutants to obtain fluorescent proteins. Examples are : Cyan Fluorescent Protein (CFP) (Tyr66Trp), characterized by an excitation peak at 436 nm and an emission peak at 476 nm[95,99]; Yellow Fluorescent Protein (YFP) (Thr203Tyr) characterized by redshifting spectra, with an excitation peak at 516 nm and an emission peak at 529 nm[95,96]; and Red Fluorescent Protein (RFP) discovered from corals, with a long excitation tail[100]. CFP-YFP pair allows monitoring very large distances, and despite cross-talk in the excitation and emission spectra, it has been the most widely used FRET pair.

For the study of PPIs, as in the case of Bcl-2 Bax, the chromophores are fused to different proteins and we speak of intermolecular FRET[97]. When chromophores are fused to the same molecule, we have intramolecular FRET[97].
Unfortunately, FRET has some limitations in the physical process and signal measurement. The excitation of the chromophore has to take place by an external source of illumination, such as a laser, leading to an elevation of the noise floor. This can occur in two ways: direct excitation of the acceptor chromophore and photobleaching mechanisms, causing loss of signal. Using FRET as an assay in HTS can lead to false negatives due to the risk of damaging photosensitive compounds, preventing any subsequent characterization. Finally, cell structures, especially membranes, tend to absorb external light, inducing autofluorescence that annihilates the signal[101]. To overcome these drawbacks, Bioluminescence Resonance Energy Transfer (BRET) has been developed[97].

- BIOLUMINESCENCE RESONANCE ENERGY TRANSFER (BRET)

The Bioluminescence Resonance Energy Transfer (BRET) is a naturally occurring phenomenon that can be observed in the sea pansy *Renilla reniformis*, and other organisms.
The BRET method is based on the Förster resonance energy transfer and involves resonance energy transfer between a light-emitting enzyme and a fluorescent acceptor. This technique is considered very versatile and is also a widely used method for monitoring protein-protein interactions in living cells as well as conformational changes within proteins or molecular complexes[98].

Whereas in FRET the donor is a fluorophore that transfers its excited-state energy to the acceptor, another fluorophore that emits fluorescence at a longer wavelength, in BRET a luciferase is used as the energy donor. The use of the luciferase instead of the fluorophore avoids the consequences of donor excitation in FRET, such as tissue damage by excitatory light, photobleaching, and simultaneous excitation of the acceptor by the donor excitatory light. However, in both methods, donor and acceptor are genetically or chemically fused to proteins or compounds under study.
Bioluminescence occurs when the luciferase emits light in the presence of its corresponding substrate. The fluorophore, usually a fluorescent protein, absorbs light at a given wavelength and re-emits light at a longer wavelength and the transfer of energy leads to the excitation of the acceptor fluorophore, which re-emits light at a longer wavelength.

Therefore, the emission spectrum of the donor must overlap with the excitation spectrum of the acceptor.

A necessary condition for resonance energy transfer to occur is that the donor and acceptor are fairly close together (<10 nm). If the distance between donor and acceptor is greater than 10 nm, only the donor signal is detected, whereas, if the 10 nm distance is met and the two proteins interact, a BRET signal can be detected.

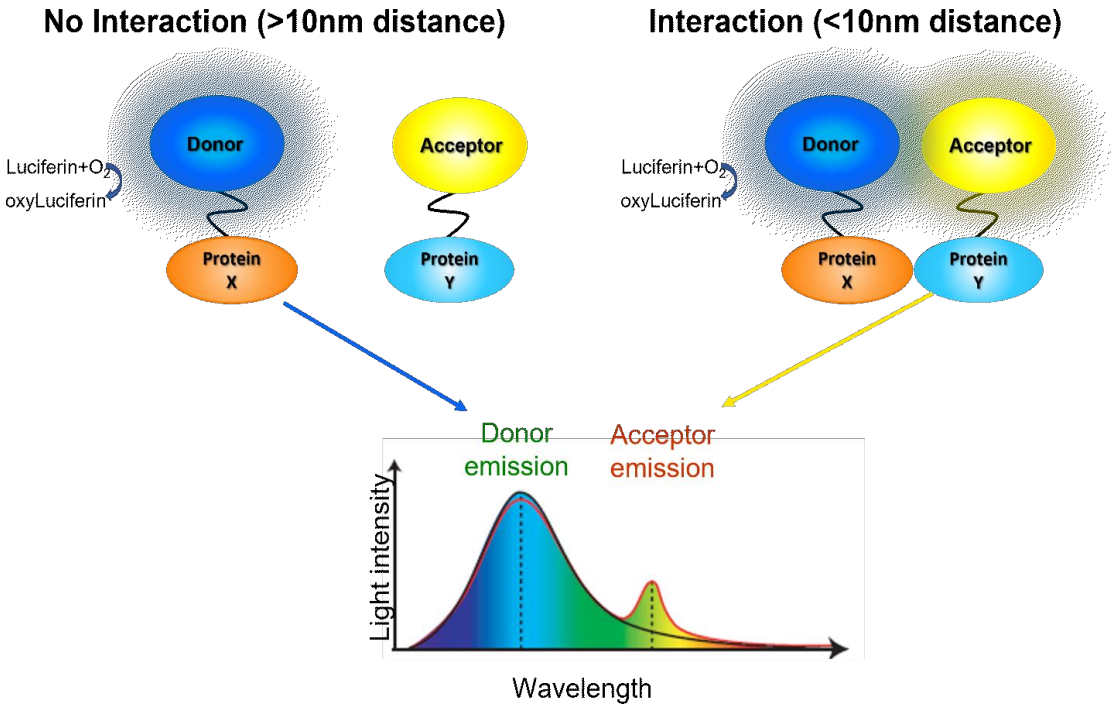

Figure 6. BRET-based assay: the energy transfer can occur only when the donor and the acceptor are sufficiently close (modified from[102])

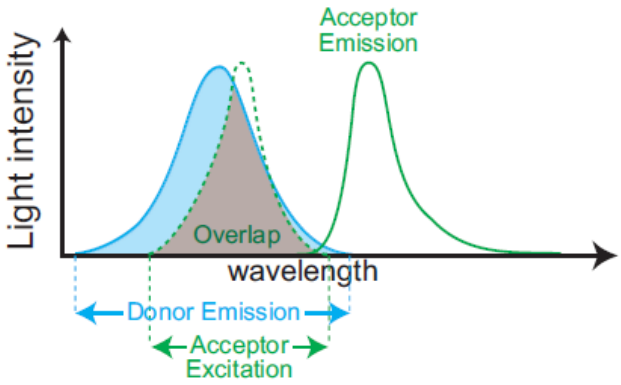

Figure 7. Representation of the emission spectrum of the donor that overlap with the excitation spectrum of the acceptor[102].

To study protein-protein interactions, one protein is fused to the donor and the other to the acceptor**.**

The BRET signal strength is influenced by three parameters:

1. Distance between donor and acceptor. It is inversely proportional to the intensity of the transfer signal: the energy transfer decreases progressively as the distance between the donor and the acceptor increases from 1 to 10 nm, which turns out to be the maximum distance for the Förster resonance energy transfer to take place (Figure 6)[91,103].

2. The relative orientation of BRET partners, due to the dipole-dipole nature of the resonance energy transfer mechanism. Lack of BRET signalling between two proteins does not mean they are not interacting. The weakening or complete absence of BRET signaling may be due to the incorrect orientation of donor and acceptor. Therefore, to overcome this problem, it is essential to test different combinations in which the proteins of interest are fused to donor and acceptor at the C- or N-terminal ends and to use different linker peptides characterized by high flexibility. The strategy often used is to change the insertion site of the donor and acceptor in the protein of interest. (Figure 8)[91,104].

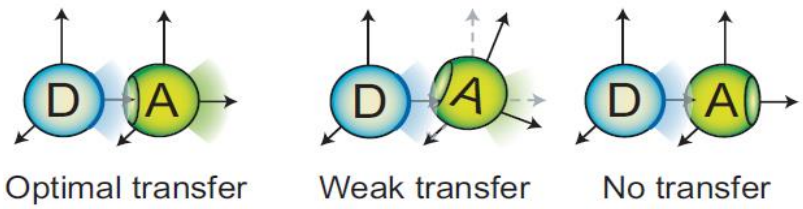

Figure 8. Different orientations of BRET partners[102].

3. Acceptor/donor ratio. As we know, protein interactions take place in finite spaces such as cell organelles, cell membranes, cytoplasm, or extracellular space. The finite space and increasing protein expression can lead to accidental encounters between proteins and a non-specific BRET signal would occur because the proteins are more likely to collide. To verify the specificity of the signal, BRET

donor saturation assays are performed, where a fixed amount of luciferase is co-expressed with increasing amounts of acceptor-tagged protein[105–108]. If the BRET signal is specific, it increases hyperbolically and reaches a plateau representing complete saturation of all donor-acceptor molecules.

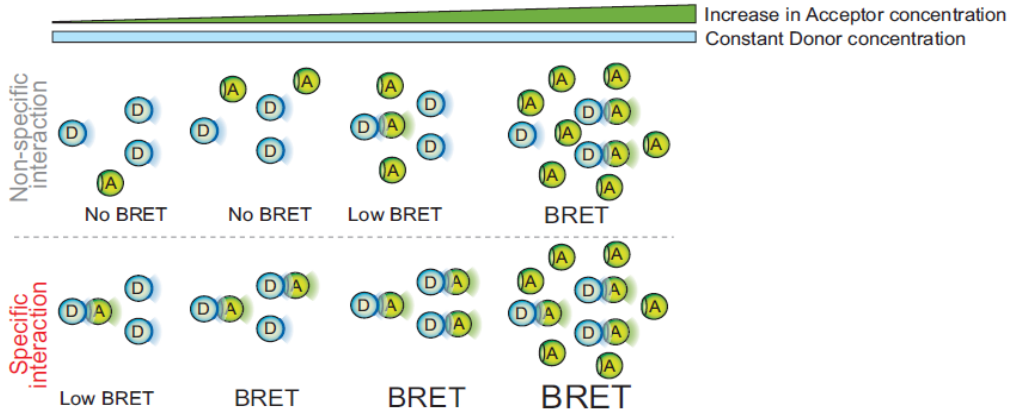

Figure 9. Representation of the acceptor/donor ratio[102].

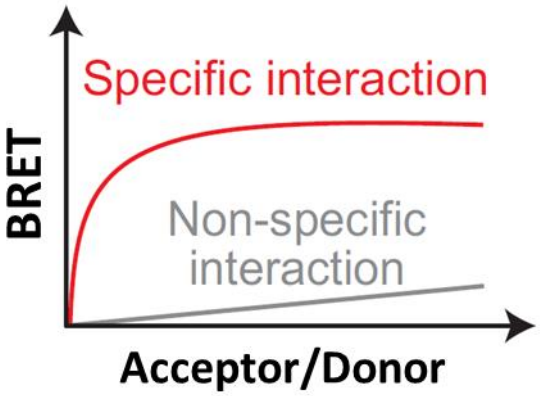

Figure 10. Donor saturation assay for analysis to set up a P2I2 BRET-based screening assay[109].

Since 1999, the BRET methodology has been increasingly used in laboratories and several new substrates and new donor/energy acceptor pairs have been developed[102]. In BRET1, the original version, coelenterazine h was used as the substrate for Renilla 36-kDa luciferase (Rluc). Maximum Rluc emission is observed at 480 nm, an appropriate wavelength for excitation of YFP, which re-emits light at 530 nm[110]. YFP variants with identical excitatory properties are YFP topaz[106,108,111,112], YFP citrine[113–115], YFP venus[83,116], and YPet[117,118]. BRET2, a variant of BRET1, uses DeepBlueCTM or coelenterazine 400a, a chemical derivative of coelenterazine h that shifts the maximum light emission of Rluc to 395 nm[102,119]. Appropriate acceptors are GFP2 and GFP10 with excitation and emission maxima of 400 and 510 nm, respectively[102]. The advancement gained with version 2 was a greater spectral separation of the donor and acceptor emission peaks. DeepBlueCTM, however, has up to 300 times less light emission[114]. BRET3 is based on the use of firefly luciferase (from *Photinus pyralis*) as a donor[102]. This 62 kDa luciferase emits light at 565 nm in the presence of its substrate D-luciferin, ATP, O_2, and Mg^{2+}[120–122]. Different acceptors are used: the 24 kDa fluorescent protein DsRed (ex: 558 nm/em: 583 nm); Cy3-labelled peptides (ex: 547 nm/em: 563 nm) or Cy3.5 (ex: 591 nm/em: 604 nm)[123,124]. Another BRET version uses quantum dots (QDs) as acceptors. QDs are semiconductor

nanocrystals excited at any wavelength from UV to 530 nm, and their light emission wavelength, which depends on their diameter, can cover the blue to near-infrared spectrum[125]. They are therefore suitable energy acceptors for assays based on BRET1 and BRET2[102].

Other luciferases have been cloned from marine organisms for application in BRET assays. One of these, the NanoLuc luciferase (NLuc), was developed from *Oplophorus gracilirostris*, is characterized by a small size (19 kDa) and a specific activity about 150-fold higher than RLuc[126–131]; NLuc can be combined with YFP or other mutated versions, such as YPF topaz, Citrine, Venus and YPet.

- History and evolution of Antibiotic and Antimicrobial Resistant

Antibiotics are the wonder drugs of the 20th century. The term antibiotic comes from ancient Greek (*antì* and *biòs*) and means 'against life'. In the mid-nineteenth century, Louis Pasteur observed that some microorganisms destroy others - a phenomenon later known as antibiosis [132]. Selman A. Waksman, in 1943, was the first that proposed the definition of "antibiotic" to "denote any class of organic molecule that inhibits or kills microbes by specific interactions with bacterial targets, without any consideration of the source of the particular compound or class" [133].

Antibiotic agents can be classified according to their mode of action:

- Bactericides, which completely kill bacterial cells, but no lysis or cell rupture occurs. They bind tightly to their cellular targets and are not removed by dilution[134].
- Bacteriolytic, which completely kills bacterial cells through cell lysis. Such compounds may inhibit cell wall synthesis or damage the cytoplasmic membrane[134].
- Bacteriostatic, which inhibit growth but do not kill. These often inhibit protein synthesis through binding to ribosomes. Their binding to the target is not tight, and when the concentration of the antibiotic is lowered, it is released from the ribosome, and growth resumes[134].

Antibiotics generally target an enzyme or process that is essential for bacterial growth and survival, while causing little or no harm to the eukaryotic host. At the molecular level, the antibiotic molecule binds to the target at a particular site, forming a molecular complex that blocks its functions[134]. The targets of antibiotics currently in use are DNA replication and repair, DNA transcription, protein synthesis, cell wall biosynthesis, and cytoplasmic membrane function.

In general, antibiotics and other chemotherapeutic agents are grouped according to their mechanism of action or, more usually, their chemical structure[134]. The main classes of antibiotics include quinolones, which inhibit DNA replication; various drugs, such as the antituberculous drug rifampicin, which inhibits DNA-directed RNA polymerase; tetracyclines and aminoglycosides, which inhibit protein synthesis by binding to the 30S ribosomal subunit; macrolides, lincosamides, chloramphenicol, and analogues which inhibit protein synthesis by binding to the 50S ribosomal subunit; β-lactams, which inhibit cell wall biosynthesis; glycopeptides, that inhibit cell wall synthesis[134–136].

The use of particular substances to treat infectious diseases is much more deeply rooted in time than we may think. From the Assyrians and Babylonians to the Europeans, there are traces of the use of "nature's magic bullets". An example was the fortunate discovery in Northern Italy, in 1991, of the "Ice Man" who lived some 5322 years ago[137,138]. Medical studies have identified the presence of a ball made of the fungus *Piptoporus betulinus*, among his belongings. This ball of *Piptoporus betulinus* would have served to expel the parasite *Trichuris trichura* from the rectum of the man. *Piptoporus betulinus* contains oils that are toxic to metazoans, have antimicrobial activity against mycobacteria, and contain toxic resins that are powerful laxatives[132]. Many references to the benefits of using mushrooms and moulds come from the ancient Egyptians, Greeks, and Romans also. In an early 17th century writing, a Buddhist nun's intervention against what was later known as an infectious disease is described: she dried 3 to 4-week old scabs of mild smallpox patients and asked people who were well to inhale the powder so that she could prevent the disease in the rest of the population[132]. The first person who documented the use of moulds to treat infections was John Parkinson in his book "*Theatrum Botanicum*", published in 1640[139]. From 1870 to 1890, several observations were made that mould had antibacterial activity. In 1897, Ernest Duchesne observed how Arabian grooms treated saddle

sores with mould and decided to analyse it. He characterized it as *Penicillium notatum* and used it to successfully treat induced typhoid in guinea pigs[140]. Salvarsan was the first antimicrobial agent in the world and it was synthesized by Enrlich in 1910. This agent was utilized as a remedy for syphilis[141]. Alexander Fleming was considered the "Medicine's accidental hero". Two cases of serendipity struck Fleming's laboratory. The first was when, while working at St. Mary's Hospital in London, he demonstrated a "zone of inhibition" around bacterial growth[142]. Due to an accidental sneeze, drops of lysozyme fell onto a petri dish containing a bacterial culture. Around the mucus, the culture did not grow. Lysozyme was later shown to have antibacterial activity only against non-pathogenic bacteria. The second was in 1928 when, returning to his laboratory after some time, he found mould in the Staphylococcus plate he had left uncovered. Between the mould and the staphylococci was a blue-green spotted mould, identified as *Penicillium notatum*. The culture filtrate, capable of killing the bacteria, was called "Penicillin"[132,142]. It was not until 1940 that penicillin became available as an antimicrobial agent, saving many lives of soldiers engaged in World War II. At the same time, sulphonamides were beginning to make their way into the world of antimicrobial agents. In 1933 Prontosil, a combination of sulphonamide and dye was used to successfully treat a boy dying of staphylococcal septicemia. Sulphonamides allegedly saved the lives of Winston Churchill and the son of Franklin D. Roosevelt[139]. These continuous discoveries and observations led to the Golden Age of antibiotic discovery. From 1940 to 1970, there was a peak in the discovery and also in the synthesis of new compounds. Initially, as with streptomycin and vancomycin, the primary source was other naturally occurring microorganisms. Indeed, streptomycin was isolated in 1944 from *Streptomyces griseus*[141] and vancomycin was extracted in 1952 from *Streptomyces orientalis* and used in patients from 1958 onwards[143]. While new antibiotics such as cephalosporins (1960), ampicillin (1961), and β-lactams (1976) were being developed, this period also saw the emergence of a parallel and conflicting pathway of pathogen resistance to antibiotics (Figure 11).

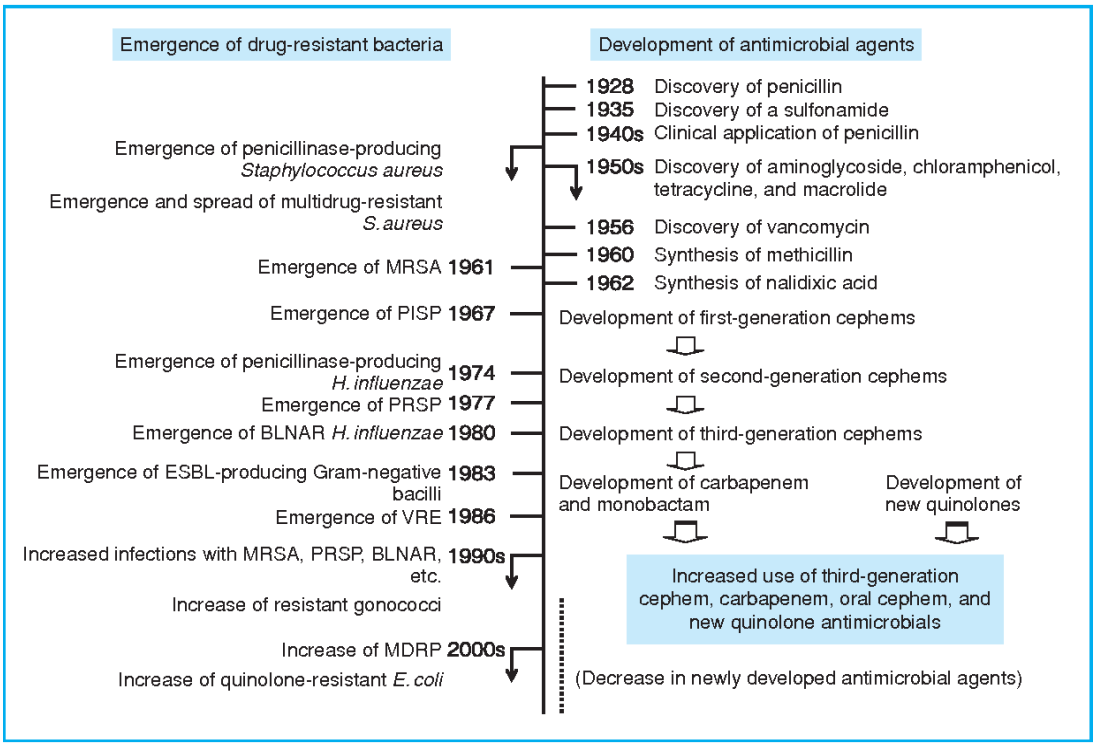

Figure 11. Trend of development of antimicrobial agents and emergence of drug-resistant bacteria [141].

Thus, if on one side some diseases caused by bacterial infections were being eradicated, on the other hand some diseases recurred that could no longer be treated with antibiotics that previously had a positive effect.

Increasing misuse of antimicrobial agents, including in sectors such as agriculture and aquaculture, has increased the emergence of antimicrobial resistance (AMR). To date, antibiotic resistance has caused more than 7 million deaths annually and the situation could worsen by 2050, when the number of deaths per year could be around 10 million[144–146]. Due to increased tolerance and resistance to antibiotics, there has been a spread of multi-drug resistant 'ESKAPE' pathogens (*Enterococcus faecium*, *Staphylococcus aureus*, *Klebsiella pneumoniae*, *Acinetobacterium baumannii*, *Pseudomonas aeruginosa,* and *Enterobacter spp*.). In addition, multi-drug resistance is now also common in pathogens such as *Staphylococcus aureus* and *Mycobacterium tuberculosis*.

The first mechanism of antibiotic resistance was reported in 1944 in an isolate of *Staphylococcus aureus,* that was able to inactivate penicillin by producing penicillinase. This mechanism was similar to that noted four years earlier in *Escherichia coli*[147–149]. Around the mid-1950s in Japan, genetically transfectable antibacterial resistance was identified, introducing the concept of the possible presence of antibiotic genes diffusible by bacterial conjugation in an entire population of pathogenic bacteria[133,150,151]. Since the mid-1960s, the identification of new and effective antibiotic scaffolds using the traditional Waksman platform approach has been challenging[152–154]. This platform was created by microbiologist Rutgers Selman Waksman, and involved the screening of soil actinomycetes on a stacked bacteria field. Actinomycetes are bacteria that commonly produce antibiotics in their soil environment and the development of an inhibition zone on the plate allowed the identification of microbes capable of producing antibiotics. Streptomycin was identified using this methodology.

Bacterial resistance may be intrinsic or acquired. In the first case, bacteria are naturally insensitive to the antibiotic and this may be due to the absence or inaccessibility of the target by the antimicrobial. An example would be the outer membrane of Gram-negative bacteria. In the second case, however, an initially sensitive bacterium becomes resistant through mutations or the acquisition of genetic material. Conjugation is the most common way in which resistance genes are picked up. The formation of a bridge allows cell-cell contact, thus transferring the genetic material, which occurs through mobile genetic elements: plasmids, transposons, or integrons.[149].

Bacteria use several strategies to combat antibiotics (Figure 12):

a) Deactivation of antibiotics. Many resistance enzymes are capable of degrading or modifying different classes of antibiotics, such as β-lactams, aminoglycosides, phenolics, and macrolides[155]. Modification can occur by adding chemical groups to the key active centers of the antibiotics, impairing their activity and preventing the antibiotics from binding to their targets, partly due to steric hindrance[152]. A prime example of an enzyme capable of modifying the antibiotic is β-lactamase, which includes serine-β-lactamase and metallo-β-lactamase. Aminoglycoside antibiotics are also particularly susceptible to modification due to their many exposed hydroxyl and amide groups[156]. Aminoglycoside-modifying enzymes (AMEs) comprise three main classes: acetyltransferases, phosphotransferases, and nucleotidyltransferases[156,157].
b) Modification of targets. One example is the chloramphenicol-florphenicol resistance methyltransferase (*cfr*), which could specifically methylate A2503 in the 23S rRNA, thus conferring resistance to five classes of antibiotics: phenolics, pleuromutilins, streptogramins, lincosamides, and oxazolidonones[158,159]. The *cfr* gene is also usually found on conjugative plasmids, facilitating their wide intra- and inter-species spread[160]. Bacterial resistance to colistin has also developed. Initially, resistance to colistin was limited to chromosomal changes such as pmrA/pmrB activation of arnBCADTEF and pmrE, which collectively modifies LPS by the addition of 4-amino-4-deoxy-L-

arabinose. Recent studies have identified the mobilized colistin resistance gene (*mcr*) in bacteria of both animal and human origin[161]. A phosphoethanolamine encoded by *mcr* transferase can add phosphoethanolamine to lipid A, thereby reducing colistin binding by lowering the negative charge of the LPS[152].

c) Prevention of intracellular accumulation. This type of resistance can be implemented by downregulating porins or replacing porins with more selective channels[152]. This leads to the reduced permeability of the OM, limiting the entry of antibiotics into bacterial cells. This mechanism, for example, is implemented against carbapenems in Enterobacterales[162]. Efflux pumps are mainly responsible for the resistance of Gram-negative pathogens to many clinically used drugs. There are two types of efflux pumps: efflux pumps with strict substrate specificity (e.g. Tet pumps), and multidrug-resistant (MDR) efflux pumps, which carry a wide range of structurally different substrates[152]. An example of MDR efflux pumps is the resistance division pump (RND), which is a clinically relevant efflux transporter with a wide range of substrates in almost all Gram-negative bacterial pathogens[152]. Among others, the RND pump is encoded by a plasmid carrying a new *tmexCD1-toprJ1* gene cluster. This has been identified in *Klebsiella pneumoniae*, and confers resistance to several drugs including tigecycline[163].

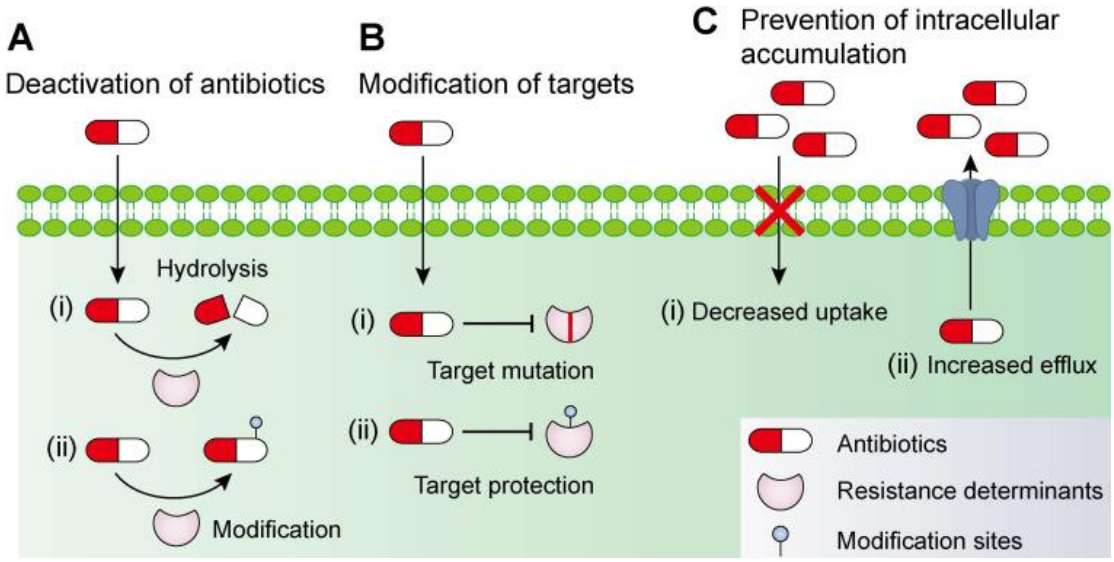

Figure 12. Molecular mechanisms of antimicrobial resistance in bacterial pathogens [152].

- Bacterial DNA Replication

DNA replication is a necessary and fundamental process of genomic duplication. The transmission of genetic instructions is essential to all living organisms and viruses[164]. This process requires extreme precision, speed, and fidelity and involves numerous protein factors. For example, in *in vitro* experiments, the rate of base incorporation in *E. coli* is ~1000 bp/s, while the rate of spontaneous base-pair substitutions is about 2×10^{-10} mutations per nucleotide per generation[164,165]. The numerous proteins involved form a multi-protein complex called "Replisome". The activity of the replisome is carried out through a hierarchy of weak functional interactions (Kd values range from low pM to high μM) and irreversible steps involving nucleotide hydrolysis or incorporation[166].

Replication consists of 3 different stages: initiation, elongation, and termination.

The initiation step is highly controlled to ensure that chromosomes are only duplicated once per cell division. Bacterial chromosomes are circular double-stranded DNA (dsDNA) with a single initiation locus, *oriC.* The *oriC* is comprised of an array of "DnaA boxes", that ensure the recognition of the origin by DnaA, the initiator protein. Another important element is the AT-rich DNA unwinding element (DUE) for strand separation[167]. DnaA boxes are bound by DnaA-ATP and DnaA-ADP. The two DNA template strands are then separated in the AT-rich region. After separation of the strands, the two single-strand DNA (ssDNA) are stabilized by *Single-Strand Binding proteins* (SSB). SSB is a monomeric protein that is associate in tetramers. DNA wraps itself tightly around SSB (these proteins also interact with other proteins involved in the replication)[168]. Two $DnaB_6$-$(DnaC)_6$ complexes are recruited and loaded on the separated ssDNA. DnaB is DNA-unwinding helicase and DnaC is the helicase loader. Helicase activity causes positive supercoils of the DNA in the front. Topoisomerases eliminate supercoils by transiently cutting through the DNA skeleton. In this way, the DNA linking number is changed. Topoisomerases are divided into the following categories: i) type IA and IB, which cut a single strand and do not require ATP hydrolysis; - ii) type II, which cut both strands and require ATP hydrolysis[168]. DnaG primase, a DNA-dependent RNA polymerase, interacts with the N-terminal of $DnaB_6$, promoting the dissociation of DnaC. At this moment, $DnaB_6$ moves to the apices of the bubble to form two replication forks, while DnaG synthesized RNA primers for an extension by DNA polymerase[164,169,170].

DNA polymerase III holoenzyme (HE) is the major replicative polymerase involved in the elongation step, in *E. coli*. This multiprotein complex involves 10 different proteins. Proteins are organized as follows: αεθ polymerase core, β_2 sliding clamp, and $\delta\tau_n\gamma_{3-n}\delta'\psi\chi$ clamp loader complex. These three assemblies are functionally distinct but physically interconnected[169]. β_2 sliding clamp is loaded, by clamp loader, onto the primer terminus synthesized by DnaG. The interaction between clamp and polymerase core (α, the subunit with polymerase activity, and ε, the 3'-5' proofreading exonuclease) takes place using a short linear clamp-binding motif (CBM) to the two symmetrically related CMB-binding pockets of β_2 sliding clamp. Pol III can synthesize DNA at high speed, ~1000 Nt/s, and with high processivity, >150 kb[166,169,171].

Genomic stability also depends on the correct termination of replication. In *E. coli* replication ends at the region opposite to *oriC*. Here there are 10 termination sites (Ter), which consist of 23 bp. Their sequence determines the binding affinity to the monomeric termination protein Tus[172]. Tus binds to Ter with high affinity. The ten Ter sites are arranged in groups of five, with opposite orientations. The replisome passes the first group and is blocked at the second. The two replication forks converge at the terminal region and there is proper segregation of the chromosomes[169].

- Bacterial DNA Replication as Antibiotic Target

Only two classes of antibiotics, in current clinical use, inhibit the process of DNA replication: quinolone and aminocoumarin. These drugs inhibit the action of DNA gyrase, a type II topoisomerase that introduces negative supercoils in DNA ahead of replication forks to enable continued strand separation by the helicase during DNA replication[170,173].

Aminocoumarin comes from coumarin. The derivates of coumarin are used in various fields of medicine. The main sources of the coumarin system are plants from the families of *Rutaceae, Rubiceae, Asteraceae, Apiaceae, Oleaceae, Fabaceae, Solanaceae,* and *Hippocastanaceae*, as well as bacteria of *Aspergillus* and *Streptomyces* strains[174].
In 1950 Novobiocin, a derivative of coumarin, was the first inhibitor of type IIA bacterial topoisomerases that was introduced in clinical use. Novobiocin was a product of *Streptomyces spheroides* and *Streptomyces niveus* fermentation[173]. Antibacterial activity is due to its ability to bind to the B subunit of DNA gyrase in bacteria and inhibit DNA supercoiling by blocking ATPase activity[174–176]. The problem with Novobicin and other coumarin derivatives was their poor activity on Gram-negative bacteria, their toxic hyperbilirubinemia, and additional problems, such as poor ADME characteristics[173,177].

The second class of antibiotics that inhibit the DNA replication of bacteria, is quinolones. This class is known to have a dual-target: DNA gyrase and topoisomerase IV. The dual action of the antibiotic class is explained by the sequence homology between the genes encoding gyrA and gyrB (gyrase) and parC and parE (topoisomerase IV)[178–186]. Quinolones and fluoroquinolones (the main subclass of quinolone antibiotics in use) bind the enzyme-DNA complex and stabilize the DNA strand breaks created by DNA gyrase and topoisomerase IV. The drug-enzyme-DNA complex causes the stop of the replication fork. The antibacterial activity of this class could take place in two stages: (1) conversion of the topoisomerase-quinolone-DNA complex into an irreversible form; (2) generation of a double-strand break by denaturation of the topoisomerase[186]. In addition to the emergence of bacterial resistance to these compounds, toxicity has also been observed. The major adverse effects include phototoxicity, CNS disturbances, tendonitis, and cardiac QT prolongation[173].

Considering the inactivity and toxicity of the antibiotics I have just described; researchers have shifted their attention to the search for new molecules using various drug discovery techniques. The bacterial replication system is essential for the viability of all organisms, and different protein complexes act at different stages. For this reason, the whole process is considered an attractive system for investigation[187]. There are currently inhibitors of proteins involved in bacterial DNA replication, which I will list below. The proteins of interest will also be briefly introduced, to highlight their functional domains and the different interactions they establish with other proteins in the replicative apparatus. Only the SSB and bacterial sliding clamp inhibitors will be discussed in subsequent chapters.

- DnaA protein is highly conserved among Gram-positive and Gram-negative bacteria[188]. Its role is to recognize and assemble at sites within *oriC* and to unwind a region within *oriC* to allow the entry of the complex DnaB-DnaC[187]. DnaA is a multifunctional protein: i) binds DnaA boxes and other sites (τ, I and C sites) that are present within *oriC*; ii) binds adenine-containing nucleotides, acid phospholipids, and other chromosomal sites; iii) binds other numerous proteins; iv) self-oligomerizes[187].

The protein consists of four different domains, through which it can interact with other different proteins[187,189–198] and with itself, as it self-interacts in the oligomerization process (first domain)[189,199–201], contacts the β and γ phosphates of the bound nucleotide, chelates the magnesium ion complexed to ATP, and binds and hydrolyzes ATP (third domain)[202–204]. The other two domains are binding motifs: the second domain mediates interaction between the first and third domains, while the fourth domain mediates binding of DnaA to oriC[187,205–210].
Inhibitors of this protein belong to the class of bis-indoles, which compete with ATP binding. The bis-indoles bind to the third domain of DnaA. Of interest is that an increase in the length of an aliphatic alkyl side chain introduced on bis-indoles correlates with an increase in their inhibitory activity, suggesting that these alkyl chains bind to a hydrophobic surface near the ATP-binding pocket[187,211].

- The helicase DnaB. Different studies have revealed the dynamic movement of the N- and C-terminal domains of DnaB during DNA unwinding. The C-terminal domains of hexameric DnaB are closest to the junction between single-stranded and duplex DNA in an artificial replication fork[212–214]. Each C-terminal domain binds and hydrolyses nucleotides to drive DNA translocation and unwinding[213,215–218]. Translocation occurs in the 5'→3' direction on the single-stranded DNA to which DnaB is bound[216,219–221]. The DNA strand passes through the central cavity of DnaB, apparently interacting with specific residues lining the cavity during movement while the other parental DNA strand is excluded[222,223]. DnaB interacts with DnaA, DnaC, DnaG, and τ subunit of DNA polymerase III holoenzyme[224,225]. Myricetin, a flavonol, inhibits the ATPase activity of *E. coli* DnaB by a non-competitive mechanism[226]. A study on DnaB from *Klebsiella pneumoniae* showed that myricetin impairs ssDNA-stimulated ATP hydrolysis[227].

- DnaG. This protein is responsible for the synthesis of oligonucleotide primers. DnaG consists of three functional domains: (i) helicase-binding domain, at the C-terminus, which interacts with DnaB; (ii) RNA polymerase domain (RPD), responsible for primer synthesis[228–232]; (iii) zinc-binding domain (ZBD), which binds DNA and may be able to recognize sites in template DNA to initiate primer synthesis[233,234]. Observations made by FRET analysis, crosslinking experiments and gel filtration assays support a model in which two or possibly three DnaG molecules are bound to DnaB. Through their specific interactions, these molecules cooperate to select the site on the parental DNA from which to initiate primer synthesis. In particular, the ZBD of a first primase molecule can interact with the RPD of a second primase molecule that is bound to the DNA[232,235]. The inhibitors of this protein belong to different chemical classes: phenolic monosaccharides and furans, imidazoles, and pyrimidine derivatives. Their mechanisms of action are not yet well understood. The first group may inhibit primase binding to ssDNA[236]. The second group was identified by *in silico* docking of compounds to the RNA polymerase domain[237].

- DNA Polymerase III Holoenzyme. This enzyme is essential for the viability of bacterial organisms. As described above, DNA Polymerase III Holoenzyme is organized into three subunits: αεθ polymerase core, β_2-sliding clamp, and $\delta\tau_n\gamma_{3-n}\delta'\psi\chi$ clamp loader complex. The three components of αεθ polymerase have three different roles. α subunit has the active site for DNA polymerization. This subunit establishes several interactions, including the one with β_2-sliding clamp (which I will discuss later). The protein α interacts with the single-strand DNA template and τ subunit of the clamp loader complex. Gram-positive bacteria with a low GC content uses two separate DNA replicases to copy the chromosome[238–244]. One, named PolC, is thought to synthesize both the leading strand and also

the lagging strand[187]. ε subunit has 3'-to-5' exonuclease activity. The role of this subunit is to eliminate an incorrectly inserted nucleotide so that DNA synthesis can proceed. In DNA polymerase III of *E. coli* the active site of the polymerase is located in a polypeptide separated from the ε subunit containing the proofreading exonuclease domain.
The clamp loader is composed of δ, δ', ψ, χ and three copies of DnaX protein[245–247]. The full version of this protein forms τ; the truncated version of this protein forms γ. The δ, δ' subunits, and DnaX protein are AAA+ proteins[202,248,249]. The function of the complex is to load the sliding clamp onto DNA[187]. The binding of ATP by the δ subunit and its subsequent hydrolysis is coordinated with conformational changes in both the sliding clamp and the clamp loader[241,245–247]. Once the sliding clamp is loaded onto the DNA, it associates with the central subset of DNA polymerase III and can then proceed with the elongation phase of replication. The τ subunit interacts with the α subunit to dimerize the central subset of DNA polymerase III so that synthesis of the main and lagging strands is simultaneous[250]. Two protomers of the τ subunit also interact with the DnaB helicase to increase both the rate of nucleotide incorporation and the rate of unwinding by the DnaB helicase [187,250–252]. In addition, DNA polymerase is stabilized on DNA by the interaction between the χ subunit and SSB[253,254]. Inhibitors of this system are nucleotide analogs. The 6-anilinouracil, benzyl guanine and 3-deazaguanine derivatives inhibit both DNA polymerase III and PolC of Gram-positive bacteria by interfering with the base pairing of dGTP with the cytosine base in the parental DNA, trapping the DNA-bound polymerase in an inactive complex[187,238,255–257]. BisQuinols (quinazolin-2-ylamino-quinazolin-4-ols) interfere with the binding of the enzyme to DNA[187,258].

- DNA Ligase. In *E. coli* we find two DNA ligases: DNA ligase A and DNA ligase B. The first binds Okazaki fragments, while the second act in the base excision or mismatch repair pathway. Both the enzymes use NAD^+ as a cofactor. Several DNA ligase A inhibitors that compete with the NAD^+ binding site have been identified[259–265]: 6-azaindazoles as AMP-competitor inhibitors[266]; adenosine analogues[267,268]; arylamino compounds, that inhibit by a non-competitive mechanism[263,269]; glycosyl ureides, glycosylamines, and tetracyclic indoles[261,265].

- Protein-Protein interactions in bacteria

Many PPIs play crucial roles in bacterial viability, in fact, DNA replication, transcription, and bacterial translation, as well as many other processes, are determined by important protein-protein interactions. Targeting the interactions between two proteins is, therefore, another strategy to fight antibiotic resistance, and in addition interactions between proteins have revealed an abundance of druggable antibiotic targets [270]. One of the mechanisms of resistance implemented by bacteria is to modify the target of the antibiotic, causing a decrease in the affinity between antibiotic and target, which however continues to maintain its biological function. This results in resistance that is amplified in a population[270]. If a mutation occurs at the protein-protein interface on one of the interacting proteins, in particular a hot-spot residue, it leads to inhibition of the drug, but also of the partner protein, leading to continued disruption or reduced protein-protein affinity[270]. For bacteria to overcome PPI inhibition by a small molecule and still maintain homeostasis, two simultaneous complementary mutations on two distinct proteins are required [270]. The probability of complementary double mutations is significantly lower than that of a mutation based on a single enzyme [270].

- Protein-Protein Interactions in bacterial DNA replication as a potential new antibiotic target

If until now molecules that target the enzymatic activity of potential targets involved in replication have been listed and analysed, now we must consider molecules that target protein-protein interactions. As mentioned above, PPIs are involved in many processes important for bacterial viability, and from a genetic point of view, there is an important difference in the conservation of proteins involved in bacterial informational processes. The DNA replication protein sequences are moderately conserved, unlike those involved in RNA transcription and protein translation, which are much more conserved[170].
Comparing the genomes of *E. coli* and *Bacillus subtilis*, they share 11-49% sequence identity concerning the proteins that make up the basic replication module[271].
Within the replication system itself, sequence motifs comprising enzyme active sites as well as whole proteins containing them are much more conserved than regions mediating protein-protein interactions[170].
Notable exceptions, however, are the protein-protein interaction systems present in the SSB and β_2-sliding clamp, which are highly conserved across bacterial genera.

- Single-stranded DNA-binding protein (SSB)

SSB plays an essential role in bacterial replication. After the action of helicases, SSB binds to ssDNA and protects it from nucleases. In addition, SSB acts in DNA recombination and repair and inhibits the formation of aberrant DNA structures. The active form of SSB is a homotetramer[187].
SSB interacts with a variety of proteins through a domain near its C-terminus[272,273]. This linear motif (LM) is conserved across 280 bacterial species and is characterized by NH_2-DDDIPF-COOH motif in *E. coli*[270].
SSB interacts directly with the α and χ subunits of the DNA polymerase III holoenzyme[253,254,274–280], with DNA polymerases II, IV, and V of *E. coli*[281–283], with proteins (PriA, PriB, and PriC) that function in the restart of collapsed replication forks[274,278,279,284–287], and with primase[275,288]. The interaction of SSB with the primase stabilizes the binding between the primase and the primer it has synthesized. This ensures the association of the primase with DnaB[228–231,289–294]. The SSB-χ interaction interrupts the SBB interaction with the primase, allowing the release of the primase and subsequent loading of the sliding clamp onto the DNA[253,254,275,277].
An advantage that makes SSB an excellent target is also its significant structural difference from its eukaryotic counterpart (replication protein A, RPA)[295].

By screening 50,400 compounds from Chemical Diversity, Maybridge, and Chembridge using high-speed fluorescence polarisation and subsequent dose-dependent assessment of SSB/Exonuclease I (ExoI) complex destruction, Keck's research group identified four inhibitors, CFAM, BCBP, BOTP, and MPTA of SSB-ExoI binding in *E. coli*[284]. The IC_{50} values of the four compounds ranged from 8 to 80 μM[296]. Crystallography showed that only CFAM interacts with the LM residues present at the C-terminus of SSB. This molecule also has the lowest IC_{50} value. Bacterial growth inhibitory activity was tested against a panel of bacterial strains that included Gram-positive microorganisms like *Listeria monocytogenes*, *Staphylococcus aureus*, and *Bacillus subtilis*, and the Gram-negative pathogens *E. coli* (wt and imp4213), *Neisseria gonorrhoeae*, *Neisseria meningitidis,* and *Neisseria lactamica*[297], with good results. In addition, MIC values were determined against one Gram-positive (*B. subtilis*) and one Gram-negative (*E. coli* imp4213) model. The MIC values against *B. subtilis* were 40, 11, 16 μM for CFAM, BCBP, and MPTA, respectively, while the MIC values against the membrane-compromised *E. coli* were 36, 62, and 10 μM, respectively[296]. Voter's research group, on the other hand, focused on PPI inhibitors of *Klebsiella pneumonia* SSB. Starting with a library of more than 72,000

compounds from Life Chemicals Inc. (Munich, Germany), and using orthogonal fluorescence polarisation assays, they identified nine selective inhibitors of the SSB/PriA interaction with IC_{50} values of <40 μM[298]. Oakley and his research group instead implemented a fragment-based drug discovery (FBDD) approach to identify disruptors of the SSB-DnaG interaction[299]. Using SPR competition assay and saturation-transfer difference NMR (STD-NMR), thirty fragments were initially identified. Subsequent structure optimizations based on the physico-chemical properties of the identified fragments resulted in a fragment with a good dissociation constant (K_D = 1.2 mM).

- β-sliding clamp

The *dnaN* gene encodes the sliding clamp, the processivity factor of the polymerase core. It works as a sliding platform and tethers the DNA polymerase to the template during replication[300]. It increases the processivity and speed of replication by ~5000-fold and 100-fold, respectively[301–305].
The β_2-sliding clamp protein is a ring-shaped homodimer that is composed of two monomers in a head-to-tail arrangement to generate two identical interfaces[300]. Each monomer (β-sliding clamp) has a molecular weight of 40.6 kDa and the structure (Figure 13) has been determined at a resolution of 1.85 Å[306].

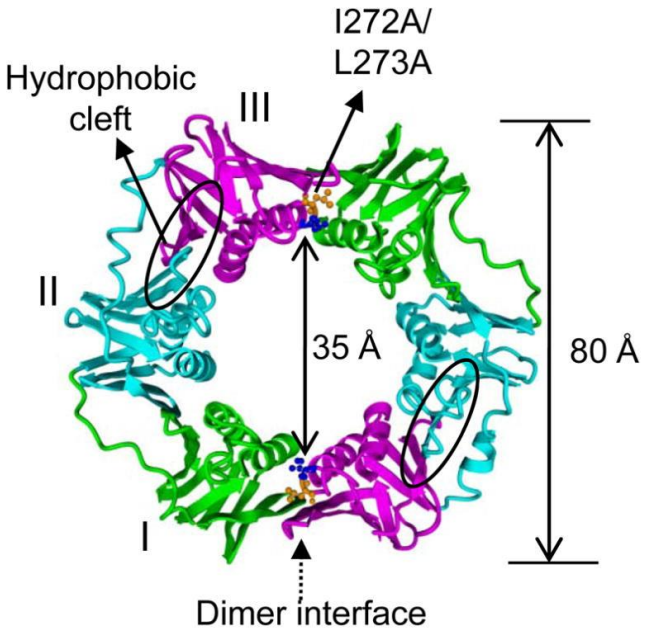

Figure 13. Ribbon representation of the crystal structure of the β_2-sliding clamp (PDB entry 1MMI)[300,306].

Structural studies revealed that β_2-sliding clamps have a pseudo-sixfold symmetry[305]. Each monomer consists of three domains that retain little primary structure but have good retention of tertiary structure. Each domain consists of two α-helices and two four-stranded antiparallel β-sheets; adjacent α-helices and a long curved β-sheet provide the interdomain interactions[305]. In Figure13, each monomer domain is represented by a different color: domain I in green, domain II in blue, and domain III in magenta[300]. The outer diameter of the ring is 80 Å, and the inner diameter is 35 Å, which easily accommodates double-stranded DNA[300,306,307]. Binding between the β_2-sliding clamp and DNA occurs through interactions between the positively charged residues within the clamp and the negatively charged DNA backbone. A hydrophobic gap between domains II and III is also evident. In addition, residues Ile272 and Leu273 are highlighted because they are essential for interaction at the β-dimer interface and a double mutation would result in a monomeric protein[300]. In evolutionary terms, the architecture and mechanism of processivity clamps are well conserved[245,308–311]. Both

β_2-sliding clamp, bacteriophage T4 gp45, and eukaryotic PCNA form planar ring structures with six similarly folded domains, although there is no detectable sequence similarity between the clamps[310]. Clamp proteins run on DNA and bind many proteins. The β_2-sliding clamp interacts with all five *E. coli* DNA polymerases[312–322]. In addition, it interacts with replication initiation factors DnaA[323] and Had[324]; mismatch repair proteins MutS and MutL; and DNA ligase A[305]. Of particular note are the interactions that β-sliding clamp establishes with δ subunit of the clamp loader and α subunit of the DNA polymerase III core. δ binds β-sliding clamp via the hydrophobic pocket and modulates the affinity of the clamp loader for β-sliding clamp, allowing clamp loading[325]. α, as described above, is the core of the replicative polymerase and the direct interaction between β-sliding clamp and the α subunit confers processivity to the polymerase[326].

In 2001 Dalrymple et al. identified a universal protein-protein interaction motif in eubacterial DNA replication and repair system: a pentapeptide with the consensus QLsLF (where s is a small amino acid) at, or near, the C-terminus of known eubacterial PolB proteins[316]. As we can see in Figure14, a similar sequence has also been found in the eubacterial PolC family and in members of the DnaE family, at positions equivalent to each other. Peptide sequence variants have also been identified in most eubacterial members of the UmuC and DinB1 families, with a significantly lower level of conservation of the proposed β-binding motifs than in the above families[316]. From the alignment of all β-sliding clamp interacting protein sequences using the consensus sequence, the percentage occurrence of amino acids was analysed and it was seen that in position one Gln is present 76.4% of the time and in position two Leu is present 41.6% of the time. A position not well determined by the presence of only one amino acid is position three, where for 34% of the times a Ser is present and for 22.8% an Asp. For the last two positions, fourth and fifth, instead, Leu is found in 81.2% of the sequences and Phe in 76.8%. In this way, it was possible to determine the composition of the consensus sequence: QL[SD]LF[316].

Through yeast two-hybrid assay and mutagenesis experiments, the abilities of the various β-sliding clamp binding motifs to interact with the protein were analysed. Specifically, about the α subunit, it was seen that β-sliding clamp-mediated β-galactosidase expression was directed by regions of α (DnaE) containing the binding motif (QADMF) for β-sliding clamp but was not observed when the β-sliding clamp binding motif was absent. The functionality of the proteins listed in Figure 14 was analysed in the same way and it was seen that they too had different activity if mutations in the binding sequence for β-sliding clamp were present[316]. A very interesting piece of information derived from these experiments is that, by mutagenising the α-subunit sequence in the consensus sequence (QLDLF), the expression of β-galactosidase increases. Subsequently, Dohrmann et al[327] conducted mutagenesis experiments on the sequence of the α subunit and then went on to quantify the KD of binding between the wt form of the α subunit (QADMF) and β-sliding clamp and between the variants of the α subunit and β-sliding clamp by Surface plasmon resonance. Through these experiments, they managed to confirm the previous finding, i.e., that by mutating the wt sequence of α to QLDLF there is an incredible increase in β-sliding clamp binding strength of about 120-fold, while mutating it to AAAKK significantly reduces β-sliding clamp binding. Subsequently, the same assay was conducted by Yin et al[328], but on the consensus sequence (QLDLF) using fluorescence polarization (FP) assay, and they noted that mutations at the level of the last two amino acids (QLDLF → QLDGG) led to a strong decrease in binding strength.

Phylogenetic analyses revealed that the residues that fold the binding site are highly conserved. Altogether, these results identify an evolutionarily conserved binding pocket for protein binding onto β-sliding clamps[329].

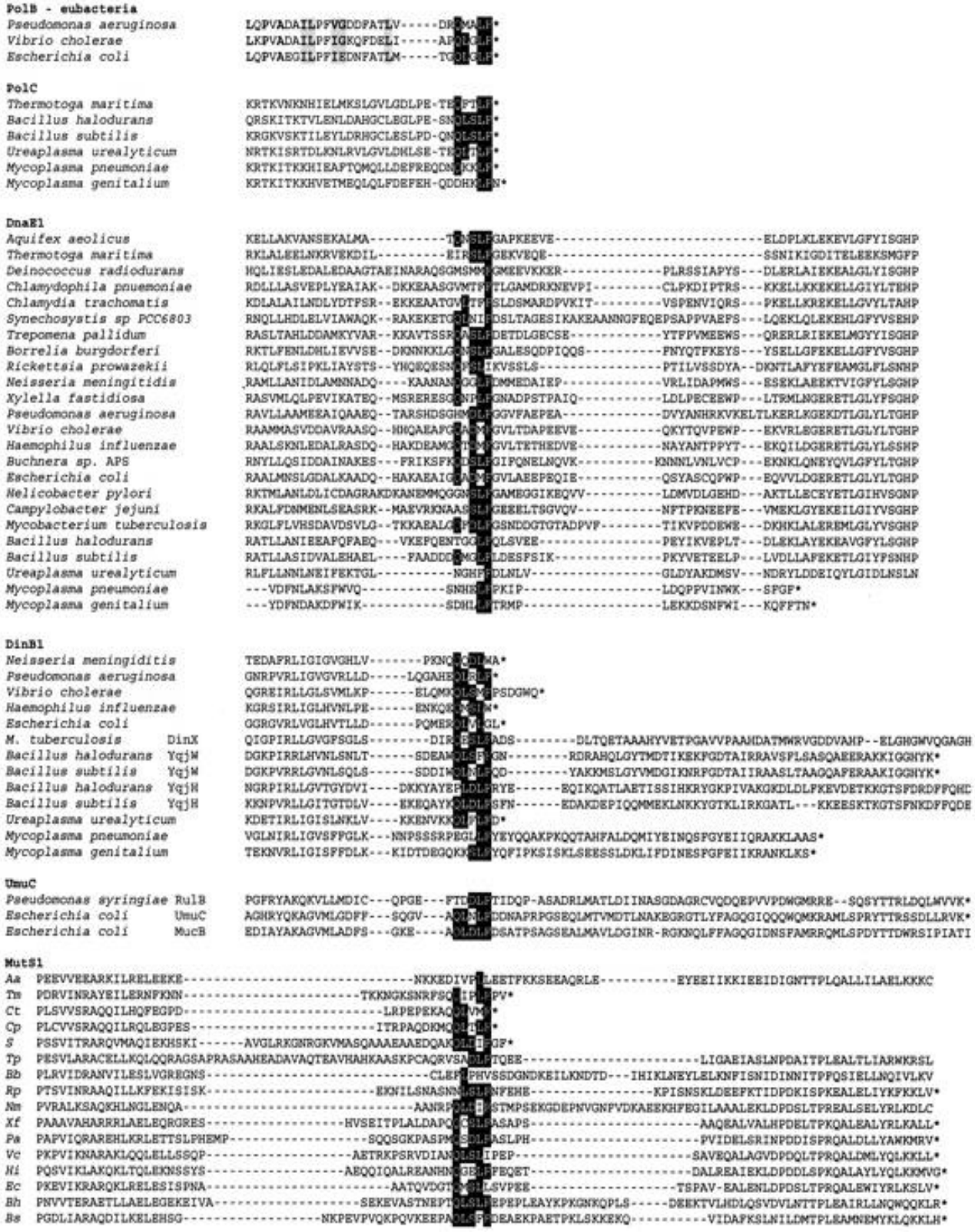

Figure 14. (Modified) Alignment of the regions containing the putative β-binding peptides from members of the eubacterial PolB, PolC, DnaE1, DinB1, UmuC, and MutS1 families[316].

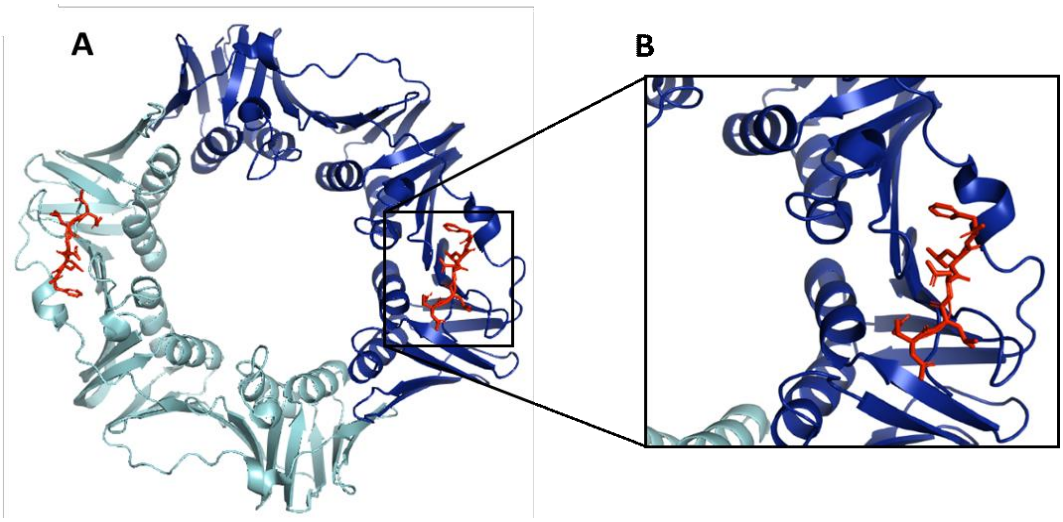

Figure 15. (A) Representation of β_2-sliding clamp co-crystallised with the consensus peptide. (B) Zoom of the consensus peptide. PDB 3Q4J[328].

Figure 15 shows β_2-sliding clamp co-crystallized with the consensus peptide. The structural analysis identified and analysed the β sites that interact most closely with the peptide. The consensus pentapeptide $Ac_0Q_1L_2D_3L_4F_5$ in complex with *E. coli* β-sliding clamp was published by Yin and his research group[328]. In this structure the N-terminal sub motif $Ac_0Q_1L_2$ dipeptide occupies subsite II, making three H-bonds to the amide backbone of M362, P363, and R365, and an H-bond to a bridging water molecule (W_0)[328]. The side chain of L_2 is involved in hydrophobic interactions with P363. The non-polar C-terminal L_4F_5 dipeptide sub motif occupies subsite I and makes interactions with the hydrophobic side chains of L177, V247, V360, and M362[328].
The β_2-sliding clamp has three key characteristics that make it an attractive target for the development of new antibiotics: (i) it is essential for DNA replication and repair; (ii) it is highly conserved among different bacterial pathogens; (iii) its structure differs from its eukaryotic counterpart.

For this reason, there are studies that have already identified β-sliding clamp inhibitors:

1. Georgescu et al. used fluorescence anisotropy trituration screening to identify an *E. coli* β-sliding clamp inhibitor from the Rockefeller University chemical library of 30,600 molecules and identified the compound RU7, a rhodanine, with a Ki=10 μM[330].
2. Wijffels et al. used a virtual screening of two different databases, National Cancer Institute and an in-house collection of 32,000 compounds. They were able to identify a biphenyl molecule that showed an IC_{50} = 40 μM[331].
3. Yin et al. initially analysed 352 compounds from Zenobia's First Pass Screen fragment library by fragment-based screening using x-ray crystallography. They identified 4 compounds that did not have high affinity when analysed in vitro using a competition assay between consensus peptide and β_2-sliding clamp. In an attempt to improve their binding affinities, they then performed a docking-based screening followed by a fluorescence polarisation (FP) assay of the selected candidates. The most promising molecule was a tetrahydrocarbazole derivative (Molecule 8) that completely occupies subsite I of *E. coli* sliding clamp. This molecule can inhibit replication by 100% at 250 μM and has a MIC of 313 μM for Gram-negatives (*E. coli* and *Acinetobacter baylyi*) and of 156 μM for Gram-positives (*Staphylococcus aureus* and *Bacillus subtilis*). One year later, further SAR investigations by the same research group led to the identification of another tetrahydrocarbazole derivative that showed a >4-fold increase in its affinity for *E. coli* sliding clamp[332].

4. Yin and Oakley's group, based on evidence that non-steroidal anti-inflammatory drugs (NSAIDs) have antimicrobial activity, studied the binding affinity of some NSAIDS (nonsteroidal anti-inflammatory drugs), whose mechanism was unknown, for β_2-sliding clamp of *E. coli*. Using fluorescence polarisation-based competition assay they analysed 20 commercial NSAIDS, of which vedaprofen, bromfenac, and carprofen show Ki < 300 μM. These three compounds also have higher antibacterial activity assessed against two Gram-negative (*E. coli* and *Acinetobacter baylyi*) and two Gram-positive (*Staphylococcus aureus* and *Bacillus subtilis*) bacteria, and Vedaprofen is the most active compound that had a MIC of 156 μM against Gram-positive bacteria. Of these, inhibition of DNA polymerase activity *in vitro* was verified: Vedaprofen and Bromfenac completely inhibit at 500 μM and Carprofen at 1 mM[333].
5. Another approach for searching for inhibitors of the protein-protein interaction was to use the structure of the natural pentapeptide QL(S/D)LF as a model. Wolff's group succeeded in identifying a short peptide with a higher affinity for β-sliding clamp (IC_{50} = 1.12 μM, measured by surface plasmon resonance). They attempted to improve the peptide's performance by replacing the leucine residue with a cyclohexyl-L-alanyl group (Cha), and by incorporating two chlorine atoms into the terminal benzyl ring of phenylalanine. The resulting peptide was shown to have a 15-fold higher binding affinity for the sliding clamp than the first peptide and to reach the 10^{-8} M range (IC_{50} = 0.077 μM)[334].
6. Løbner-Olesen and co-workers performed a study in which a library of 900,000 cyclic peptides was generated intracellularly using the circular split-intein binding of peptides and proteins (SICLOPPS)[74]. The aim was to identify molecules capable of inhibiting PPIs in the β_2-sliding clamp of *Staphylococcus aureus*. They were able to identify three peptides capable of disrupting the DnaN-DnaN interaction; two of them inhibited *Staphylococcus aureus* growth with MIC values of approximately 50 μM[335].
7. Kling et al. focused their study on tuberculosis. They identified griselimycin and its metabolically more stable analogs (methyl-griselimycin, MGM, and cyclohexyl-griselimycin, CGM) as active compounds against *Mycobacterium tuberculosis* with MIC values of 1, 0.6, and 0.06 μg/mL respectively. Surface plasmon resonance (SPR) showed that the compounds bind with high affinity to *Mycobacterium tuberculosis* sliding clamp (K_D ranging from 1.0×10^{-10} M to 2.0×10^{-10} M). No binding was detected between the same compounds and the human sliding clamp. Griselimycin and cyclohexyl-griselimycin bind the hydrophobic pocket between domains II and III[336].
8. Pandey et al selected 5 *E. coli* β_2-sliding clamp inhibitors found by Yin and co-workers, 4 from the study by Yin et al.[332], and 1 from the study by Yin et al.[334] and showed that they also inhibit the β-clamp/DNA ligase interaction of *Helicobacter pylori*. Only two molecules, 5-chloroisatin and difluorobenzamide, are shown to inhibit the growth of the bacterium with MIC values of 18 μM and 824 μM respectively[337].

β-sliding clamp characteristics and all the studies done so far suggest that it is a good target for the research of new antibiotics, as it interacts with many proteins and its function is very important for bacterial viability. Of particular relevance is the interaction it establishes with the α subunit: in fact, destroying this interaction would lead to the interruption of the replicative process and therefore the interruption of bacterial proliferation. Setting β-sliding clamp as a target of possible antibiotics would allow hitting a wide range of bacterial organisms, as the protein is highly conserved between Gram-positive and Gram-negative bacteria and, in addition, is different from its eukaryotic counterpart, so antibiotics would affect only prokaryotic organisms. The presence of studies that have been able to identify molecules that target β-sliding clamp could be helpful for the development of molecules with increased antimicrobial activity and having a target,

still not largely studied, involved in an interaction between proteins is an attractive starting point, as it could be less subject to mutations that would lead to the onset of resistance.

2. AIM OF THE PROJECT

Over the last two years, the health crisis that hit the world has forced many research groups and pharmaceutical companies to put aside research on very important topics that could cause growing problems as the years go by, such as the increasing bacterial resistance to antibiotics. The discovery and use of antibiotics to treat human and non-human infections are threatened by the presence of more and more pathogenic bacteria that are resistant to the antibiotics currently in use. This calls for the development of new drugs capable of hitting new targets. Unfortunately, research and development of a new drug is an expensive and sometimes lengthy process. Nowadays target-based discovery represents a very interesting approach to identify molecules capable of interacting with and modulating the biological activity of the target of interest. This approach is based on the screening of large libraries of small molecules to identify 'hit compounds' targeting a protein of interest. Of particular interest are protein-protein interactions (PPIs) as they may represent a new target for novel classes of antibiotics because they mediate numerous biological functions, both in physiological and pathological conditions. A PPI inhibitor can bind in pockets on the surface of a protein, leaving no room for the partner protein to make the necessary bonds for native interaction.

Replication is an essential process for the propagation of all organisms and is a very interesting pharmacological target. Interest has been focused on the bacterial interaction between the β-sliding clamp protein and the α-subunit of DNA polymerase III Holoenzyme. The β-sliding clamp is the processivity factor of the polymerase core, while the α-subunit presents the active site for DNA polymerization and the direct interaction between these two proteins ensure the processivity of the polymerase. A very interesting point to note is that several other proteins, involved in both DNA replication and repair, interact with β-sliding clamp using a highly conserved binding motif, called the consensus sequence, which is also conserved in the portion of the α-subunit that interacts with the β-sliding clamp.

Given the biological importance of the β-sliding clamp, this thesis aims to identify compounds capable of targeting the β-sliding clamp and thereby interfering with the interaction that the protein establishes with the α-subunit and, eventually, with the other interacting partners.

To do so, we used a high-throughput (HT) platform, with a screening yield of up to 800 compounds/day and combined *in vivo* and *in vitro* sequential assays as a new antibiotic discovery pipeline.

The proposed pipeline includes:

1. yBRET (yeast Bioluminescent Resonance Energy Transfer) assay, a highly sensitive *in vivo* HT assay, which allows to reproduce the β-sliding clamp - α interaction in the hyper-permeable strain *Δerg6* of yeast *Saccharomyces cerevisiae* and to search for compounds that inhibit the interaction, while monitoring the toxicity of these compounds towards a eukaryotic model organism. The efficiency of different yeast growth conditions and donor/acceptor ratios were compared to identify the optimal conditions to perform the screening. The assay allowed the screening of two libraries of pre-existing compounds and one library of compounds selected *in silico*. This latter library was obtained by virtual screening, which employed a pharmacophore model based on the consensus peptide previously co-crystallized with β-sliding clamp, and a ligand-based pharmacophore model that was constructed by incorporating features derived from already known inhibitors of the interaction, such as tetrahydrocarbazole derivative (Mol8)[333], the RU7 derivative of rhodanine[330] and vedaprofen[334] targeting β-sliding clamp subsite I. The first of these molecules was used as a reference compound in the following assays.
2. *in vitro* assays to validate and further characterize the inhibitory activity of hit compounds and of their analogs.

3. *in vivo* bacterial assays to assess the ability of selected compounds to inhibit the growth of Gram-negative and Gram-positive bacteria.

This strategy has previously proven to be an excellent tool for the identification and characterization of new molecules capable of inhibiting a bacterial PPI: in fact with this discovery platform, antimicrobial molecules capable of inhibiting the protein-protein interaction between the β'- subunit and the initiation factor σ^{70} of bacterial RNA polymerase were identified[338].

3. RESULTS AND DISCUSSION

OPTIMIZATION AND VALIDATION OF THE α SUBUNIT / β-SLIDING CLAMP INTERACTION AND CONSENSUS SEQUENCE / β-SLIDING CLAMP INTERACTION IN THE YEAST BRET PLATFORM

- α subunit – β-sliding clamp INTERACTION

Construction of fusion proteins for BRET analysis

The α-subunit of *E. coli* bacterial DNA polymerase III has two portions at the C-terminal end (aa 736-1160), identified through double-hybrid experiments, involved in interaction with the β-sliding clamp: the first binding motif includes residues 920-924 (QADMF)[316], while the other region includes two binding sites at amino acids 920-924 and 1152-1160[312].

To perform BRET it is usually necessary to try all possible combinations of fusion proteins. In this case, being β-sliding clamp the most promising target of the inhibitor molecules, this protein has been fused to the sequence of YFP and expressed constitutively, to allow inhibitors to bind to the target before the protein-protein complex is formed[98]. The expression of the donor fusion protein is instead induced, after addition of the candidate compound, by inducer supplementation. The donor fusion proteins are expressed under the control of the GAL1 galactose-inducible promoter (p415), while the acceptor fusion protein under a constitutive promoter (p416, GPD promoter), in the hyperpermeable Δ*erg6* strain of the yeast *S. cerevisiae* to maximize the uptake of the luciferase substrate and small molecule compounds.

We decided to analyse fragments of the α-subunit that contained one or all the binding regions of the β-sliding clamp: aa 736-991 portion (containing only the first binding motif) and the more extensive aa 736-1160 portion (containing both binding regions). Each of these two α-portions was cloned in-frame to NLuc in the p415 vector, in both C- and N-terminal combinations, measure β-sliding clamp binding strength by means of BRET signal. The full-length sequence of β-sliding clamp, the target of potential inhibitors, was cloned in-frame to YFP in the p416 vector with both C- and N-terminal orientations.

We performed a preliminary test, inducing the expression of the donor fusion protein with 2% galactose for 2 h, to select the combination with the higher BRET signal (Tables 1 and 2).

30 °C	Constructs	mBRET
2% gal	α (aa 736-991)-NLuc p415 / β-sliding clamp-YFP p416	18
	NLuc-α (aa 736-991) p415 / β-sliding clamp-YFP p416	86
	α (aa 736-991)-NLuc p415 / YFP-β-sliding clamp p416	5
	NLuc-α (aa 736-991) p415 / YFP-β-sliding clamp p416	18

Table 1. BRET signals are obtained with different combinations of α (aa 736-991) subunit / β- sliding clamp interaction constructs.

30 °C	Constructs	mBRET
2% gal	α (aa 736-1160)-NLuc p415 / β-sliding clamp-YFP p416	16
	NLuc-α (aa 736-1160) p415 / β-sliding clamp-YFP p416	120
	α (aa 736-1160)-NLuc p415 / YFP-β-sliding clamp p416	22
	NLuc-α (aa 736-1160) p415 / YFP-β-sliding clamp p416	33

Table 2. BRET signals are obtained with different combinations of α (aa 736-1160) subunit / β- sliding clamp interaction constructs.

The orientation of both YFP and NLuc affects the BRET signal, being the NLuc-α and β-sliding clamp-YFP the most effective orientations. NLuc-α (aa 736-1160) fragment resulted in a stronger interaction signal.

A minimum threshold value of 100 mBRET is set to be considered suitable for small molecule screening, thus, based on the results of this preliminary experiment, we selected the interaction construct combination NLuc-α (aa 736-1160) p415 / β-sliding clamp-YFP p416 to be used in subsequent analyses.

MODULATION OF EXPRESSION AT DIFFERENT GALACTOSE CONCENTRATIONS AT 30°C

To optimize the BRET assay, we monitored the BRET signal inducing the donor fusion protein of the selected interaction using different galactose concentrations (Table 3).

30 °C	NLuc-α (736-1160 aa) p415 / β-sliding clamp-YFP p416	
% gal	NLuc	mBRET
2	124600	120
0.5	156443	107
0.1	123503	103
0.05	121396	75
0.025	79506	72
0.01	14567	68
0.005	8114	29
Raffinose	163	0

Table 3. Nluc expression and mBRET values in response to different galactose concentrations for the NLuc-α (736-1160 aa) p415 / β-sliding clamp-YFP p416 interaction.

The BRET signal increases proportionally as the concentration of the inducer increases. Given the results, 0.5% galactose was chosen to perform BRET assay, because more reproducible BRET values were detected using this galactose concentration than under other conditions.

EVALUATION OF α (736-1160 aa) / β-sliding clamp INTERACTION SIGNAL SPECIFICITY

A donor saturation assay was performed to verify the specificity of NLuc-α (736-1160) / β-sliding clamp-YFP interaction. In this assay, the donor construct is expressed constitutively, and for this reason, the α-sequence (736-1160) was cloned in frame at the C-terminus of the NLuc in the p190 vector under the control of the constitutive TEF promoter. Meanwhile, the acceptor construct is expressed in an inducible manner: the complete sequence of the β-slide clamp was cloned in frame at YFP N-terminus in the p215 vector under the control of a galactose-inducible promoter (GAL1). This test is performed at 20 °C because it is the optimal temperature for proper folding of YFP and for the maturation of its chromophore, and the acceptor fusion protein is induced for 24 hours to allow the YFP chromophore to complete its maturation. We measured the BRET signal at increasing galactose concentrations, and, as shown in Figure 16, the BRET signal of the Nluc-α

(aa 736-1160) / β-clamp-YFP interaction is described by a hyperbolic curve, demonstrating the specificity of the interaction.

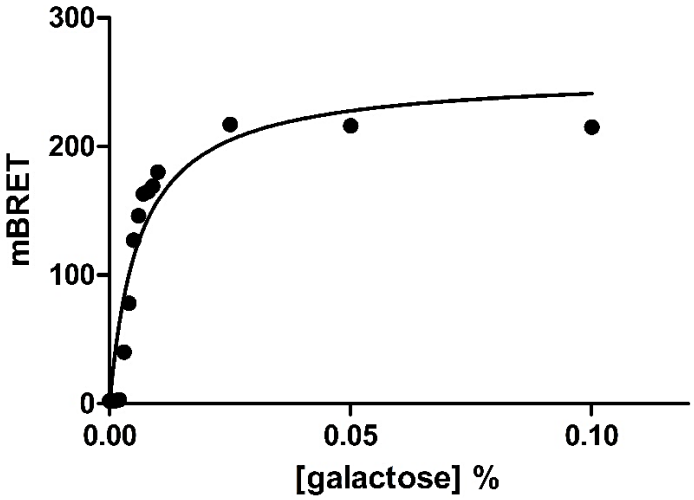

Figure 16. Energy donor saturation curve of the NLuc-α (736-1160) / β-sliding clamp-YFP interaction.

Another way to test the specificity of the interaction is to check the influence of mutations of key residues on BRET signal. Two mutant versions of the α protein were created, specifically mutating the QADMF binding site sequence between aa 920-924. A mutant version was created that should reduce the binding affinity towards β-sliding clamp by about 130 times compared with the wild type[327]: at the level of QADMF sequence, Q920 and D922 were replaced with alanine residues, and M923 and F924 were replaced with lysine residues[327]. The second mutant version should increase the binding affinity towards β-sliding clamp by approximately 120-fold compared to the wild type. This mutation involved changing aa A921 and M923 to leucine[327].

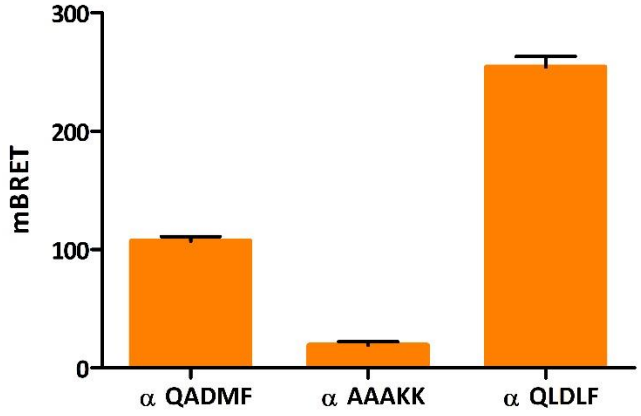

Figure 17. BRET signal comparison between wild-type and mutant combinations. The expression of the donor fusion proteins is induced for 2 h with 0.5% galactose (mean ±SD; error bars represent SD, n=3)

The BRET signal of the mutant versions was compared with the wild-type signal (Figure 17). The BRET assays confirmed the specificity of the binding between α and β-sliding clamp, validating the results found in the literature. Concerning mutations on the α amino acid chain, the AAAKK mutation reduced the BRET signal by 84%, while the QLDLF mutation increased the signal by 267%.

- Consensus sequence / β-sliding clamp INTERACTION

CONSTRUCTION OF FUSION PROTEINS FOR BRET ANALYSIS

β_2-sliding clamp of bacterial DNA polymerase III interacts with several proteins within the cell. Through the alignment of interacting β-sliding clamp protein sequences from different bacterial organisms, Dalrymple *et al*. identified a five-amino acid sequence, QL[D/S]LF, called the "consensus sequence" representative of the β-sliding clamp binding domain[316]. It is known from the literature that addition of dipeptides representative of the DNA polymerase III α-subunit sequence at both ends of the consensus results in an increase in the binding strength between the consensus and β-sliding clamp[339].

The consensus sequence IGQLDLFGV, comprehensive of dipeptides at C- and N-terminal, was cloned in frame to the NLuc in the p415 vector in both C- and N-terminal orientations, while the full-length β-sliding clamp sequence was cloned in frame to the YFP in the p416 vector in both orientations (Table 4).

30 °C	Constructs	mBRET
2% gal	Consensus-NLuc p415 / β-sliding clamp-YFP p416	205
	NLuc-consensus p415 / β-sliding clamp-YFP p416	245
	Consensus-NLuc p415 / YFP- β-sliding clamp p416	74
	NLuc-consensus p415 / YFP- β-sliding clamp p416	101

Table 4. BRET signals were obtained with different combinations of consensus sequence / β- sliding clamp interaction constructs.

High BRET signals were obtained regardless of the orientation of the partners. As in the case of α / β-sliding clamp interaction, the major influence on mBRET values is given by the fusion orientation of the acceptor. When YFP is placed at the C-terminus of the β-sliding clamp, mBRETs increase approximately 2.6-fold compared to when it is placed at the N-terminus. Although to a lesser extent, NLuc orientation also affects the BRET signal. The value of 100 mBRET is obtained for three out of four interactions analysed and, in this case, we selected the interaction NLuc-consensus p415 / β-sliding clamp-YFP p416 for further characterization.

MODULATION OF EXPRESSION AT DIFFERENT GALACTOSE CONCENTRATIONS AT 30°C

In order to optimize the BRET assay, we monitored the BRET signal of the selected interaction following the induction of the donor fusion protein with different galactose concentrations (Table 5).

30 °C	NLuc-consensus sequence p415 / β-sliding clamp-YFP p416	
% gal	NLuc	mBRET
2	83303	270
0.5	126560	245
0.1	116270	249
0.05	91425	245
0.025	47368	249
0.01	11424	234
0.005	6435	226
Raffinose	4659	194

Table 5. Nluc expression and mBRET values in response to different galactose concentrations for the NLuc- consensus sequence / β-sliding clamp interaction.

Modulation of Nluc expression is observed in response to different inducer concentrations, but a low modulation of BRET signal is detected at any galactose concentration. Considering these results, 0.5% galactose was selected since more reproducible BRET values are detected during the assay than under other conditions.

EVALUATION OF consensus sequence / β-sliding clamp INTERACTION SIGNAL SPECIFICITY

The specificity of the Nluc-consensus / β-clamp-YFP interaction was verified by a donor saturation assay. To this end, the consensus sequence was cloned in frame at the C-terminal of the NLuc in the p190 vector, while the full-length sequence of β-sliding clamp was cloned in frame at the N-terminal of YFP in the p215 vector (Figure 18). This assay was performed under the same conditions are the same as those described in section 2.1.3.

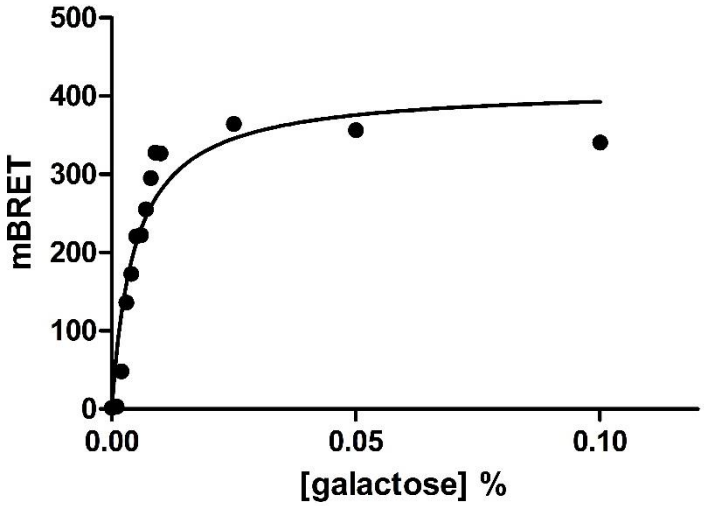

Figure 18. Energy donor saturation curve of the NLuc-consensus sequence / β-sliding clamp-YFP interaction.

The BRET signal of the Nluc-consensus sequence / β-clamp-YFP interaction is described by a hyperbolic curve, which confirms the specificity of the interaction.

To further validate the specificity of the consensus sequence / β-sliding clamp interaction, the QLDLF sequence was changed to the QLDGG sequence, which should reduce the binding affinity towards β^{328}. Yin *et al*. has conducted site-specific mutagenesis assays to analyse which of the amino acids have a greater influence on β-sliding clamp interaction by measuring the $K_D{}^{328}$. Of particular note are the mutations at the level of amino acids four and five when replaced with a Gly residue, and for this reason, we decided to make the mutation simultaneously at the level of both amino acids and evaluate the binding strength in yBRET (Figure19).

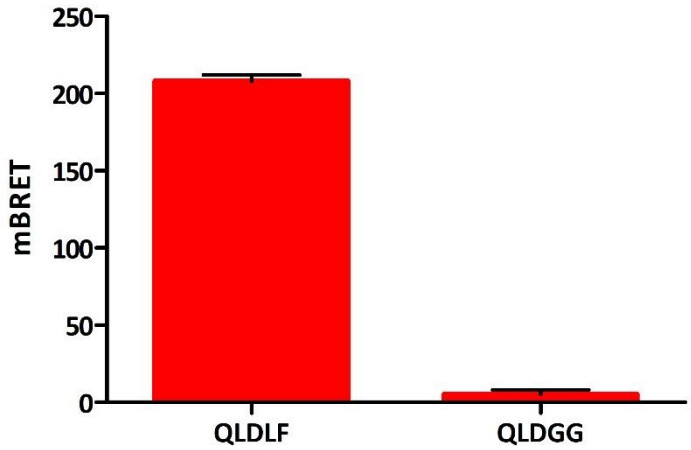

Figure 19. BRET signal comparison between wild-type and mutant combinations. The expression of the donor fusion proteins was induced for 2 h with 0.5% galactose (mean ±SD; error bars represent SD, n=3).

The BRET signal using the mutant version was reduced by 97% compared with the signal of the wild-type version, thus confirming the specificity of binding between the consensus sequence and the β-sliding clamp.

SCREENING OF SMALL MOLECULES LIBRARIES

The screenings of small molecules with possible antibacterial activity were performed with the NLuc-α (736-1160) p415 / β-sliding clamp-YFP p416 interaction at 0.5% galactose concentration. Although the consensus sequence / β-sliding clamp interaction displayed a stronger BRET signal, we preferred to test the molecules on the native interaction, as it can be inhibited more easily according to the K_D values of the two different interactions. Indeed, through Isothermal Tritation Calorymetry (ITC) assay, the strength of the β-sliding clamp / consensus sequence interaction was evaluated as K_D = 0.61 μM[340], while the K_D for the β-sliding clamp / α subunit interaction was 1.5 μM[341].

Molecules were tested in yBRET at a final concentration of 20 μM, added to exponentially growing yeasts before donor protein induction, and the BRET signal is read after a 2-hr incubation at 30 °C. From this primary screening, molecules were selected if they showed have inhibitory activity against the interaction greater than 15% and simultaneously did not reduce the NLuc signal by more than 50%, because they would then be deemed as toxic to yeast cells.

The selected molecules were re-assayed in a secondary screening at two different concentrations: 20 μM to reconfirm the previously obtained data and 10 μM to verify their activity at lower concentration.

The assays were carried out in white 96-well plates organized so that the first and last columns contained positive and negative controls (3% DMSO) and each of the remaining 80 wells contained yeasts treated with a different molecule.

- National Cancer Institute Library (NCI) and Compounds Australia Library-1 (CA, Griffith University)

The first two libraries screened were the *National Cancer Institute* (NCI, Bethesda, MD, USA) library, consisting of 1596 molecules, and the *Compounds Australia Library-1* (CA, Griffith University), consisting of 5000 molecules[338].

From the NCI library, the primary screening identified 50 molecules with inhibitory activity against the interaction above the 15%, but all molecules proved to be toxic to yeast cells and, therefore, were not further considered.

From *Compounds Australia Library-1*, nine molecules capable of inhibiting the interaction were initially identified, and three molecules (C239-0797, F393-0093 and F726-1337) were reconfirmed in secondary screening and then further tested.

- *IN SILICO* selection of compounds of the Griffith library and yBRET screening

Small non-peptide ligands able to inhibit the α subunit / β-sliding clamp interaction have already been identified[330–334,342], but still they are less potent than peptides designed on sequences inferred from native partners[327,328,331,339]. Given the limited exploitability of peptides, usually characterized by poor pharmacokinetic properties, a drug discovery campaign aimed at identifying new α-β interaction inhibitors could provide new molecules with antibacterial activity that might be further developed as potential new drugs.

The best-characterized region of interaction between the β-sliding clamp and the α subunit is about 20 Å long and can be described as composed of two subsites, a larger subsite I and a smaller subsite II. In some

crystal structures, these subsites are separated by the side chain of M362. Depending on the dimension of the co-crystallized ligand, in other crystal structures, the M362 side chain is displaced, and the ligand can undertake interactions with both subsites.

Compounds to be screened as α-β-sliding clamp protein-protein interaction inhibitors through the yBRET assay were derived from the "Open Collection Scaffolds" library and from an academic library provided by Compounds Australia (Griffith University).
Compounds were selected through a mixed approach which took into consideration i) fitting to pharmacophore models and ii) complementarity with β-sliding clamp surface evaluated with docking calculations.

As a preliminary phase in the selection of compounds to be evaluated, molecules with molecular weight lower than 250 were discarded, given the high molecular weight of known protein-protein interaction inhibitors and the extended contact surface between DNA polymerase III α-β proteins. The ligands were then transformed into their 3D structure. The following were taken into account: i) all chiral compounds with known stereochemistry, which were built with the indicated configuration; ii) all stereoisomers of compounds with unknown stereochemistry; iii) according to calculations with Epik (Schrodinger software), all protonation states available at pH =7.4±2.
Compounds belonging to the *Compounds Australia Library-1*, which had already been tested on α-β proteins of DNA polymerase III, were not considered in the construction of the second library.

Two pharmacophore models were prepared and used for compound selection. The first model was based on the main interactions undertaken by an optimized consensus sequence peptide derived from a portion of the α-subunit (Figure 5) contacting β-clamp residues[342].
In the crystal structure (PDB id 3Q4L), in which the peptide is bound to the β-subunit, subsites I and II of the β-sliding clamp are both occupied by the peptide and the M362 side chain is peripherally displaced and does not separate the two subsites. The pharmacophore model built on the peptide coordinates comprises seven features, three of which are hydrophobic and four polar. The radius of the hydrophobic features was increased (3 Å) with respect to the more restricting polar interactions (1 Å) which are additionally characterized by a directional component, to favour the selection of compounds having lipophilic substituent able to occupy the corresponding regions of the β-clamp.

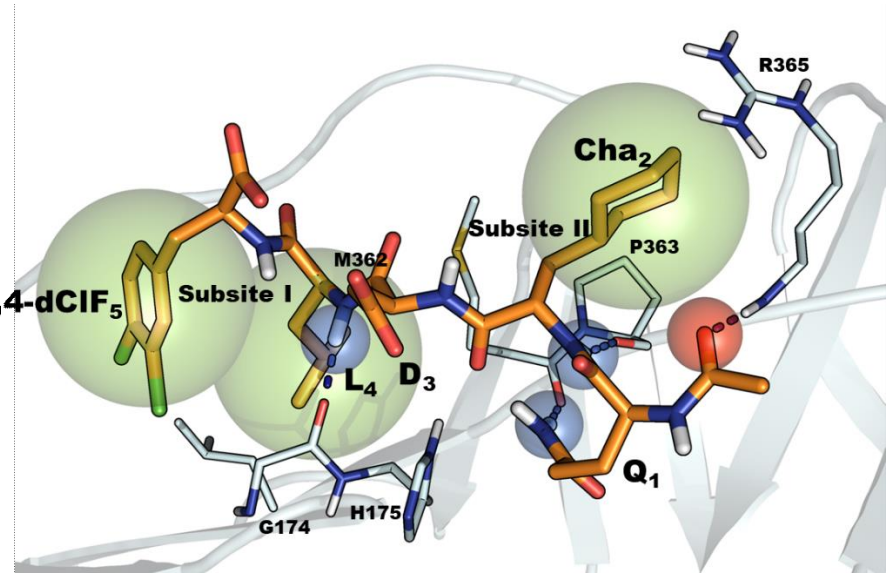

Figure 20. Pharmacophore model based on the main interactions established by an optimized consensus peptide (orange carbon sticks), co-crystallized with the β-sliding clamp (PDB id 3Q4L). Spheres represent pharmacophoric features. Larger green spheres identify hydrophobic features located in subsite I (L4 and 3,4-$dClF_5$) and subsite II (Cha_2). Blue and red spheres identify H-bond donor and acceptor sites of the peptide, respectively. The radius of each sphere is proportional to the tolerance accepted for functional groups fitting the specific feature.

The second pharmacophore model was based on interactions undertaken by small-molecule ligands (Figure 6) co-crystallized with the β-sliding clamp. A tetrahydrocarbazole derivative (compound 5b), a rhodanine (RU7) and vedaprofen were selected for the construction of the pharmacophore[330,333,334]. Some of the selected interactions are common to the different ligands, some are peculiar to a specific ligand. Overall, the crystallized inhibitors bind subsite I and the region immediately below it in the representation in Figure 9. The pharmacophore model comprises 6 features, 4 polar and 2 aromatic/hydrophobic sites. Three anionic features are present, as selected crystallized ligands undertake interaction with different basic β-sliding clamp residues.

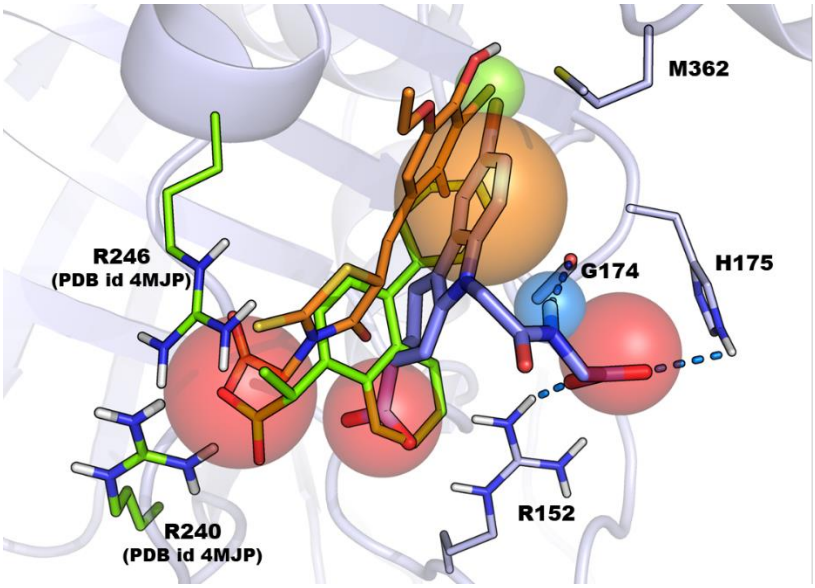

Figure 21. Ligand-based pharmacophore model obtained from interactions undertaken by small molecules co-crystallized with β-sliding clamp and targeting subsite I. Reference PDB structures are 4OVH for tetrahydrocarbazole derivative (compound 5b)[333], 3D1F for compound RU7[330] and 4MJP for vedaprofen[334]. The crystal structure of the tetrahydrocarbazole in complex with the β-sliding clamp is shown (PDB 4OVH, gray ribbons and sticks). Additionally, arginine residues bordering the subsite I are shown in the conformation captured in the crystal of the β subunit bound with vedaprofen (PDB id 4MJP, green sticks). Features: orange sphere, aromatic ring; green sphere, hydrophobic feature; blue and red spheres, H-bond donor and acceptor sites, respectively.

Pharmacophore screening was conducted by requiring structures to match at least three features. Compounds meeting this requirement were classified according to the number of matched pharmacophoric features, and then ranked with the built-in scoring function (Phase fitness score). Screening based on the first pharmacophore (built on the optimized consensus peptide) resulted in the identification of 24,351 structures from the ChemDiv library, 20,064 from the Enamine library, and 456 from the CA Academics library. The ligand-based pharmacophore model resulted in the identification of 17,218 structures from the ChemDiv library, 11,651 from the Enamine library, and 215 from the CA Academics library, ranked according to their phase fitness score.

The selected structures were then docked to the β-sliding clamp (PDB id 3Q4L). The purpose of docking was to identify compounds that could fit the β-sliding clamp binding site and exclude those structures that sterically clash with the protein and are likely characterized by poor or no binding affinity. Once docked, a short energy minimization was performed to relieve minor steric clashes. For each compound, the value of the scoring function GlideScore (GScore) was recorded, which, is taken as an indication of the possibility to interact with the binding site or to collide with the β-sliding clamp.

To define the set of compounds to be screened on recombinant *E. coli* proteins by BRET assay, a customized consensus function was set up, taking into account both the Phase fitness score (indicating the quality of each structure's fitting to the pharmacophore sites) and of the GScore (indicating the structure's stereo-electronic complementarity with the protein counterpart). Structures were ranked according to the consensus scoring function and the top 4000 non-redundant compounds were selected from the peptide pharmacophore and 935 compounds from the ligand-based pharmacophore screening. Top-ranked ligands identified according to the consensus score tend to occupy subsite I, although compounds selected through the peptide pharmacophore may also occupy the entire β-clamp binding site (subsite I and subsite II). Additionally, 25 compounds were selected based on their structural similarity to three molecules previously identified from *Compounds Australia Library-1*.

After *in silico* selection, 4960 potential inhibitors of the interaction between the α-subunit and β-sliding clamp were identified. The molecules were pooled in a targeted small-molecule library, the *Compounds Australia Library-2* (CA, Griffith University). From the primary screening, where all the molecules are tested at the concentration of 20 μM, 53 molecules were identified that could inhibit the interaction of interest and at the same time are not toxic to the yeast cells. Subsequently, the 53 molecules were retested in secondary screening, and only three molecules were confirmed.

The six hits (three from *Compounds Australia Library*-1 and three from *Compounds Australia Library*-2) were purchased from ChemDiv (San Diego, CA USA) along with 29 structural analogues (Table 6), to more extensively investigate the inhibitory activity of these chemical classes. For information on the structure, see Table 11.

Small molecule library	HIT commercial ID	N° structural analogs	Analogs commercial ID
Compounds Australia Library-1	C239-0797	0	
	F393-0093		
	F726-1337		
Compounds Australia Library-2	D479-0063	3	D428-0018
			D428-0071
			D479-0091
	L862-1652	7	L862-1364
			L862-1373
			L862-1593
			L862-1654
			L863-2005
			L863-2164
			L863-2310
	L010-0518	19	D430-0343
			D576-0080
			L010-0068
			L010-0480
			L010-0495
			L010-0504
			L010-0548
			L011-0481
			L011-0498
			L011-0513
			L367-0038
			L367-0072
			L367-0497
			L533-0208
			L533-0362
			L534-0053
			P510-0634
			P510-0674
			P843-0212

Table 6. List of selected hits with structural analogues.

In vitro VALIDATION

All molecules and structural analogues were tested in two different in vitro assays: Protein Thermal Shift and Competitive Enzyme-Linked Immunosorbent Assay (ELISA). The Protein Thermal Shift allows to verify that the target of the molecule is β-sliding clamp; the Competitive Enzyme-Linked Immunosorbent Assay (ELISA), allows to identify molecules able to displace the interaction of interest.
For both these assays, the tetrahydrocarbazole derivative (Molecule 8 or Mol8) was used as reference compound.

To perform these *in vitro* assays, *E. coli* β-sliding clamp, α-subunit, and consensus sequence proteins were expressed and purified.

- Proteins Expression and Purification

β-sliding clamp

The β-sliding clamp protein sequence was cloned in frame with the MycTag sequence, which is required for the ELISA assay, and with a six-histidine tag (HisTag), which is required for the purification step. The two Tags were cloned at the C-terminal end of the protein sequence. The entire β-sliding clamp sequence was cloned into pET28 (b) vector, expressed in *E. coli* BL21 CodonPlus strain for 20 hours at 20 °C with 1 mM IPTG, purified through affinity chromatography and the eluted fractions stored in 20 mM Tris-HCl pH 7.5, 0.5 mM EDTA, 20%(v/v) glycerol.

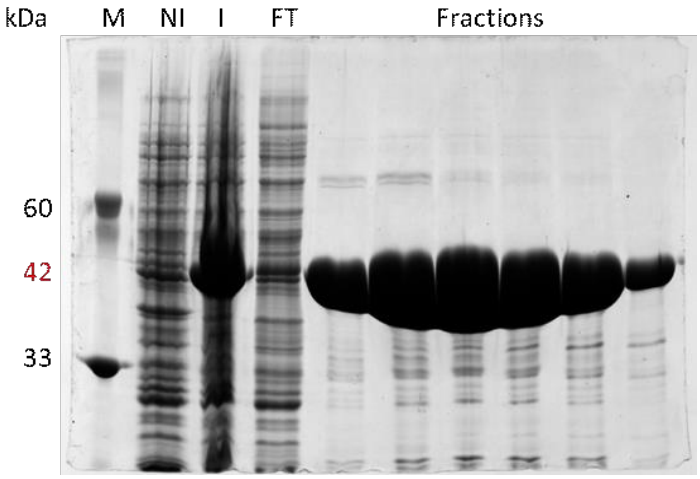

Figure 22. SDS-PAGE of β-sliding clamp-MycTag purification. The protein has a molecular weight of 42 kDa. (M = marker; NI = not induced; I = induced; FT = Flow Through).

Using the Lambert-Beer formula, the concentration of the protein was deduced. Through the calculation of ε = 16180 M^{-1} cm^{-1} in ProtParam and the OD_{280} nm obtained from spectrophotometric measurement, the concentration of our protein after purification (Figure 22) was 3.7 µg/µL giving a yield of 56 mg of protein per litre of culture.

α subunit

We initially proceeded with the expression and purification of the same portion (736-1160) used in the yBRET assays. The α (736-1160) sequence was cloned into pET28 (b) in frame with the six-histidine tag (HisTag) and

expressed in the *E. coli* BL21 CodonPlus strain for 20 hours at 20 °C with 1mM IPTG in LB medium and for 24 hours at 20 °C in autoinduction medium.

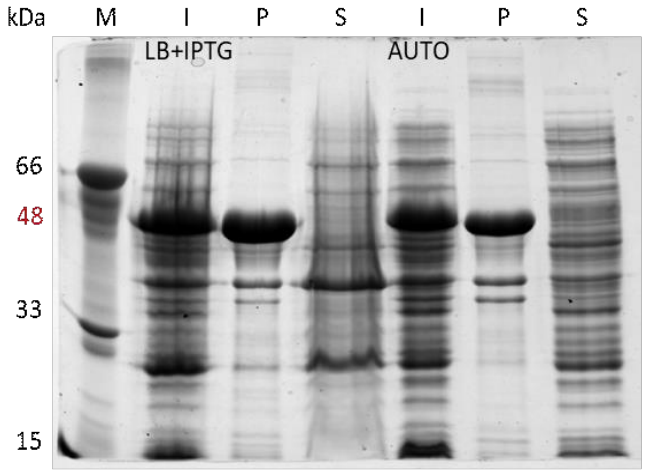

Figure 23. SDS-PAGE of α (736-1160) subunit expression. The protein has a molecular weight of 48 kDa (M = marker; I = induced; P=pellet; S=Supernatant; LB=Luria-Bertani medium; AUTO= Autoinducer medium).

The protein resulted insoluble under both expression conditions (Figure 23).

The protein was then expressed in a BL21 (DE3) strain carrying the pKJE7 (Takara3) plasmid. This plasmid encodes for multiple molecular chaperones (DnaK of 70 kDa, DnaJ of 40 kDa, and GrpE of 22kDa), known to work cooperatively in the protein folding process. The chaperone-coding genes are under the control of *araB* promoter. Thus, the expression of target protein and chaperones can be induced individually if the target gene is placed under the control of another promoter. We then proceeded with expression for 20 hours at 20 °C in LB, with the addition of 20% arabinose to induce expression of the chaperonins and 1 mM IPTG to induce expression of the α subunit (aa 736-1160) protein.

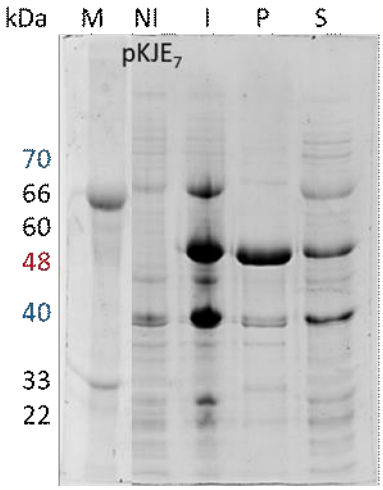

Figure 24. SDS-PAGE of α (736-1160) subunit expression in pKJE$_7$. (M = marker; NI=not induced; I = induced; P=pellet; S=Supernatant).

In this condition of expression, there is an improvement in the solubility of the protein, and it was purified with affinity chromatography, as described above.

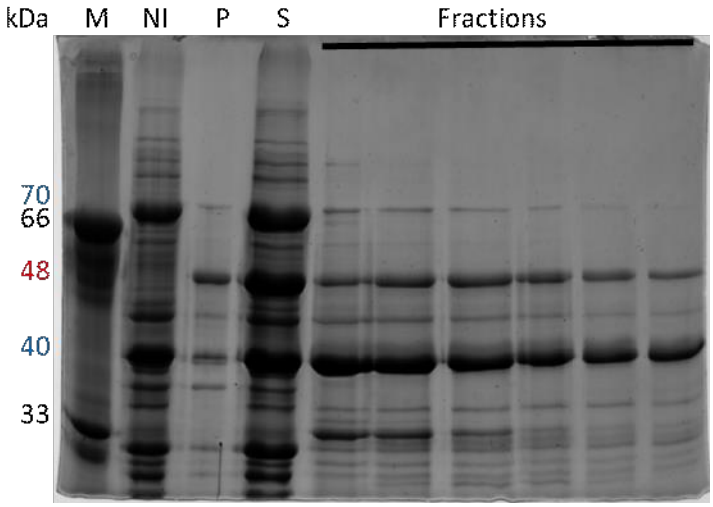

Figure 25. SDS-PAGE of α (736-1160) purification in the $pKJE_7$ strain. (M = marker; NI = not induced; I = induced; P=pellet; S=Supernatant).

Two proteins were purified after the affinity chromatography: one, displaying a molecular weight of 48 kDa, is the protein of interest, while the most abundant one, is the chaperonin DnaJ, which has a molecular weight of 40 kDa. An anion exchange chromatography was carried out to separate the proteins by exploiting their different isoelectric points: pI α (736-1160) = 6.12 and pI DnaJ = 7.98.

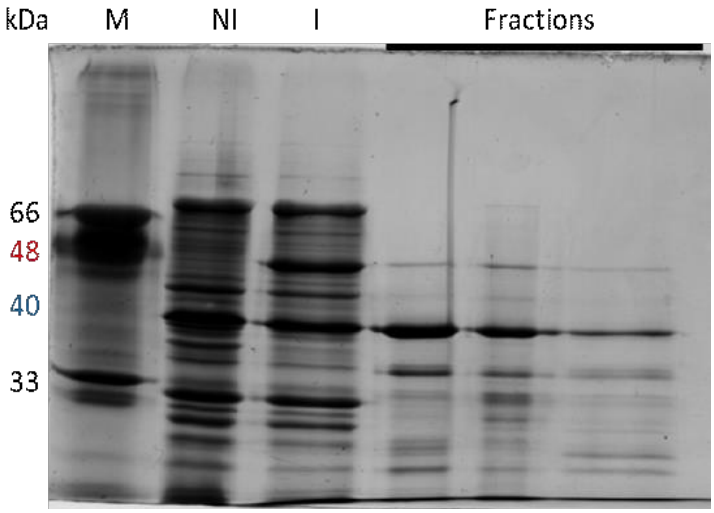

Figure 26. SDS-PAGE of anionic exchange step of α (736-1160) protein. (M = marker; NI = not induced; I = induced;).

However, also in this case, it was not possible to separate the two proteins.

A final attempt to purify the protein was made expressing α (736-1160) in the Origami strain of *E. coli*, which greatly enhances disulphide bond formation in the cytoplasm, but once again the protein was found to be insoluble.

It is probably the case that the cut made at the level of the 736 amino acid in the α sequence does not allow the protein to fold correctly, so that it requires external help to adopt its correct conformation. The entire α sequence was then cloned into the pET28 (b) vector in frame with the six-histidine tag (HisTag), expressed in the *E. coli* BL21 CodonPlus strain for 20 hours at 20 °C with 1mM IPTG, and the solubility of the protein was verified before the purification step. An improvement in protein solubility was immediately noticed. As can be seen from Figure 27, after sonication, most of the protein, which in its full-length form has a molecular weight of 140 kDa, is in the soluble fraction.

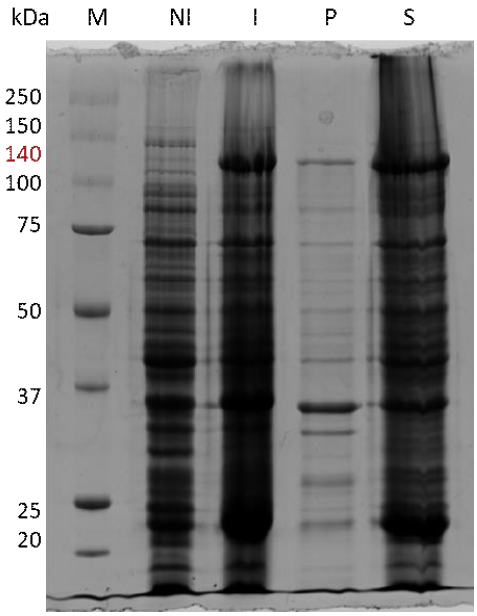

Figure 27. SDS-PAGE of α (1-1160) expression. (M = marker; NI = not induced; I = induced; P=pellet; S=Supernatant).

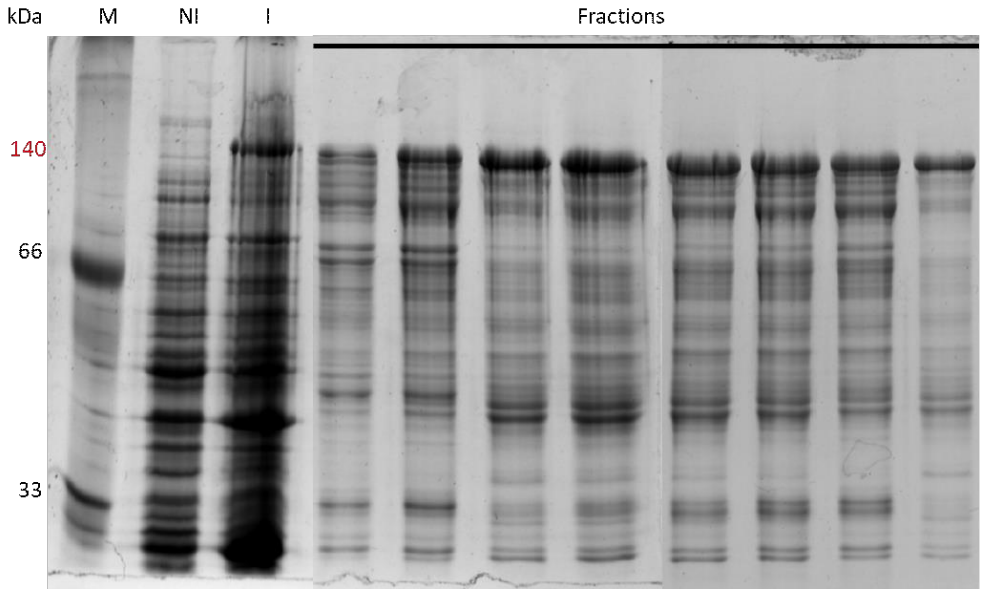

Figure 28. SDS-PAGE of α (1-1160) purification. (M = marker; NI = not ninduced; I = induced).

The purification through affinity chromatography did not lead to a pure protein (Figure 28), and this was the case even after an additional step of anion exchange chromatography.

We tried to separate the protein of interest from all other proteins via gel filtration purification, taking advantage of their different molecular weights, but again the protein was not pure (Figure 29).

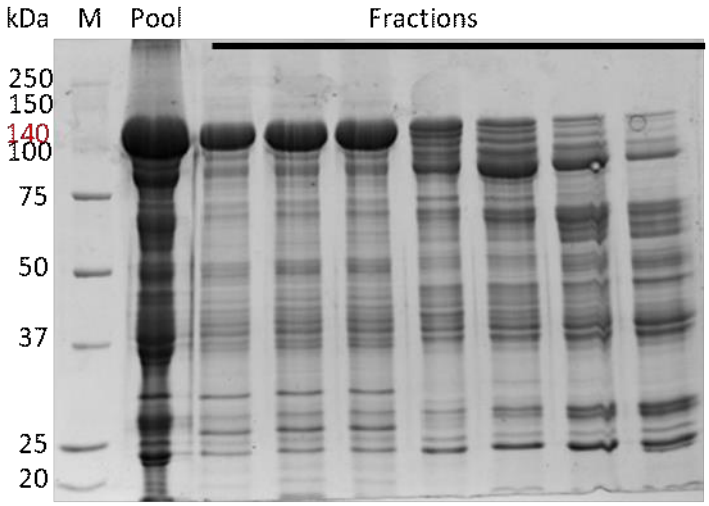

Figure 29. SDS-PAGE of α (1-1160) gel filtration. (M = marker; Pool= fractions collected from the previous purification).

The latter assay highlighted how the protein tends to be purified along with many other proteins. This is most likely due to the role of the protein itself, which is part of the core of the αεθ polymerase, and thus it is difficult to separate this subunit from the other two. In addition, the protein establishes many other interactions, making the purification process even more difficult. Therefore, we did not obtained a protein suitable for use in the *in vitro* ELISA assay, and as an alternative we decided to express the consensus sequence QL[D/S]LF.

NLuc-consensus sequence

Having analysed the interaction between the β-sliding clamp and the consensus sequence in yBRET, we decided to express and purify the consensus sequence in frame with the Nluc sequence, since such a small sequence needs a carrier, and in frame with a six-histidine tag (HisTag), which is required for the purification step. Tests performed in yBRET had also showed that the presence of NLuc does not affect the binding of β-sliding clamp to the consensus sequence. The entire NLuc-consensus sequence was cloned into the pET28(a) vector, expressed in the *E. coli* BL21 CodonPlus strain for 4 hours at 30 °C with 1mM IPTG, purified through affinity chromatography and the eluted fractions stored in PBS and 20%(v/v) glycerol.

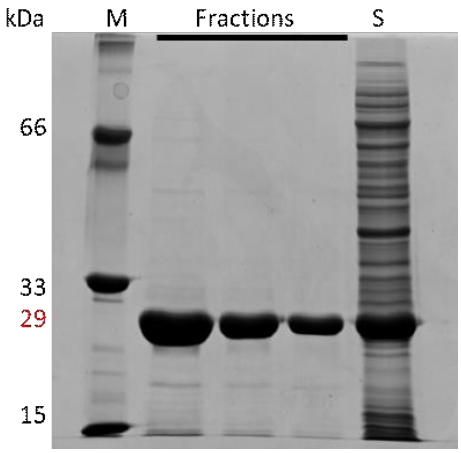

Figure 30. SDS-PAGE of NLuc-consensus sequence purification. The protein has a molecular weight of 29 kDa (M = marker; S=supernatant).

Using the Lambert-Beer formula, the concentration of the protein was deduced. Through the calculation of ε = 25440 M^{-1} cm^{-1} in ProtParam and the OD_{280} nm obtained from spectrophotometric measurement, the concentration of our protein after purification (Figure 30) was 3.47 µg/µL giving a yield of 55 mg of protein per litre of culture.

- Protein Thermal Shift Assay

The Protein Thermal Shift (PTS) assay is based on the principle that proteins unfold at a critical temperature. At lower temperatures, proteins adopt a native state that generally consists of a compact and predictable tertiary structure. At higher temperatures, proteins denature, losing secondary and tertiary elements and forming a molten globule or aggregates. Thermal stability is an intrinsic property derived from the protein sequence and defines the temperature at which thermal denaturation occurs.
The stability of a protein is related to its unfolding Gibbs free energy, ΔGu, which is temperature-dependent, so the stability of most proteins decreases as temperature increases; as temperature increases, ΔGu decreases and becomes zero at equilibrium, when folded and unfolded proteins have equal concentration. The temperature at which this state occurs is the melting temperature (Tm)[343].

In this assay, the thermal stability of a protein, and consequently its Tm, can be measured by monitoring the denaturation of the protein using a fluorescent dye (such as SYPRO Orange or ROX) while progressively increasing the temperature of the sample. These dyes are often exploited for their ease of use: when denaturation begins, proteins tend to expose hydrophobic residues buried in the inner core of the protein and these hydrophobic residues, when exposed to the solvent, interact with the dyes used in the PTS assay, allowing the detection and measurement of a measurable fluorescent signal[344].
The thermal stability of a protein is an important characteristic that can be used to assess the stability of a protein under a range of pH and buffers conditions.

If a molecule binds to a protein, in most cases the free energy contribution of the ligand causes an increase in ΔGu, which can lead to an increase in Tm, and, for this reason, the PTS can be used to identify biological ligands, a characteristic that makes it suitable also as a primary screening method for protein targets that lack a suitable functional or binding assay to identify leads for drug discovery[316]. This connection between binding and thermal stability allows ligands to be identified based on their effect on the Tm of the protein.

We used PTS to verify that β-sliding clamp was the target of both the hits identified by the BRET assay and their structural analogues.
The PTS test set-up includes a first step to assess the Tm of β-sliding clamp, by assaying different quantities of protein to identify the amount at which the Tm is most stable. 2 µg, 3 µg, 4 µg, and 5 µg of β-sliding clamp were tested; 4 µg of protein resulted the most reliable condition showing a Tm of 57 °C.
The second step is necessary to verify that the solvent in which the molecules are resuspended, DMSO in this case, does not alter the Tm of the protein, so that any temperature variation identified when the molecules are assayed against the protein of interest can be traced back exclusively to the activity of the molecule.
The Tm of β-sliding clamp was determined in the presence of 1%, 2%, and 3% DMSO and all three concentrations of solvent did not affect the Tm of the protein.

The 35 molecules (6 hits + 29 analogues) and Molecule 8 (reference compound) were tested at 100 µM in 1% DMSO. Molecule 8[332] is a tetrahydrocarbazole bound to subsite 1 of the β-subunit (PDB id 4N9A), that is analogue to compound 5b[332]. Molecule 8 (ChemDiv) was used instead of compound 5b, which is not commercially available. ΔTm was calculated using the Boltzmann method[344].

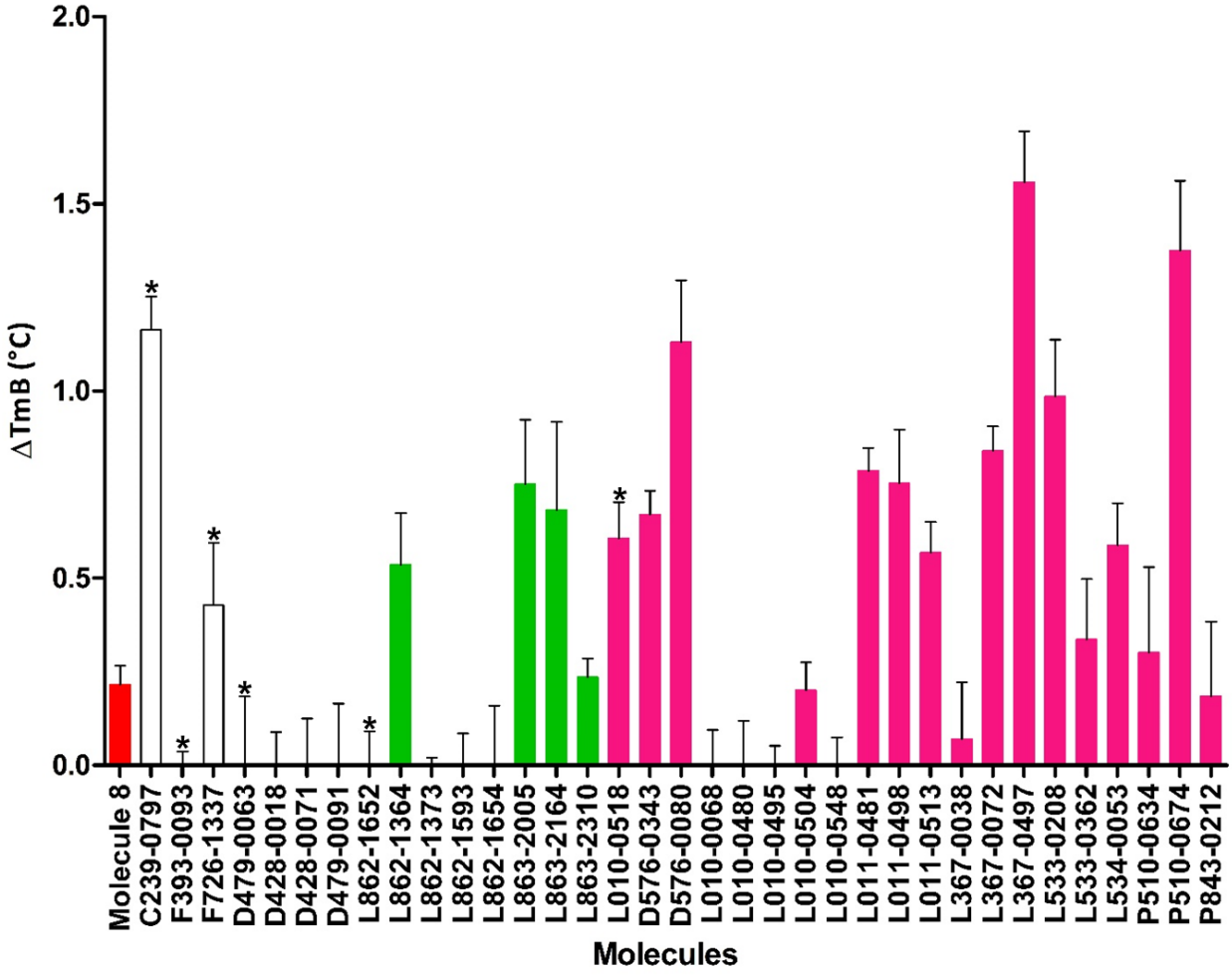

Figure 31. Protein Thermal Shift (PTS) assay results of β-sliding clamp in the presence of hits and analogues molecule. *: hits identified with the yBRET screening. Specifically, the first three derived from screening on *Compounds Australia Library-1*, and the other three from screening on *Compounds Australia Library-2*. Structural analogues follow the

corresponding hits. Molecule 8 (in red) is the reference compound. ΔTmB (ΔTm was calculated using the Boltzmann method) is reported as average of 4 replicates. Error bars: standard deviation

Fifteen molecules induced an increase in β-sliding clamp Tm of at least 0.5 °C, indicating their specificity for the target (Figure 31).

This assay suggests that three hits identified by yBRET assay, C239-0797, F726-1337 and L010-0518, belonging to three different chemical classes, inhibit the interaction between the β-sliding clamp and the α subunit because by specifically binding the β-sliding clamp. In particular, for the molecule L010-0518, which is the progenitor of the series of molecules represented with the pink colour (Figure 31), this ability is also confirmed for its structural analogues. Two other hits instead, F393-0093 and D479-0063, did not display any binding activity in this assay, and for the latter, the entire class of analogues did not appear to bind the β-sliding clamp. The hit L862-1652, on the other hand has no affinity for the protein, but four out of seven structural analogues induced an increase in Tm of the β-sliding clamp.

- Competitive Enzyme-Linked Immunosorbent Assay (ELISA)

To validate the yBRET results we also analysed the ability of all molecules to displace the interaction of interest with Competitive Enzyme-Linked Immunosorbent (ELISA) assay. Due to the difficulty in purifying the α-subunit, the assay was optimized with the interaction β-sliding clamp-MycTag / Nluc-consensus sequence. The interaction was first reproduced in ELISA using three molar concentrations of Nluc-consensus sequence (250 nM, 500 nM, and 1 µM) and four different concentrations of β-sliding clamp-MycTag (250 nM, 500 nM, 1 µM, and 2 µM) combinatorially. All combinations tested showed detectable and stable signals. The nonspecific signal was monitored using the interaction between β-sliding clamp-MycTag and NLuc as negative control. The highest signal reliability was obtained when both proteins Nluc-consensus sequence and β-sliding clamp-MycTag were assayed at 250 nM.

All molecules were initially tested at 100 µM. Ten molecules that could inhibit the interaction of at least 20% were identified. The fairly permissive threshold (20%) was chosen based on the lower K_D of the β-sliding clamp / consensus sequence interaction[340] compared with the K_D of the native β-sliding clamp / α subunit interaction[341].

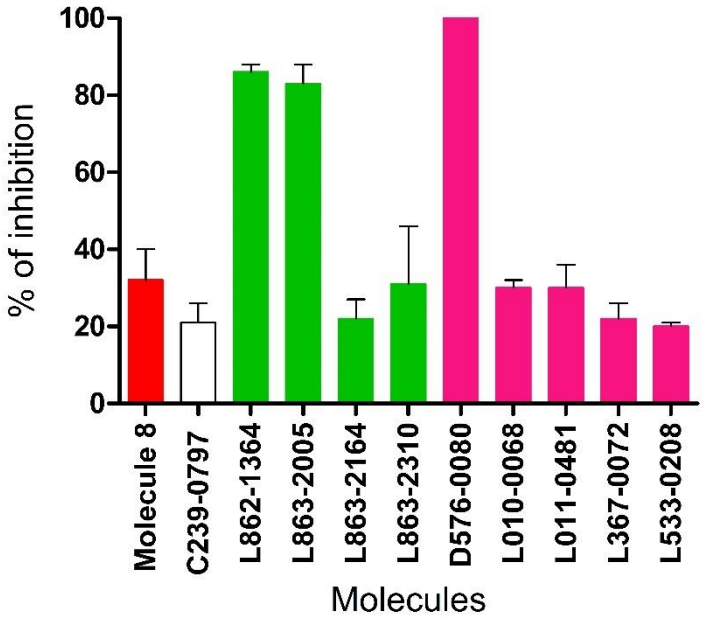

Figure 32. Molecules ability to inhibit β-sliding clamp / consensus sequence interaction, assayed in the ELISA assay. Compounds are shown in the same colour code as described for the PTS assay (Figure 31). (mean ±SD; error bars represent SD, n=3). Molecule 8 (in red) is the reference compound.

The most active compounds L862-1364, L863-2005, and D576-0080 were selected to evaluate their inhibitory capacity in a dose-response ELISA assay.

The percentage of inhibition was calculated at twelve different concentrations ranging from 0.5 µM to 150 µM. For Molecule 8 the percentage of inhibition was calculated at fourteen different concentrations, from 0.5 µM to 350 µM.

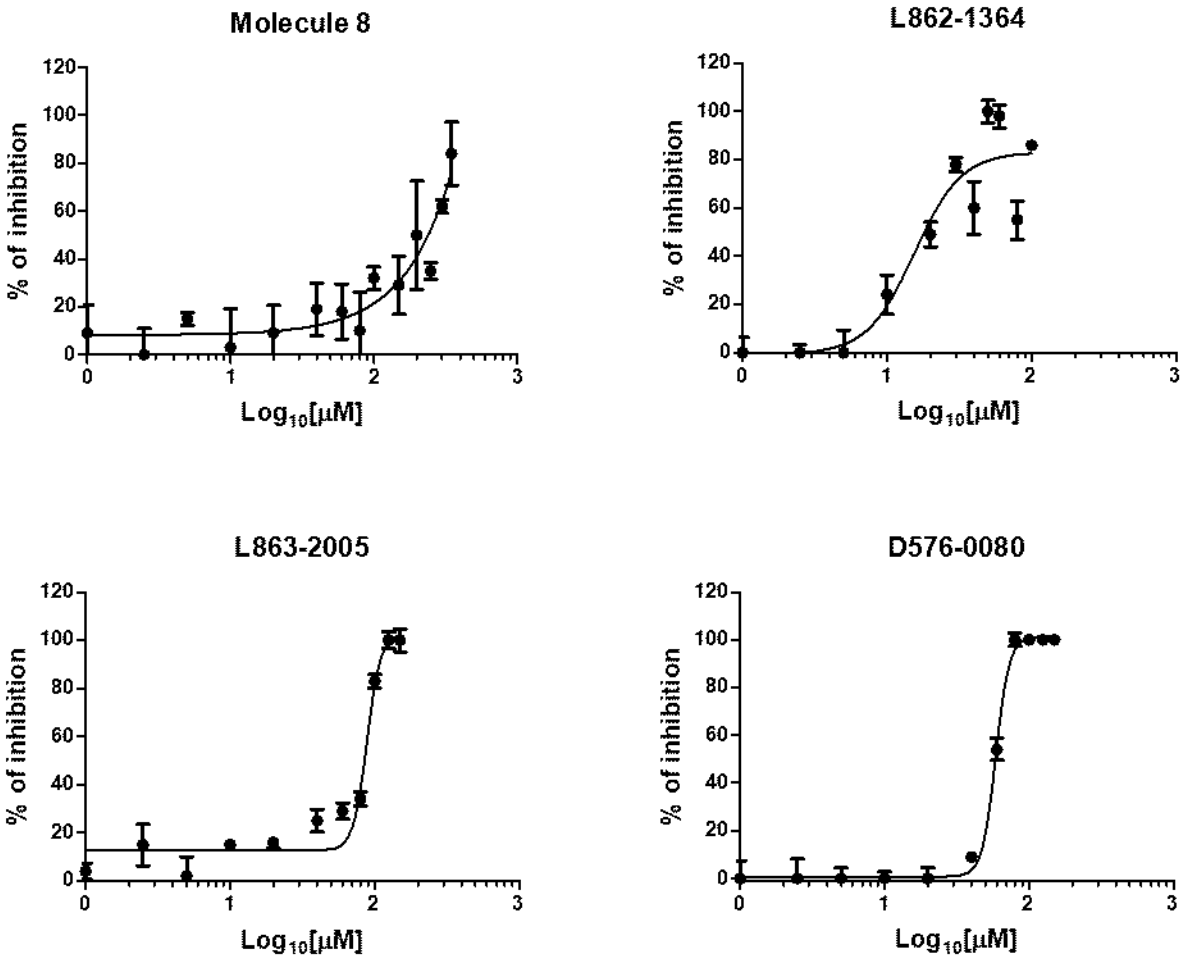

Figure 33. Inhibitory activity on the β-sliding clamp / consensus sequence interaction of the most active molecules is evaluated at different concentrations in the ELISA assay. IC50 is calculated as a measure of molecule potency.
Molecule 8: IC_{50}=nd r2=0.5812
L862-1364: IC_{50}=16.15 µM r2=0.8481
L863-2005: IC_{50}=88.52 µM r2=0.9098
D576-0080: IC_{50}=58.91 µM r2=0.9798

For Molecule 8, an attempt was made to calculate the IC_{50} with this assay, but this was not possible because, at the concentrations tested, the molecule has not yet reached the plateau of activity, i.e. the concentration value at which its activity is maximum, and the program is not supplied with the necessary data. While the molecules identified by this study reached a plateau of activity at 100 µM, Molecule 8, despite being tested at higher concentrations, up to 300 µM, was unable to reach it. This may presumably be due to a lower activity of the molecule towards the interaction of interest.

The purpose of the ELISA assay is to analyse the ability of molecules to hamper the interaction of interest. They were therefore initially tested at a concentration of 100 µM, allowing the identification of ten molecules belonging mainly to two different chemical classes that are particularly active towards the interaction. As can be seen from the histogram in Figure 16, the molecules belong to the chemical classes that also stood out in the PTS assay. They are part of the series of molecules identified with the green and pink colour, while the molecules belonging to the other chemical classes are inactive in this competitive assay. Molecules L862-1364, L863-2005, and D576-0080 showed an inhibitory activity in the range of µM (IC_{50} values from 16.15 to 88.52), which was nevertheless better than the reference Molecule 8.

- Ligand Docking

A binding hypothesis can be drawn for the two most potent compounds in the ELISA assay, L862-1364 and D576-0080, which are structural analogues of compounds initially selected from the screening on the first pharmacophore model derived from the optimized consensus peptide. Each compound was aligned on the pharmacophore model and two energy-minimizations of the protein-ligand complexes were run with the OPLS3e force field implemented in MacroModel. In the first energy-minimization distance restraints were kept on the atoms undertaking hydrogen bonds, while in the final one no restraints were applied, and the ligands were free to move. The protein was kept fixed during minimization, except for the residue side chains within 5 Å from the ligand.

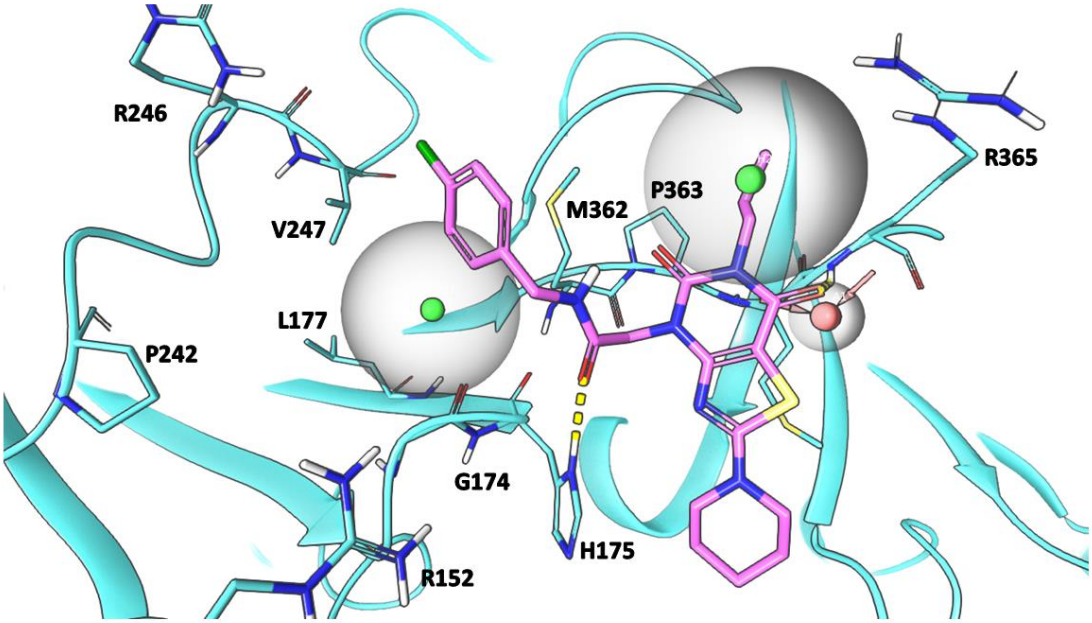

Figure 34. Putative binding mode of L862-1364 inside the binding pocket of the β-subunit. Green and red spheres represent hydrophobic and hydrogen bond acceptor pharmacophore sites, respectively. Hydrogen bonds are evidenced with yellow dashes.

L862-1364, the most potent compound in the series of tiazo-pyrimidindione derivatives, is bound to subsite II (Figure 34). Two pharmacophore points are maintained after energy-minimization: a carbonyl oxygen of the pyrimidindione ring, which is H-bonded to the backbone nitrogen of R365 (red sphere in Figure 34), and the hydrophobic site of subsite II occupied by the propyl chain. In crystal structures of proteins interacting with the β-sliding clamp the latter hydrophobic interaction is generally established by residues, such as leucine, bearing short alkyl groups[316]. Additionally, a hydrogen bond is undertaken by the ligand with H175, and the *p*-chloro-phenyl group is accommodated close to the hydrophobic region of subsite I.

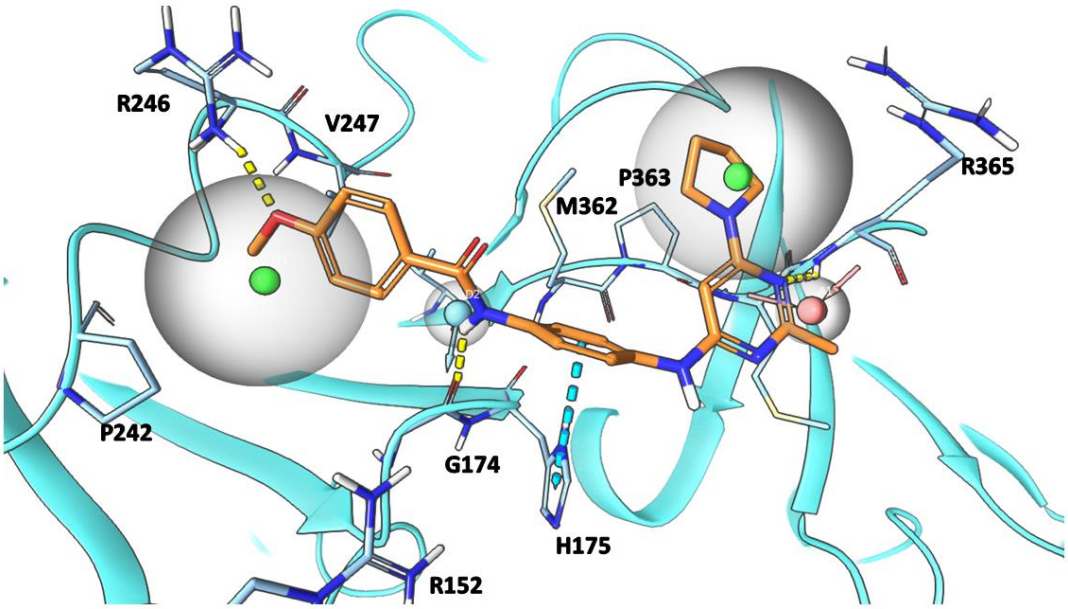

Figure 35. Putative binding mode of D576-0080 inside the binding pocket of the β-subunit. Green spheres represent hydrophobic regions included in the pharmacophore model, and hydrogen bond acceptor and donor features are represented by red and cyan spheres. Hydrogen bonds and π-π interactions are evidenced with yellow and blue dashes, respectively.

The most potent compound D576-0080, due to its elongated shape, is able to bind both subsites I and II (Figure 35). In subsite I, one of the hydrophobic sites is occupied by the anisole fragment, while the amide nitrogen undertakes a hydrogen bond with G174 backbone. On the other side of the binding pocket, a pyrimidine nitrogen undertakes a hydrogen bond with the backbone nitrogen of R365 and the pyrrolidine ring occupies the hydrophobic region of subsite II, similarly to the cyclohexyl-alanine of the optimized consensus peptide and the propyl chain of the thiazo-pirimidinone L862-1364.

In vivo CHARACTERIZATION

- Growth Inhibition Assay on Non-Pathogenic Bacteria

Once all the molecules were characterized in the *in vitro* assays, we analysed their activity *in vivo*, directly on bacteria, through a growth inhibition assay. Bacterial growth was monitored for 8 hours, in the presence of two different molecule concentrations: 20 µM and 100 µM. The inhibitory activity of all molecules was tested against two non-pathogenic bacteria: Gram-negative *E. coli*, in the presence of 2 µg/mL of Polymyxin B nonapeptide (PMBN) to increase the permeability of the outer membrane, and Gram-positive *B. subtilis*. To exclude possible toxicity on a eukaryotic organism, molecules were also tested on the yeast *S. cerevisiae*.

	E. coli		*B. subtilis*		W303	
	20 µM	100 µM	20 µM	100 µM	20 µM	100 µM
Molecule 8	0	0	24	85	0	0
C239-0797	0	30	7	8	0	23
F393-0093	0	0	0	6	7	22
F726-1337	0	5	3	14	0	9
D479-0063	0	1	0	0	0	2
D428-0018	0	12	10	7	0	9
D428-0071	0	19	0	1	0	2
D479-0091	0	11	16	7	0	8
L862-1652	47	na	28	na	29	na
L862-1364	0	26	41	21	25	26
L862-1373	25	12	0	12	39	11
L862-1593	2	4	9	0	0	13
L862-1654	0	3	2	0	0	0
L863-2005	0	9	1	0	0	20
L863-2164	0	12	8	0	0	0
L863-2310	0	4	2	21	0	0
L010-0518	0	0	3	0	32	43
D430-0343	0	24	14	16	0	25
D576-0080	99	93	14	92	0	24
L010-0068	0	0	3	13	0	0
L010-0480	17	0	0	0	3	54
L010-0495	0	0	7	0	13	16
L010-0504	0	0	0	0	0	22
L010-0548	0	0	0	0	0	13
L011-0481	100	na	0	24	14	47
L011-0498	100	82	0	26	0	36
L011-0513	0	0	21	5	0	38
L367-0038	0	0	0	0	0	5
L367-0072	0	0	13	0	2	8
L367-0497	0	0	0	0	2	10
L533-0208	0	0	16	21	18	13
L533-0362	0	0	28	7	0	26
L534-0053	0	0	25	0	0	20
P510-0634	0	0	7	0	0	3
P510-0674	0	0	13	0	0	0
P843-0212	14	0	4	0	0	0

Table 7. Percentage growth inhibition activity at 8 h for molecules tested at 20 µM and 100 µM, on Gram-negative *E. coli* DH10 in the presence of Polymyxin B nonapeptide (PMBN), on Gram-positive *B. subtilis* (WB800N), and *S. cerevisiae* (W303). Hits identified by the yBRET assay are in bold, and below are their respective structural analogues. Specifically, the molecules in white are the hits identified by screening on *Compounds Australia-1*, and in green, blue and pink are

the three identified by screening on *Compounds Australia-2* with their structural analogs. Molecule 8 (in red) is the reference compound.

None of the molecules corresponding to the first 5 hits and corresponding homologues showed strong inhibitory activity against the two prokaryotic organisms. Molecules L862-1652 and L862-1364 at 20 µM inhibited the growth of *E. coli* and *B. subtilis* by 47% and 41% respectively but resulted toxic against *S. cerevisiae*. On the other hand, molecules D576-0080, L011-0481 and L011-0498, analogues of the 6th hit, completely inhibited the growth of *E. coli* already at 20 µM, while being non-toxic to *S. cerevisiae*. When tested at 100 µM, molecule D576-0080 was also able to inhibit the growth of *B. subtilis*, although it also displayed a 24% inhibitory activity against the eukaryotic organism under investigation.

The molecules were also tested on *E. coli* in the absence of PMBN, but none of them showed activity, and even the activity of the molecules that were found to be the strongest in presence of 2 µg/mL PMBN dropped in its absence (data no shown).

- ## Minimum Inhibitory Concentration (MIC) And Minimum Bactericidal Concentration (MBC)

For the three molecules that were particularly active against *E. coli* and *B. subtilis*, MIC and MBC values were calculated against both of these organisms. Again, PMBN was added to the final concentration of 2 µg/mL to *E. coli* cells.

	Escherichia coli		***Bacillus subtilis***	
	MIC	MBC	MIC	MBC
	PMBN 2 µg/mL			
D576-0080	25 µM	25 µM	25 µM	25 µM
L011-0481	10 µM	10 µM	nd	nd
L011-0498	5 µM	25 µM	nd	nd
Molecule 8	50 µM	100 µM	100 µM	nd

Table 8. MIC and MBC values on *E. coli* and *B. subtilis*. (nd=not detected)

The molecules were tested at nine different molar concentrations (0.5 µM - 100 µM), and MIC and MBC values were determined against both of these non-pathogenic bacteria. Confirming the data obtained in the previous assay (see Table 7), the molecules proved to be particularly active against *E. coli* and with MIC and MBC values lower than the reference molecule (Molecule 8). The MIC and MBC values give us information on the mode of action of the different compounds. While molecules D576-0080 and L011-0481 have bactericidal activity at 25 µM and 1 µM respectively, molecule L01-0498 is bacteriostatic up to 5 µM but becomes bactericidal at 25 µM. A similar difference can be found for Molecule 8, which is bactericidal at a concentration of 50 µM and bacteriostatic at 100 µM. As far as the activity of the molecules against *B. subtilis* is concerned, it was only possible to calculate both values for compound D576-0080, because the other molecules most likely had to be tested at higher concentrations to be active. This molecule is bacteriostatic at 25 µM, while Molecule 8 has bactericidal activity at 100 µM.

We determined MIC and MBC also against two strains of the Gram-positive pathogen *Listeria monocytogenes* (LMG21264 and LMG13305, table 9) and against two strains of the Gram-negative pathogen *E. coli* (DSM 10973 and DSM 9025, data no shown).

	Listeria monocytogenes			
	MIC	MBC	MIC	MBC
	LMG21264	LMG21264	LMG13305	LMG13305
D576-0080	50 µM	100 µM	50 µM	50 µM
L011-0481	nd	nd	nd	nd
L011-0498	nd	nd	nd	nd
Molecule 8	nd	nd	nd	nd

Table 9. MIC and MBC values on *Listeria monocytogenes*. (nd=not detected)

In the case of *Listeria monocytogenes*, it was possible to calculate MIC and MBC values only for molecule D576-0080, thus resulting to be the molecule with highest activity also in this case as well, with bacteriostatic activity at 50 µM and bactericidal activity at 100 µM for the LMG21264 strain and bactericidal activity at a concentration of 50 µM for the LMG13305 strain.

The experiment conducted on the two pathogenic strains of *E. coli* was not successful, because both strains were found to be particularly resistant to PMBN (MIC> 64 µg/mL) and the molecules, in the absence of PMBN activity, were inactive against the bacterium.

4. CONCLUSION

Currently, many of the known β-sliding clamp inhibitors are peptides selected by virtual screening[330,332,334,337,339] and a variety of information has been obtained through *in vitro* analyses, e.g. SPR, including K_D, K_i, and IC_{50} values, but very often there is zero or little information on the *in vivo* activities of these compounds, including information on possible toxicity on eukaryotic cells. Very often these compounds have better activity against Gram-positive bacteria. Molecule 8[332], derived from a compound identified by fragment-based screening using x-ray crystallography, has known antibacterial activity against bacterial organisms, with better results against Gram-positive bacteria, and for this reason, for greater completeness of its studies, it was chosen as the bibliographic reference compound in our assays.

Following in the footsteps of the study carried out on the *E. coli* β' - σ^{70} interaction[338], a high-throughput platform combining sequential *in vivo* and *in vitro* assays was also applied in this study as an antibiotic discovery pipeline, applied to the search for small molecules capable of preventing the *E. coli* interaction between the β-sliding clamp protein and the α-subunit, proteins involved in bacterial DNA replication and part of the larger DNA polymerase III holoenzyme protein complex.

The interaction was successfully reproduced for the *in vivo* yBRET assay, where a yBRET strain was optimised for the identification of molecules preferentially targeting the β-sliding clamp, resulting in a pipeline with high-throughput screening of two different types of libraries: untargeted and target. While the former library consists of random small molecules (or molecules not selected on this target), the latter comes from *in silico* screening, where molecules were selected based on their physicochemical characteristics, to increase the probability to find molecules binding the β-sliding clamp target.

From the yBRET screening, a total of six hits were identified, three belonging to the untargeted library (C239-0797, F393-0093, and F726-1337) and three belonging to the targeted library (D479-0063, L862-1652, and L010-0518), capable of inhibiting the interaction of interest and all molecules belong to different chemical classes, which are also different from the chemical classes to which the already known β-sliding clamp inhibitors belong. Of the 3 molecules resulting from the screening of the targeted library, 29 structural analogs were also acquired (3 for D479-0063, 7 for L862-1652, and 19 for L010-0518), for a total of 35 molecules to be tested in subsequent assays. See table 6 for more information.

All candidates and the reference molecule were validated and characterised in two different *in vitro* experiments: the Protein Thermal Shift (PTS) test, to analyse the specificity of the molecules and their analogues for the β-sliding clamp, and the ELISA test to analyse the ability of the molecules to hamper the interaction of interest.

The molecules were subsequently also characterised for their ability to inhibit the bacterial growth of two non-pathogenic organisms, *E. coli* and *B. subtilis*, and for the compounds active and non-toxic towards *S. cerevisiae*, MIC values on pathogenic and non-pathogenic bacteria were also calculated, yielding values in the low to medium μM range. To determine the mode of action of the molecules, MBC assays were conducted.

Of the compounds identified by screening the untargeted library, C239-0797, F393-0093, and F726-1337, belonging to 3 different chemical classes, only the C239-0797 molecule stood out in the *in vitro* assays; in fact, in both PST and ELISA assays we saw good activity: in the first assay, it abundantly exceeds the temperature threshold that we set to identify molecules with a good affinity towards β-sliding clamp, in the second assay, on the other hand, although with a low percentage of inhibition of the interaction, it is a molecule that manages to bind the target, inhibiting the β-sliding clamp/consensus sequence interaction. On

the other hand, unfortunately, the molecule appears to be inactive at the concentrations tested against bacterial organisms.

Of the compounds identified by screening the targeted library, D479-0063, L862-1652, and L010-0518, which also belong to 3 different chemical classes and for which several analogues have been acquired, we find different situations. For the first class of compounds, D479-0063 and analogues, we have no relevant data both *in vitro* and *in vivo*, leading us to consider this class as a false positive result from the yBRET screening. This is different for the molecule L862-1652 and analogues, where good results were found in the *in vitro* assays. In the PTS, 3 structural analogues, but not the hit L862-1652, exceeded the temperature threshold that allows us to identify molecules with a good affinity towards β-sliding clamp and in particular, the molecules L862-1364 and L863-2005 inhibited the interaction in ELISA by more than 80%, thus allowing us to calculate IC_{50} values, which are 16.15 µM and 88.52 µM respectively. Again, unfortunately, the molecules were not shown to be active against bacteria. Finally, good results in both *in vitro* and *in vivo* assays were obtained with the class of molecules headed by the molecule L010-0518: 11 molecules bind specifically to β-sliding clamps in the PTS assay and of these, 5 are active in the ELISA assay. Of particular interest is the molecule D576-0080, which has the highest interaction inhibition value in ELISA, i.e. 100%, and an IC_{50} value of 58.91 µM. In this class of compounds, *in vivo*, three molecules, D576-0080, L011-0481, and L011-0498, were shown to completely inhibit the growth of *E. coli*, and only the first of the three was also capable of completely inhibiting the growth of *B. subtilis*. For these three molecules, MIC and MBC values were also calculated on pathogenic and non-pathogenic bacteria, obtaining values in the low-to-medium µM range, promising values compared to those of the already known β-sliding clamp inhibitor compounds.

Results obtained from the PTS assay highlighted three chemical classes that may bind to the target, while excluding chemical classes that could presumably be false positives of the yBRET assay.

The ELISA assay, optimised with the β-sliding clamp / consensus sequence strong interaction (with the NLuc protein as a carrier), partly confirmed the results obtained with the PTS assay. Some of the molecules that showed ability to bind the target can displace the interaction of interest, although with low potency, most likely due to the different K_D of the β-sliding clamp / α subunit and β-sliding clamp / consensus sequence interactions. In this assay, the molecules with the highest inhibitory activity belonged to the two chemical classes identified in the PTS assay, although none of the hits identified by the yBRET assay recurred in these assays. This could still be due to the different K_D of the two interactions used in the two different assays.

For the two strongest compounds in the ELISA test, L862-1364 and D576-0080, a binding hypothesis could be made. L862-1364, the most potent compound in the series of thiazo-pyrimidindione derivatives, is bound to subsite II. The most potent compound D576-0080, due to its elongated shape, can bind both subsites I and II. The pyrrolidine ring occupies the hydrophobic region of subsite II, similarly to the cyclohexyl-alanine of the optimised consensus peptide and the propyl chain of the thiazo-pyrimidinone L862-1364.

Molecules identified as active in binding the target or inhibiting the interaction in *in vitro* assays are probably unable to cross the bacterial membrane barrier and their reduced functionality against bacteria may be due to this reason. On the other hand, molecules capable of inhibiting bacterial growth were bactericidal against the organisms tested, but their antibacterial activity decreased in the absence of the membrane permeabiliser PMBN.

Further experiments will be conducted to better characterize the most potent chemical class here identified. These will include the purchase of new analogues to identify molecules with higher activity and for SAR

studies; the Isothermal Titration Calorimetry, to quantify the affinity to the target; and the *in vitro* replication assay, as functional validation. These results will be used for structural design of more potent inhibitors.

In parallel, these new antimicrobials will be assayed for their antimicrobial activity against other bacterial strains, including the 'ESKAPE' bacterial pathogens (*Enterococcus faecium*, *Staphylococcus aureus*, *Klebsiella pneumoniae*, *Acinetobacter baumanii*, *Pseudomonas aeruginosa* and *Enterobacter species*) and other bacteria that are resistant to currently available antibiotics.

5. MATERIALS AND METHODS

- **Chemicals**

D(+)-galactose and D(+)-raffinose were purchased from ACROS Organics (Geel, Belgium). Yeast nitrogen base without amino acids and Bacto peptone were purchased from BD Biosciences (Franklin lakes, NJ). D(+)-glucose, Bacto yeast extract, dimethylsulfoxyde (vehicle control),3,3'5-triiodo-L-thyronine sodium salt (T3), and the different amino acids complements were purchased from Sigma (St. Louis, MO).

- **Reagents**

Coelenterazine h was purchased from Interchim (Montluçon, France) and Nano-Glo Luciferase Assay Substrate from Promega (Madison, WI). The antibodies used are anti-Myc (#ab1261; Abcam, Cambridge, UK).

- **Equipment**

TriStar² LB942 Multidetection Microplate Reader luminometer (Berthold Technologies, Bad Wildbad, Germany) microplate reader was used with the following emission filters: • NLuc: counting time, 2.00 s; emission filter (No. 39450), 480 nm (±10 nm); • YFP: counting time, 2.00 s; emission filter (No.39451), 530 nm (±12.5 nm). Measurement operation is performed by well, and each plate is read three times in a cycling manner.

Affinity chromatography for purification was performed in a pure ÄKTA system and a 5 mL HiTrapQFF nickel column was used.

QuantStudio™ 3 Real-Time PCR Systems.

- **Strains**

S. cerevisiae erg6 yeast strain (BY4742 background: MATa; his3Δ1; leu2Δ 0; met15Δ 0; ura3Δ 0; YML008c::kanMX4) was obtained from Open Biosystems (Huntsville, AL, USA) and employed in the yBRET system.

E. coli DH10B™ T1R strain (F- mcrA Δ(mrr-hsdRMS-mcrBC) ϕ80lacZΔM15 ΔlacX74 recA1 endA1 araD139 Δ(ara,leu)7697 galU galK - rpsL nupG tonA) (Invitrogen); exploited for vector construction, bacterial growth inhibition assay, MIC and MBC assays.

E. coli BL21-CodonPlus (DE3)-RIL strain (F– ompT hsdS(rB – mB –) dcm+ Tetr gal λ (DE3) endA Hte [argU ileY leuW Camr); exploited for protein overexpression (Agilent Technologies). These competent cells carry extra copies of the arg U, ile Y, and leu W tRNA genes. Te tRNAs encoded by these genes recognize the AGA/AGG (arginine), AUA (isoleucine), and CUA (leucine) codons, respectively.

E. coli BL21(DE3) pKJE7 strain F — , ompT, hsdSB (rB — mB —), gal, dcm; DE3 lysogen contains T7 polymerase upon IPTG induction. This strain is deficient of lon and omp-t proteases and is therefore suitable for the expression of non-toxic proteins. In particular, this strain could co-express the plasmid of interest and the plasmid and $pKJE_7$ (Takara3). The two different plasmids are designed to enable the efficient expression of multiple molecular chaperones known to work cooperatively in the protein folding process.

E. coli Origami(DE3)pLysS strain Δ(ara-leu)7697 ΔlacX74 ΔphoA PvuII phoR araD139 ahpC galE galK rpsL F'[lac^+ $lacI^q$ pro] (DE3) gor522::Tn10 trxB pLysS (Cam^R, Str^R, Tet^R); these host strains are K-12 derivates that have mutations in both the thioredoxin reductase (trxB) and glutathione reductase (gor) genes.

B. subtilis WB800N strain (nprE aprE epr bpr mpr::ble nprB::bsr Δvpr wprA::hyg cm::neo; NeoR); exploited for bacterial growth inhibition assay, MIC and MBC assays.

S. cerevisiae W303-1A strain (leu2-3,112 trp1-1 can1-100 ura3-1 ade2-1 his3-11, 15) was used for growth inhibition assay.

L. monocytogenes LMG 21264, and *L. monocytogenes* LMG 13305 were acquired from Belgian co-ordinated collections of Micro-organisms.

E. coli DSM 10973, and *E. coli* DSM 9025 were acquired from Leibniz Institute DSMZ-German Collection of Microorganisms and Cell Cultures.

- **Vectors**

All sequences used in this study were amplified with PCR and inserted in frame with the donor or the acceptor using *CpoI* restriction enzyme digestion and DNA ligation. The centromeric vectors p415 (*LEU2*, *GAL1* inducible promoter) and p416 (*URA3*, *GPD* constitutive promoter) were used to express the chimeric proteins[345]. *TRP1* selectable marker gene cannot be employed with *erg6* mutant strain, because *trp1-erg6* double mutant is synthetic lethal. Donor proteins were cloned into p415, and acceptor proteins were cloned into p416. Both C- or N-terminal fusion vectors are available upon request. Vector p190 (*LEU2*, *TEF* constitutive promoter) and p215 (*URA*, *GAL1*) were used to express chimeric proteins in the donor saturation assay.

pET 28b (+) was used for: i) the expression of *dnaN* gene in *E. coli* as fusion with MycTag at the C-terminal end and N-terminal His Tag®/thrombin/T7•Tag® configuration plus an optional C-terminal His Tag sequence, respectively. ii) the expression of *dnaE* gene in *E. coli* as a fusion with N-terminal His Tag®/thrombin/T7•Tag® configuration plus an optional C-terminal His Tag sequence.

pET 28a (+) was used for the expression of consensus sequence in *E. coli* as a fusion with Nluc sequence at the C-terminal and an N-terminal His•Tag®/thrombin/T7•Tag® configuration plus an optional C-terminal His•Tag sequence.

- **BRET calculation and screening analysis protocol**

The BRET ratio was calculated by dividing the signal measured at 530 nm by the signal measured at 480 nm. Then, the BRET signal was calculated as the BRET ratio subtracted by the BRET background ratio (obtained when the donor protein was expressed alone) and multiplied by 1000 to express results in milliBRET (mBRET): BRET = (BRET ratio −Background BRET ratio) x 1000[98].

The assortment rationale takes into account three factors: (i) an interaction inhibition of at least 15% on average, compared to the untreated plate-specific controls; (ii) a median mBRET percentage of below 85% compared to the median calculated on the non-treated plate-specific controls: (iii) an SSMD statistic considered to be at a minimum "weak inhibition" (SSMD is the ratio of the mean to the standard deviation of the difference between a test compound and a negative reference group with no specific inhibition/activation effects).

- **Small molecule libraries**

Molecule 8 was purchased from ChemDiv (San Diego, CA USA).

Two libraries were available in our laboratory: *Australia Compound Library-1*, and *National Cancer Institute* (NCI), which contained compounds of synthetic and natural origin.

The compounds of *Australia Compound Library-2* were selected through *in silico* screening (details in paragraph 3.2).

- **Expression and purification of β-sliding clamp and NLuc-consensus and Expression of sequence α (736-1160) subunit α subunit full length**

- **β-sliding clamp and NLuc-consensus sequence**

Induction was performed in *E. coli* BL21-CodonPlus (DE3)-RIL strain for both the protein, but for β-sliding clamp the induction was carried out overnight at 20 °C, while, for NLuc-consensus sequence the induction was carried out for 4 hours at 30 °C. Both inductions were performed with the addition of 1 mM isopropyl-b-D-thiogalactopyranoside (IPTG), followed by sonication to lyse cell. The soluble proteins were then purified by affinity chromatography using a pure ÄKTA system with HiTrapQFF nickel column (5 mL, GE Healthcare). 50 mL of supernatant from 1 L of bacterial lysate were loaded onto the column previously equilibrated in buffer A (Tris-HCl 25 mM pH 8; NaCl 0.3 M; imidazole 20 mM), and elution of the protein was carried out with 30 mL imidazole linear gradient to 500 mM in the same buffer. Finally, 2 mL fractions are collected and analysed by UV-vis spectrophotometry and SDS-PAGE.

- **α (736-1160) subunit**

Induction was performed in *E. coli* BL21(DE3) pKJE7 strain with overnight induction at 20 °C and with the addition of 1 mM isopropyl-b-D-thiogalactopyranoside (IPTG), and 0.5 mg/mL of L-arabinose, followed by sonication to lyse cell. The chaperone genes were downstream of *araB* promoter. The soluble protein was then purified by affinity chromatography using a pure ÄKTA system with HiTrapQFF nickel column (5 mL, GE Healthcare). 50 mL of supernatant from 1 L of bacterial lysate was loaded onto the column previously equilibrated in buffer A (Tris-HCl 25 mM pH 8; NaCl 0.3 M; imidazole 20 mM), and elution of the protein was carried out with 30 mL imidazole linear gradient to 500 mM in the same buffer. After affinity chromatography, anionic exchange was carried out utilizing two different buffers were used for this purpose: i) Tris-HCl 25 mM pH 8; ii) Tris-HCl 25 mM pH 8 + 2 M NaCl. The purity of the proteins was checked on SDS-PAGE.

- **α subunit full length**

Induction was performed in *E. coli* BL21-CodonPlus (DE3)-RIL strain with overnight induction at 20 °C and with the addition of 1 mM isopropyl-b-D-thiogalactopyranoside (IPTG), followed by sonication to lyse cell. The soluble protein was then purified by affinity chromatography using a pure ÄKTA system with HiTrapQFF nickel column (5 mL, GE Healthcare). 50 mL of supernatant from 1 L of bacterial lysate was loaded onto the column previously equilibrated in buffer A (Tris-HCl 25 mM pH 8; NaCl 0.3 M; imidazole 20 mM), and elution of the protein was carried out with 30 mL imidazole linear gradient to 500 mM in the same buffer. After affinity chromatography, the protein was subjected to anion exchange chromatography and was used two different buffers: i) Tris-HCl 25 mM pH 8; ii) Tris-HCl 25 mM pH 8 + 2 M NaCl. After this step, the protein was subjected to gel filtration chromatography on a Superdex 200 Increase 10/300 GL column (24 ml, GE Healthcare). Bovine serum albumin (66 kDa), ovalbumin (44.3 kDa), and lysozyme (14.5 kDa) were used as calibration standards. The purity of the protein was checked on SDS-PAGE.

- **Protein Thermal Shift assay**

In each well of the RP, LF, SEMI Sk, 96 well plate (0.2mL) (#AB19700 from BIOplastics) were added 5 µL of Ptrotein Thermal Shift™ Buffer. 12.5 µL of 4 µg of β-sliding clamp in 20 mM Tris-HCl pH 7.5, 0.5 mM EDTA was incubated with 1 µl of the compounds at 100 µM (or DMSO as control) for 1 hour at 37 °C and added to the wells. The Protein Thermal Shift™ Dye was diluted to 8X in 20 mM Tris-HCl pH 7.5, 0.5 mM EDTA, and 2.5 µl of the solution was added to each well. After pipetting up and down 10 times to mix well, the plate is sealed with MicroAmp® Optical Adhesive Film, spinned at 1000 rpm for 1 minute and placed on ice, protected from light. Using QuantStudio™ Design & Analysis Software, the file of execution of the experiment was set up and by QuantStudio™ 3 Real-Time PCR Systems the experiment was conducted. The data related to the melting temperature, are analysed by Protein Thermal Shift™ Software v1.4. Each experiment was performed in quadruplicate. In total have been prepared: • 4 replicates of each reaction; • 4 replicates of no protein controls (NPCs); • 4 replicates of ligand only controls (LOCs).

- **ELISA assay**

The NLuc-consensus sequence was diluted to 250 nM in phosphate-buffered saline (PBS), and 100 µl of the solution was added into NUNC Maxisorp microtiter plate wells. Following overnight incubation at 4 °C wells were washed three times with 300 µl of PBS and blocked with 400 µl of 1% (w/v) BSA in PBS at RT for 2 h. Plates were then washed three times with wash buffer (PBS, 0.3% (v/v) Tween-20). 100 µl of 250 nM β-sliding clamp-MycTag diluted in PBS was incubated with 3.5 µl of the compounds at different concentrations (or DMSO as control) for 1 hour at 37 °C and added to the wells followed by incubation at RT for 1 h. Wells were washed three times with 300 µl of wash buffer, 100 µL of goat anti-Myc tag antibody (1:50000 in PBS) were added, and the plate was incubated at RT for 1 h. Interactions were detected by the addition of 100 µl of ABTS substrate to each well. The signal was measured, after 15 minutes of incubation at 30°C, reading absorbance at 415 nm using a microplate reader (TriStar² LB 942, Berthold Technologies). The inhibitory activity of each compound was then calculated as IC_{50} value.

- **Antimicrobial activity**

The antimicrobial activity of hit compounds was evaluated by monitoring bacterial growth in the presence of two different molecule concentrations. Bacteria were grown at exponential phase before growth inhibition test and then diluted to OD_{600} nm = 0.006. W303-1A yeast strain was grown in YPD (Yeast peptone Dextrose) at 30 °C until OD_{600} nm = 0.5 before growth inhibition assay. Bacterial (or yeast) growth was monitored for 8 h in the presence of molecules dissolved in DMSO, or of an equivalent quantity of DMSO as negative control (5% DMSO final concentration). The assay was conducted in triplicate in a 96-well plate by monitoring the growth of the cells every 30 minutes, reading the absorbance with a microplate reader (TriStar² LB 942, Berthold Technologies). Polymyxin B Nonapeptide used on Gram-negative bacteria was purchased from Sigma-Aldrich (Saint Louis, USA).

- **Minimum Inhibitory Concentration (MIC) And Minimum Bactericidal Concentration (MBC)**

The antimicrobial activity of D576-0080, L011-0498, and L011-0481 was determined by the minimum inhibitory concentration (MIC) assay. The assays were performed in 96-well microplates in 20% MH broth in PBS. A mid-log phase bacterial suspension at 3×10^5 CFU/mL in 20% MH broth was used, and the microplates were incubated at 37 ˚C for 24 hours. The MIC value was taken as the lowest concentration of compound that results in complete inhibition of visible bacterial growth after an appropriate incubation time. Results

are derived from at least two independent experiments performed in triplicate. For *Listeria monocytogenes* strains, the assay was conducted in LB broth.

For minimum bactericidal concentration (MBC) 8 µL from each well is taken and deposited on Petri dish containing MH agar medium. Subsequently, plates are incubated for 24 hours and growth observed. The MBC value was taken as the lowest concentration of an antibacterial agent that results in killing a particular bacterium after an appropriate incubation time.

- **Statistical analysis**

To calculate IC_{50} for inhibitory activity in ELISA assay was conducted in triplicate, using at least ten different compound concentrations. Data were analysed in Prism (GraphPad Software Inc.) using nonlinear regression curve fitting.

Student T-test was used to find significant differences when comparing compound inhibitory activities.

Table 10. List of oligonucleotides used in this study.

Primer name (restriction enzyme	Sequence (5'→3') restriction enzyme underlined
β-sliding clamp FW (*BamHI*)	TAAATATAAAGGATCCATGAAATTTACCGTAGAACGTGAGC
β-sliding clamp RE no stop codon (*EcoRI*)	AATTATTTTAGAATTCCAGTCTCATTGGCATGACAACAT
β-sliding clamp FW (*EcoRI*)	TAAATATAAAGAATTCATGAAATTTACCGTAGAACGTGAGC
β-sliding clamp RE stop (*XhoI)*	AATTATTTTACTCGAGtcaCAGTCTCATTGGCATGACAACAT
β-sliding clamp RE stop (*SalI*)	AATTATTTTAGTCGACTCACAGTCTCATTGGCATGACAACAT
β-sliding clamp FW (*CpoI*)	TAAATATAAACGGTCCGATGAAATTTACCGTAGAACGTGAGC
β-sliding clamp mutagenesis internal CpoI site	TGAGCGGTCCATTAGGTGGTC
β-sliding clamp mutagenesis internal CpoI site	GACCACCTAATGGACCGCTCA
β-sliding clamp for cloning in pET 28 vector FW (*NcoI)*	TAAATATAAACCATGGCGGTCCGATGAAATTTACCGTAG
β-sliding clamp with partial MycTag RE	TCCTCGCTAATCAGCTTCTGTTCCGGACCGATCAGTCTCATTGG
MycTag for fusion (*NotI* and *CpoI*)	AATTATTTTAGCGGCCGCCAGGTCTTCCTCGCTAATCAGCTTCTGTTCCGG
α to amplified from aa 736 FW *(CpoI)*	TAAATATAAACGGTCCGATGATCAACGCTGAACTGGCGAT
α (736-1160) RE no stop codon *(CpoI)*	AATTATTTTACGGACCGATGTCAAACTCCAGTTCCACCTGC
α (736-1160) RE with stop codon *(CpoI)*	AATTATTTTACGGACCGTCAGTCAAACTCCAGTTCCACCTGC
Mutagenesis QADMF → QLDLF of α FW	GAAGCTATCGGTCAGCTGGATCTGTTCGGCGTGCTGG
Mutagenesis QADMF → QLDLF of α RE	CCAGCACGCCGAACAGATCCAGCTGACCGATAGCTTC
Mutagenesis QADMF → AAAKK of α FW	CGCCTTTTTTCGCGGCCGCACCGATAGCTTCCGCTTTCG
Mutagenesis QADMF → AAAKK of α RE	GCGGCCGCGAAAAAAGGCGTGCTGGCCGAAGAG
α (1-1160) for In-Fusion cloning in pET28 (*NdeI/NotI)* FW	CGCGCGGCAGCCATATGATGTCTGAACCACGTTTCGTAC
α (1-1160) for In-Fusion cloning in pET28 (*NdeI/NotI)* RE	TGCTCGAGTGCGGCCGCTTAGTCAAACTCCAGTTCCACCT
consensus sequence FW stop codon	GTCCGATCGGTCAGTTGGATTTGTTCGGCGTGTGACG
consensus sequence RE stop codon	GACCGTCACACGCCGAACAAATCCAACTGACCGATCG
consensus sequence FW no stop codon	GTCCGATGATCGGTCAGTTGGATTTGTTCGGCGTGATCG
consensus sequence RE no sto codon	GACCGATCACGCCGAACAAATCCAACTGACCGATCATCG
Mutagenesis QLDLF→QLDGG FW stop codon	GTCCGATCGGTCAGTTGGATGGTGGTGGCGTGTGACG
Mutagenesis QLDLF→QLDGG RE stop codon	GACCGTCACACGCCACCACCATCCAACTGACCGATCG

Table 11. Structures of molecules tested in both *in vitro* and in *vivo* assays. The molecules designated with an asterisk are the hits identified after the yBRET assay. Specifically, the first three are from screening on *Compounds Australia Library-1*, and the other three are from screening on *Compounds Australia Library-2*, and the molecules following the molecules with an asterisk are their structural analogs. Molecule 8 (in red) is the reference compound.

Molecule	Structure
C239-0797*	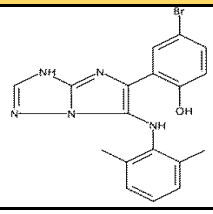
F393-0093*	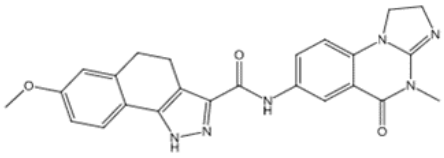
F726-1337*	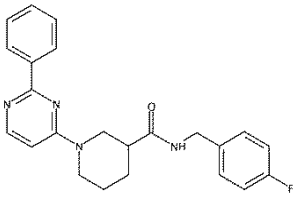
D479-0063*	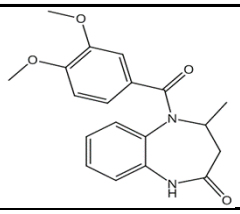
D428-0018	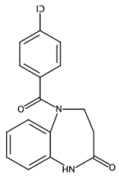
D428-0071	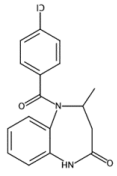
D479-0091	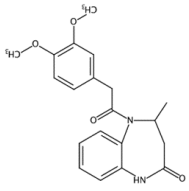

L862-1652*	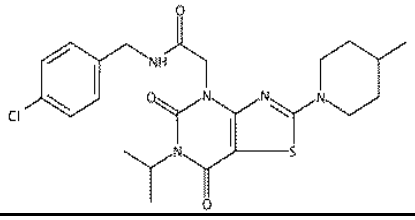
L862-1364	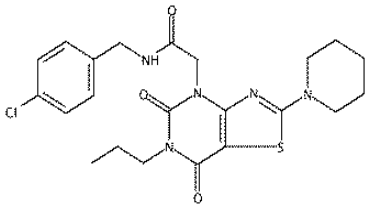
L862-1373	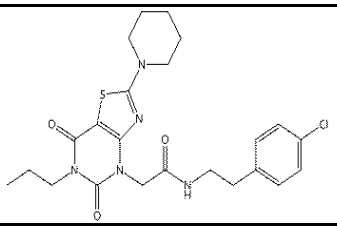
L862-1593	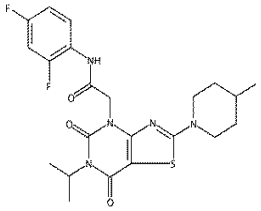
L862-1654	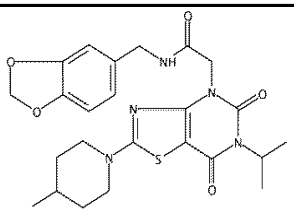
L863-2005	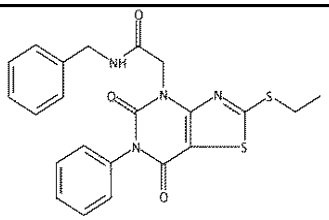
L863-2164	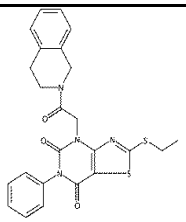
L863-2310	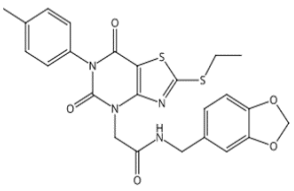

L010-0518*	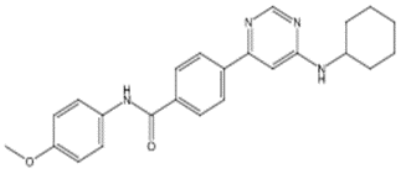
D430-0343	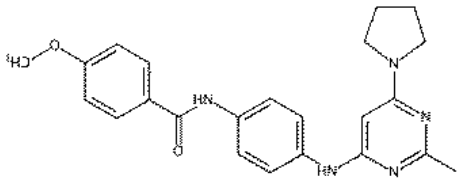
D576-0080	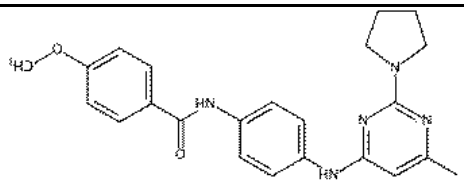
L010-0068	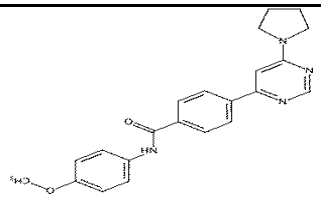
L010-0480	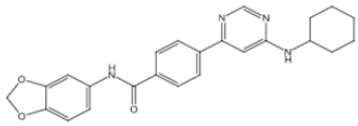
L010-0495	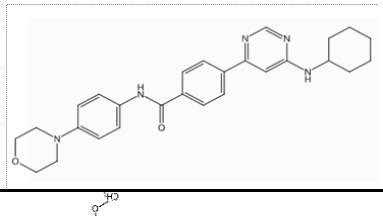
L010-0504	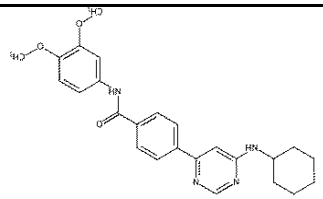
L010-0548	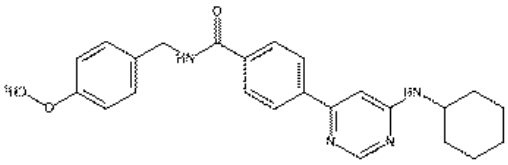
L011-0481	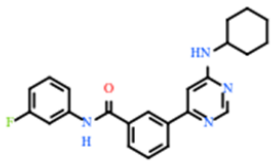
L011-0498	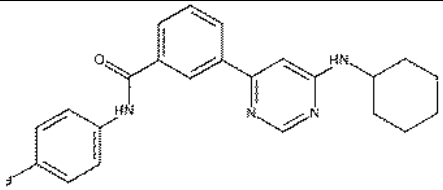

L011-0513	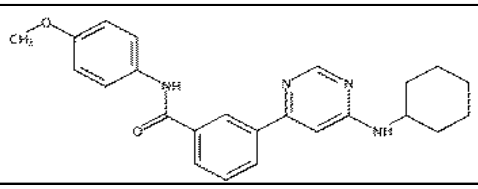
L367-0038	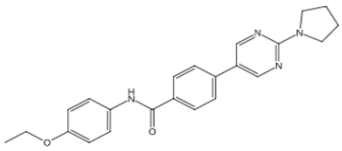
L367-0072	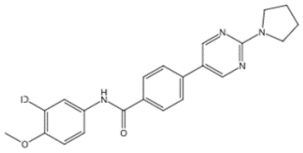
L367-0497	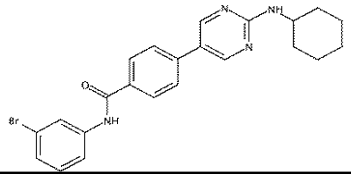
L533-0208	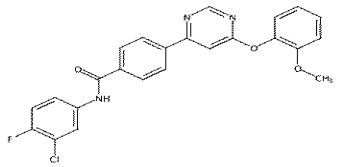
L533-0362	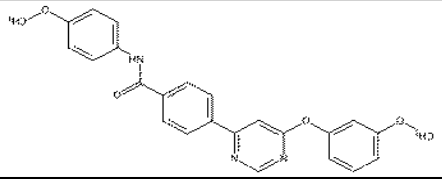
L534-0053	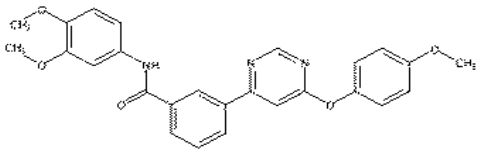
P510-0634	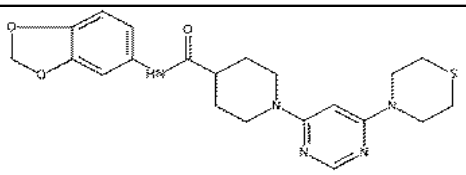
P510-0674	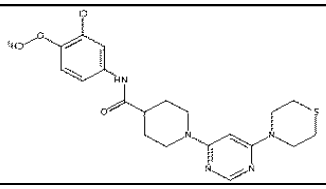
P843-0212	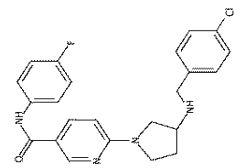
Molecule 8	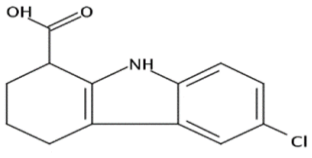

6. Abbreviations

hGH human growth hormone

2P2I Protein–Protein Interaction Inhibition

ADME Absorption Distribution Metabolism Excretion

AMEs Aminoglycoside-modifying enzymes

AMR Antimicrobial Resistance

ATP Adenosine Triphosphate

BFP Blue Fluorescent Protein

bp base pairs

BRET Bioluminescence Resonance Energy Transfer

BSA Bovine Serum Albumin

CBM Clamp-binding motif

CFP Cyan Fluorescent Protein

CFU Colony-Forming Unit

CGM Cyclohexyl-griselimycin

Cha Cyclohexyl-L-alanyl group

CNS Central Nervous System

CRISPR-Cas Clustered Regularly Interspaced Short Palindromic Repeats

Da Dalton

DHPS Dihydropteroate Synthase

DMSO Dimethyl Sulfoxide

DNA Deoxyribonucleic Acid

Dr. PIAS Druggable Protein-protein Interaction Assessment System

dsDNA double-stranded DNA

DUE DNA unwinding element

EDF Extracellular Death Factor

EDTA Ethylenediaminetetraacetic Acid

ELISA Enzyme-Linked Immunosorbent Assay

EMA European Medicines Agency

FBDD Fragment screening and Fragment-Based Drug Design

FDA Food and Drug Administration

FIC First-in-class

FLIM Fluorescence-Lifetime Imaging Microscopy

FP Fluorescence Polarization

FRET Förster Resonance Energy Transfer

gal Galactose

GAL1 Galactose-Inducible promoter

GFP Green Fluorescent Protein

GPCRs G protein-coupled *receptors*

GScore GlideScore

gyr gyrase

HE Holoenzyme

hGHbp human Growth Hormone bound receptor

His-Tag Histidine tag

HIV Human Immunodeficiency Virus

HPV Human Papillomavirus

HSQC Heteronuclear Single Quantum Correlation

HT High-Throughput

HTS High-Throughput Screening

i.e. in example

IAP Inhibitors of Apoptosis

IC_{50} Half Maximal Inhibitory Concentration

IL-2 Interleukin-2

iPPI-DB inhibitors of Protein-Protein Interaction Database

iPS induced Pluripotent Stem cell

IPTG Isopropyl β- d-1-thiogalactopyranoside

ITC Isothermal Titration Calorimetry

LB Luria-Bertani

LM Linear Motif

MBC Minimum Bactericidal Concentration

mBRET milliBRET

MD Molecular Dynamics

MDR Multidrug Resistant

MGM Methyl-Griselimycin

MH Mueller Hinton

MIC Minimum Inhibitory Concentration

MSCS Multiple Solvent Crystal Structure

NAD Nicotinamide Adenine Dinucleotide

NFC Near Field Communication

NIHCM Foundation Health Care Management Research and Educational Foundation

NLuc NanoLuc luciferase

NMEs New Molecular Entities

NMR Nuclear Magnetic Resonance

PBS Phosphate-Buffered Saline

PDD Phenotypic Drug Discovery

PFAM20 Protein Families (database)

PMBN Polymyxin B Nonapeptide

PPIs Protein-Protein Interactions

PTS Protein Thermal Shift

QDs Quantum Dots

RFP Red Fluorescent Protein

Rluc Renilla luciferase

RNA Ribonucleic Acid

RND Resistance-Nodulation-Division

RPA Replication Protein A

RPD RNA Polymerase Domain

RT Room Temperature

SAR Structure–Activity Relationship

SCOP19 Structural Classification of Proteins

SICLOPPS Split-Intein Circular Ligation Of Peptides and Proteins

SPR Surface Plasmon Resonance

SSB Strand Binding Proteins

ssDNA single-strand DNA

STD-NMR Saturation-Transfer Difference NMR

TDD Target-based Drug Discovery

Ter Termination sites

Tm Melting Temperature

TS Thermal Shift

USAN United States Adopted Names

UV Ultraviolet

wt wild type

yBRET yeast BRET

YFP Yellow Fluorescent Protein

YPD Yeast peptone Dextrose

ZBD zinc-binding domain

7. Bibliography

1. Chan HCS, Shan H, Dahoun T, Vogel H, Yuan S. Advancing Drug Discovery via Artificial Intelligence. *Trends Pharmacol Sci*. 2019;40(8):592-604. doi:10.1016/j.tips.2019.06.004

2. Eder J, Herrling PL. Trends in Modern Drug Discovery. *Handb Exp Pharmacol*. 2015;(January):251-263. doi:10.1007/164

3. Schrör K. Acetylsalicylic acid. 2008.

4. Lee JA. Foreword: Phenotypic Drug Discovery: A Personal Perspective. *RSC Drug Discov Ser*. 2021;2021-Janua(77):IX-XX. doi:10.1039/9781839160721-FP009

5. Moffat JG, Vincent F, Lee JA, Eder J, Prunotto M. Opportunities and challenges in phenotypic drug discovery: An industry perspective. *Nat Rev Drug Discov*. 2017;16(8):531-543. doi:10.1038/nrd.2017.111

6. Swinney DC, Anthony J. How were new medicines discovered? *Nat Rev Drug Discov*. 2011;10(7):507-519. doi:10.1038/nrd3480

7. Shi Y, Inoue H, Wu JC, Yamanaka S. Induced pluripotent stem cell technology: a decade of progress. *Nat Rev Drug Discov*. 2017;16(2):115-130. doi:10.1038/nrd.2016.245.Induced

8. Fellmann C, Gowen BG., Lin P-C, Doudna JA., Corn JE. Cornerstones of CRISPR-Cas in drug development and therapy. *Nat Rev Drug Discov*. 2017;16(2):89-100. doi:10.1038/nrd.2016.238.Cornerstones

9. Overington JP, Al-Lazikani B, Hopkins AL. How many drug targets are there ? PubMed Commons. *Nat Rev Drug Discov*. 2006;5(12):10. http://www.ncbi.nlm.nih.gov/pubmed/17139284%0Ahttp://dx.doi.org/10.1038/nrd2199.

10. Weber A, Casini A, Heine A, et al. Unexpected Nanomolar Inhibition of Carbonic Anhydrase by COX-2-Selective Celecoxib: New Pharmacological Opportunities Due to Related Binding Site Recognition. *J Med Chem*. 2004;47(3):550-557. doi:10.1021/jm030912m

11. Roskoski R. Properties of FDA-approved small molecule protein kinase inhibitors: a 2022 update. *Pharmacol Res*. 2021;175(December 2021):106037. doi:10.1016/j.phrs.2021.106037

12. NIHCM 24 pp (National Institute for Health Care Management Research and Educational Foundation 2002). NIHCM 24 pp (National Institute for Health Care Management Research and Educational Foundation, 2002).

13. Stumpf MPH, Thorne T, De Silva E, et al. Estimating the size of the human interactome. *Proc Natl Acad Sci U S A*. 2008;105(19):6959-6964. doi:10.1073/pnas.0708078105

14. Venkatesan K JR, Vazquez A, Stelzl U, Lemmens I, Hirozane-Kishikawa T, Hao T. An empirical framework for binary interactome mapping. *Nat Methods*. 2009;6(1):83-90. doi:10.1038/nmeth.1280.An

15. Belitsky M, Avshalom H, Erental A, et al. The Escherichia coli Extracellular Death Factor EDF Induces the Endoribonucleolytic Activities of the Toxins MazF and ChpBK. *Mol Cell*.

2011;41(6):625-635. doi:10.1016/j.molcel.2011.02.023

16. Letai A, Bassik MC, Walensky LD, Sorcinelli MD, Weiler S, Korsmeyer SJ. Distinct BH3 domains either sensitize or activate mitochondrial apoptosis, serving as prototype cancer therapeutics. *Cancer Cell*. 2002;2(3):183-192. doi:10.1016/S1535-6108(02)00127-7

17. London N, Raveh B, Schueler-Furman O. Druggable protein-protein interactions - from hot spots to hot segments. *Curr Opin Chem Biol*. 2013;17(6):952-959. doi:10.1016/j.cbpa.2013.10.011

18. Nooren IMA, Thornton JM. NEW EMBO MEMBER ' S REVIEW Diversity of protein ± protein interactions. 2003;22(14).

19. Monod J, Wyman J, Changeux JP. On the nature of allosteric transitions: A plausible model. *J Mol Biol*. 1965;12(1):88-118. doi:10.1016/S0022-2836(65)80285-6

20. Goodsell DS, Olson AJ. Structural symmetry and protein function. *Annu Rev Biophys Biomol Struct*. 2000;29:105-153.

21. Scott DE, Bayly AR, Abell C, Skidmore J. Small molecules, big targets: Drug discovery faces the protein-protein interaction challenge. *Nat Rev Drug Discov*. 2016;15(8):533-550. doi:10.1038/nrd.2016.29

22. Moreira IS, Fernandes PA, Ramos MJ. Hot spots—A review of the protein – protein interface determinant amino-acid residues. 2007;(October 2006):803-812. doi:10.1002/prot

23. Smith MC, Gestwicki JE. Features of protein – protein interactions that translate into potent inhibitors : topology , surface area and affinity. 2012;14(July):1-20. doi:10.1017/erm.2012.10

24. Sheng C, Dong G, Miao Z, Zhang W, Wang W. State-of-the-art strategies for targeting protein-protein interactions by small-molecule inhibitors. *Chem Soc Rev*. 2015;44(22):8238-8259. doi:10.1039/c5cs00252d

25. Clackson T, Wells JA. A hot spot of binding energy in a hormone-receptor interface. *Science (80-)*. 1995;267(5196):383-386. doi:10.1126/science.7529940

26. Bogan AA, Thorn KS. Anatomy of Hot Spots in Protein Interfaces. 1998.

27. London N, Raveh B, Movshovitz-attias D, Schueler-furman O. Can self-inhibitory peptides be derived from the interfaces of globular protein – protein interactions? 2010:3140-3149. doi:10.1002/prot.22785

28. Klepeis JL, Lindorff-larsen K, Dror RO, Shaw DE. Long-timescale molecular dynamics simulations of protein structure and function. 2009. doi:10.1016/j.sbi.2009.03.004

29. Mattos C, Ringe D. Locating and characterizing binding sites on proteins. *Nature*. 1996;14:595-599.

30. Hajduk PJ, Huth JR, Fesik SW. Druggability Indices for Protein Targets Derived from NMR-Based Screening Data. 2005:2518-2525.

31. Shuker SB, Hajdilk PJ, Meadows RP, Fesik SW. Discovering High-Affinity Ligands for Proteins: SAR by NMR. *Science (80-)*. 1996;274:1531-1534.

32. Kozakov D, Hall DR, Chuang G, et al. Structural conservation of druggable hot spots in

protein – protein interfaces. 2011;108(33). doi:10.1073/pnas.1101835108

33. Metz A, Christopher P, Kopitz H, Pfei S, Baringhaus K, Gohlke H. Hot Spots and Transient Pockets : Predicting the Determinants of Small-Molecule Binding to a Protein À Protein Interface. 2012;(iii):120-133.

34. Fischer G, Rossmann M, Hyvönen M. Alternative modulation of protein-protein interactions by small molecules. *Curr Opin Biotechnol*. 2015;35:78-85. doi:10.1016/j.copbio.2015.04.006

35. Flygare JA, Beresini M, Budha N, et al. Discovery of a potent small-molecule antagonist of inhibitor of apoptosis (IAP) proteins and clinical candidate for the treatment of cancer (GDC-0152). *J Med Chem*. 2012;55(9):4101-4113. doi:10.1021/jm300060k

36. Vu B, Wovkulich P, Pizzolato G, et al. Discovery of RG7112: A small-molecule MDM2 inhibitor in clinical development. *ACS Med Chem Lett*. 2013;4(5):466-469. doi:10.1021/ml4000657

37. Ding Q, Zhang Z, Liu J-J, et al. Discovery of RG7388, a Potent and Selective p53−MDM2 Inhibitor in Clinical Development. *J Med Chem*. 2013;56:5976-5983.

38. Zhao Y, Yu S, Sun W, et al. A potent small-molecule inhibitor of the MDM2-p53 interaction (MI-888) achieved complete and durable tumor regression in mice. *J Med Chem*. 2013;56(13):5553-5561. doi:10.1021/jm4005708

39. Wang S, Sun W, Zhao Y, et al. SAR105838: An optimized inhibitor of MDM2-p53 interaction that induces complete and durable tumor regression. *Cancer Res*. 2015;74(20):5855-5865. doi:10.1158/0008-5472.CAN-14-0799.SAR405838

40. Arkin MMR, Wells JA. Small-molecule inhibitors of protein-protein interactions: Progressing towards the dream. *Nat Rev Drug Discov*. 2004;3(4):301-317. doi:10.1038/nrd1343

41. Giordanetto F, Schäfer A, Ottmann C. Stabilization of protein-protein interactions by small molecules. *Drug Discov Today*. 2014;19(11):1812-1821. doi:10.1016/j.drudis.2014.08.005

42. Merdanovic M, Mönig T, Ehrmann M, Kaiser M. Diversity of allosteric regulation in proteases. *ACS Chem Biol*. 2013;8(1):19-26. doi:10.1021/cb3005935

43. Hammoudeh DI, Daté M, Yun MK, et al. Identification and characterization of an allosteric inhibitory site on dihydropteroate synthase. *ACS Chem Biol*. 2014;9(6):1294-1302. doi:10.1021/cb500038g

44. Higueruelo AP, Jubb H, Blundell TL. Protein-protein interactions as druggable targets: Recent technological advances. *Curr Opin Pharmacol*. 2013;13(5):791-796. doi:10.1016/j.coph.2013.05.009

45. Higueruelo P, Schreyer A, Bickerton GRJ, Pitt WR, Groom CR, Blundell TL. Atomic Interactions and Profile of Small Molecules Disrupting Protein – Protein Interfaces : the TIMBAL Database. 2009;(1):457-467. doi:10.1111/j.1747-0285.2009.00889.x

46. Bouzidi S, Basse MJ, Morelli X, Roche P, Chetrit B. 2P2Idb : a structural database dedicated to orthosteric modulation of protein – protein interactions. 2013;41(November 2012):824-827. doi:10.1093/nar/gks1002

47. Labbé CM, Laconde G, Kuenemann MA, Villoutreix BO, Sperandio O. iPPI-DB: A manually

curated and interactive database of small non-peptide inhibitors of protein–protein interactions. *Drug Discov Today*. 2013. doi:10.1016/j.drudis.2013.05.003

48. Lo MC, Aulabaugh A, Jin G, et al. Evaluation of fluorescence-based thermal shift assays for hit identification in drug discovery. *Anal Biochem*. 2004;332(1):153-159. doi:10.1016/j.ab.2004.04.031

49. Navratilova I, Hopkins AL. Emerging role of surface plasmon resonance in fragment-based drug discovery. *Future Med Chem*. 2011;3(14):1809-1820. doi:10.4155/fmc.11.128

50. Lepre CA, Connolly PJ, Moore JM. (, 2010). In: Merz, K. M. Jr., Ringe, D. & Reynolds CH, ed. *Drug Design*. Cambridge Univ. Press; :41–58.

51. Davies TG, Tickle IJ. Fragment Screening Using X-Ray Crystallography. *Top Curr Chem*. 2012;317:33-59. doi:10.1007/128

52. Bruce Turnbull W, Daranas AH. On the Value of c: Can Low Affinity Systems Be Studied by Isothermal Titration Calorimetry? *JACS*. 2003;125:14859-1866. doi:10.2307/450776

53. Biazzo-Ashnault DE, Park YW, Cummings RT, et al. Detection of insulin receptor tyrosine kinase activity using time-resolved fluorescence energy transfer technology. *Anal Biochem*. 2001;291(1):155-158. doi:10.1006/abio.2001.5027

54. Namkung Y, Le Gouill C, Lukashova V, et al. Monitoring G protein-coupled receptor and β-arrestin trafficking in live cells using enhanced bystander BRET. *Nat Commun*. 2016;7. doi:10.1038/ncomms12178

55. Mullard A. Protein–protein interaction inhibitors get into the groove. *Nat Rev Drug Discov*. 2012;11(4):173-175. doi:10.1049/et.2016.0418

56. Entzeroth M, Flotow H, Condron P. Overview of high-throughput screening. *Curr Protoc Pharmacol*. 2009;(SUPPL. 44):1-27. doi:10.1002/0471141755.ph0904s44

57. Vassilev LT, Vu BT, Graves B, et al. In Vivo Activation of the p53 Pathway by Small-Molecule Antagonists of MDM2. *Science (80-)*. 2004;303(5659):844-848. doi:10.1126/science.1092472

58. Grasberger BL, Lu T, Schubert C, et al. Discovery and cocrystal structure of benzodiazepinedione HDM2 antagonists that activate p53 in cells. *J Med Chem*. 2005;48(4):909-912. doi:10.1021/jm049137g

59. Allen JG, Bourbeau MP, Wohlhieter GE, et al. Discovery and optimization of chromenotriazolopyrimidines as potent inhibitors of the mouse double minute 2-tumor protein 53 protein-protein interaction. *J Med Chem*. 2009;52(22):7044-7053. doi:10.1021/jm900681h

60. Blackburn TJ, Ahmed S, Coxon CR, et al. Diaryl- and triaryl-pyrrole derivatives: Inhibitors of the MDM2-p53 and MDMX-p53 protein-protein interactions. *Medchemcomm*. 2013;4(9):1297-1304. doi:10.1039/c3md00161j

61. Nero TL, Morton CJ, Holien JK, Wielens J, Parker MW. Oncogenic protein interfaces: Small molecules, big challenges. *Nat Rev Cancer*. 2014;14(4):248-262. doi:10.1038/nrc3690

62. Kenny CH, Ding W, Kelleher K, et al. Development of a fluorescence polarization assay to screen for inhibitors of the FtsZ/ZipA interaction. *Anal Biochem*. 2003;323(2):224-233.

doi:10.1016/j.ab.2003.08.033

63. White PW, Titolo S, Brault K, et al. Inhibition of human papillomavirus DNA replication by small molecule antagonists of the E1-E2 protein interaction. *J Biol Chem*. 2003;278(29):26765-26772. doi:10.1074/jbc.M303608200

64. Hajduk PJ, Greer J. A decade of fragment-based drug design: Strategic advances and lessons learned. *Nat Rev Drug Discov*. 2007;6(3):211-219. doi:10.1038/nrd2220

65. Schuffenhauer A, Ruedisser S, Marzinzik A, Jahnke W, Selzer P, Jacoby E. Library Design for Fragment Based Screening. *Curr Top Med Chem*. 2005;5(8):751-762. doi:10.2174/1568026054637700

66. Rees DC, Congreve M, Murray CW, Carr R. Fragment-based lead discovery. *Nat Rev Drug Discov*. 2004;3(8):660-672. doi:10.1038/nrd1467

67. Harner MJ, Frank AO, Fesik SW. Fragment-Based Drug Discovery Using NMR Spectroscopy. *J Biomol NMR*. 2013;56(2):65-75. doi:10.1007/s10858-013-9740-z.Fragment-Based

68. Erlanson DA, Wells JA, Braisted AC. Tethering: Fragment-based drug discovery. *Annu Rev Biophys Biomol Struct*. 2004;33:199-223. doi:10.1146/annurev.biophys.33.110502.140409

69. DeLano WL, Ultsch MH, De Vos AM, Wells JA. Convergent Solutions to Binding at a Protein-Protein Interface. *Science (80-)*. 2000;287.

70. Rudin CM, Hann CL, Garon EB, et al. Phase II study of single-agent navitoclax (ABT-263) and biomarker correlates in patients with relapsed small cell lung cancer. *Clin Cancer Res*. 2012;18(11):3163-3169. doi:10.1158/1078-0432.CCR-11-3090

71. Emerson SD. NMR characterization of interleukin-2 in complexes with the IL-2Ralpha receptor component, and with low molecular weight compounds that inhibit the IL-2/IL-Ralpha interaction. *Protein Sci*. 2003;12(4):811-822. doi:10.1110/ps.0232803

72. Braisted AC, Oslob JD, Delano WL, et al. Discovery of a potent small molecule IL-2 inhibitor through fragment assembly. *J Am Chem Soc*. 2003;125(13):3714-3715. doi:10.1021/ja034247i

73. Jesus Perez de Vega M, Martin-Martinez M, Gonzalez-Muniz R. Modulation of Protein-Protein Interactions by Stabilizing/Mimicking Protein Secondary Structure Elements. *Curr Top Med Chem*. 2006;7(1):33-62. doi:10.2174/156802607779318325

74. Tavassoli A. SICLOPPS cyclic peptide libraries in drug discovery. *Curr Opin Chem Biol*. 2017;38:30-35. doi:10.1016/j.cbpa.2017.02.016

75. Cheng T, Li Q, Zhou Z, Wang Y, Bryant SH. Structure-based virtual screening for drug discovery: A problem-centric review. *AAPS J*. 2012;14(1):133-141. doi:10.1208/s12248-012-9322-0

76. Ripphausen P, Nisius B, Bajorath J. State-of-the-art in ligand-based virtual screening. *Drug Discov Today*. 2011;16(9-10):372-376. doi:10.1016/j.drudis.2011.02.011

77. Sugaya N, Furuya T. Dr. PIAS: An integrative system for assessing the druggability of protein-protein interactions. *BMC Bioinformatics*. 2011;12. doi:10.1186/1471-2105-12-50

78. Meireles LMC, Dömling AS, Camacho CJ. ANCHOR: A web server and database for analysis of protein-protein interaction binding pockets for drug discovery. *Nucleic Acids Res*. 2010;38(SUPPL. 2):407-411. doi:10.1093/nar/gkq502

79. Lerner E, Cordes T, Ingargiol A, et al. Toward dynamic structural biology: two decades of single-molecule Förster resonance enrgy transfer. *Science (80-)*. 2018;359:1. doi:10.1126/science.aan1133.Toward

80. Jia Y, Talaga DS, Lau WL, Lu HSM, DeGrado WF, Hochstrasser RM. Folding dynamics of single GCN-4 peptides by fluorescence resonant energy transfer confocal microscopy. *Chem Phys*. 1999;247(1):69-83. doi:10.1016/S0301-0104(99)00127-5

81. Jabaiah AM, Getz JA, Witkowski WA, Hardy JA, Daugherty PS. Identification of protease exosite-interacting peptides that enhance substrate cleavage kinetics. *Biol Chem*. 2012;393(9). doi:10.1515/hsz-2012-0162.Identification

82. Kettling U, Koltermann A, Schwille P, Eigen M. Real-time enzyme kinetics monitored by dual-color fluorescence cross-correlation spectroscopy. *Proc Natl Acad Sci U S A*. 1998;95(4):1416-1420. doi:10.1073/pnas.95.4.1416

83. Nagai Y, Miyazaki M, Aoki R, et al. A fluorescent indicator for visualizing cAMP-induced phosphorylation in vivo. *Nat Biotechnol*. 2000;18(3):313-316. doi:10.1038/73767

84. Algar WR, Hildebrandt N, Vogel SS, Medintz IL. FRET as a biomolecular research tool — understanding its potential while avoiding pitfalls. *Nat Methods*. 2019;16(9):815-829. doi:10.1038/s41592-019-0530-8

85. Piston DW, Kremers GJ. Fluorescent protein FRET: the good, the bad and the ugly. *Trends Biochem Sci*. 2007;32(9):407-414. doi:10.1016/j.tibs.2007.08.003

86. Szöllosi J, Damjanovich S, Mátyus L. Application of fluorescence resonance energy transfer in the clinical laboratory: Routine and research. *Commun Clin Cytom*. 1998;34(4):159-179. doi:10.1002/(SICI)1097-0320(19980815)34:4<159::AID-CYTO1>3.0.CO;2-B

87. Ma L, Yang F, Zheng J. Application of fluorescence resonance energy transfer in protein studies. *J Mol Struct*. 2014:87-100. doi:10.1016/j.molstruc.2013.12.071.Application

88. Sun Y, Hays NM, Periasamy A, Davidson MW, Day RN. Monitoring Protein Interactions in Living Cells with Fluorescence Lifetime Imaging Microscopy. *Methods Enzym*. 2012;(504):371-391. doi:10.1016/B978-0-12-391857-4.00019-7.Monitoring

89. Nakanishi J, Takarada T, Yunoki S, Kikuchi Y, Maeda M. FRET-based monitoring of conformational change of the β2 adrenergic receptor in living cells. *Biochem Biophys Res Commun*. 2006;343(4):1191-1196. doi:10.1016/j.bbrc.2006.03.064

90. Wang S, Vafabakhsh R, Borschel WF, Ha T, Colin G. Structural dynamics of potassium channel gating revealed by single molecule FRET. *Nat Struct Mol Biol*. 2016;23(1):31-36. doi:10.1038/nsmb.3138.Structural

91. Kasprzak AA. The use of FRET in the analysis of motor protein structure. *Methods Mol Biol*. 2007;392:183-197. doi:10.1007/978-1-59745-490-2_13

92. Schaap M, Hancock R, Wilderspin A, Wells G. Development of a steady-state FRET-based assay to identify inhibitors of the Keap1-Nrf2 protein-protein interaction. *Protein Sci*.

2013;22(12):1812-1819. doi:10.1002/pro.2384

93. Nougalli Tonaco IA, Borst JW, De Vries SC, Angenent GC, Immink RGH. In vivo imaging of MADS-box transcription factor interactions. *J Exp Bot*. 2006;57(1):33-42. doi:10.1093/jxb/erj011

94. Tsien RY. The green fluorescent protein. *Annu Rev Biochem*. 1998;67:509-544. doi:10.1146/annurev.biochem.67.1.509

95. Olenych SG, Claxton NS, Ottenberg GK, Davidson MW. The Fluorescent Protein Color Palette. *Curr Protoc Cell Biol*. 2007;36(1):1-34. doi:10.1002/0471143030.cb2105s36

96. Xu X, Gerard ALV, Huang BCB, Anderson DC, Payan DG, Luo Y. Detection of programmed cell death using fluorescence energy transfer. *Nucleic Acids Res*. 1998;26(8):2034-2035. doi:10.1093/nar/26.8.2034

97. Boute N, Jockers R, Issad T. The use of resonance energy transfer in high-throughput screening: BRET versus FRET. *Trends Pharmacol Sci*. 2002;23(8):351-354. doi:10.1016/S0165-6147(02)02062-X

98. Corbel C, Sartini S, Levati E, et al. Screening for Protein-Protein Interaction Inhibitors Using a Bioluminescence Resonance Energy Transfer (BRET)–Based Assay in Yeast. *SLAS Discov*. 2017;22(6):751-759. doi:10.1177/2472555216689530

99. Miyawaki A, Llopis J, Heim R, et al. Fluorescent indicators for Ca2+ based on green fluorescent proteins and calmodulin. *Nature*. 1997;388(6645):882-887. doi:10.1038/42264

100. Campbell RE, Tour O, Palmer AE, et al. A monomeric red fluorescent protein. *Proc Natl Acad Sci U S A*. 2002;99(12):7877-7882. doi:10.1073/pnas.082243699

101. Leavesley SJ, Rich TC. Overcoming limitations of FRET measurements. *Cytometry*. 2016;89(4):325-327. doi:10.1002/cyto.a.22851.Overcoming

102. Bacart J, Corbel C, Jockers R, Bach S, Couturier C. The BRET technology and its application to screening assays. *Biotechnol J*. 2008;3(3):311-324. doi:10.1002/biot.200700222

103. Wu PG, Brand L. Resonance energy transfer: Methods and applications. *Anal Biochem*. 1994;218(1):1-13. doi:10.1006/abio.1994.1134

104. Clegg RM, Murchie AIH, Zechel A, Lilley DMJ. Observing the helical geometry of double-stranded DNA in solution by fluorescence resonance energy transfer. *Proc Natl Acad Sci U S A*. 1993;90(7):2994-2998. doi:10.1073/pnas.90.7.2994

105. Mercier JF, Salahpour A, Angers S, Breit A, Bouvier M. Quantitative assessment of β1- and β2-adrenergic receptor homo- and heterodimerization by bioluminescence resonance energy transfer. *J Biol Chem*. 2002;277(47):44925-44931. doi:10.1074/jbc.M205767200

106. Couturier C, Jockers R. Activation of the leptin receptor by a ligand-induced conformational change of constitutive receptor dimers. *J Biol Chem*. 2003;278(29):26604-26611. doi:10.1074/jbc.M302002200

107. Ramsay D, Carr IC, Pediani J, et al. High-affinity interactions between human α1A-adrenoceptor C-terminal splice variants produce homo- and heterodimers but do not generate the α1L-adrenoceptor. *Mol Pharmacol*. 2004;66(2):228-239.

doi:10.1124/mol.66.2.228

108. Ayoub MA, Levoye A, Delagrange P, Jockers R. Preferential formation of MT1/MT2 melatonin receptor heterodimers with distinct ligand interaction properties compared with MT 2 homodimers. *Mol Pharmacol*. 2004;66(2):312-321. doi:10.1124/mol.104.000398

109. Couturier C, Deprez B. Setting up a bioluminescence resonance energy transfer high throughput screening assay to search for protein/protein interaction inhibitors in mammalian cells. *Front Endocrinol (Lausanne)*. 2012;3(SEP):1-13. doi:10.3389/fendo.2012.00100

110. Xu Y, Piston DW, Johnson CH. A bioluminescence resonance energy transfer (BRET) system: Application to interacting circadian clock proteins. *Proc Natl Acad Sci U S A*. 1999;96(1):151-156. doi:10.1073/pnas.96.1.151

111. Angers S, Salahpour A, Joly E, et al. Detection of β2-adrenergic receptor dimerization in living cells using bioluminescence resonance energy transfer (BRET). *Proc Natl Acad Sci U S A*. 2000;97(7):3684-3689. doi:10.1073/pnas.060590697

112. Angers S, Salahpour A, Bouvier M. Biochemical and biophysical demonstration of GPCR oligomerization in mammalian cells. *Life Sci*. 2001;68(19-20):2243-2250. doi:10.1016/S0024-3205(01)01012-8

113. Jiang L, Collins J, Davis R, et al. Use of a cAMP BRET Sensor to Characterize a Novel Regulation of cAMP by the Sphingosine 1-Phosphate/G13 Pathway*. *J Biol Chem*. 2007;282(14):10576-10584. doi:10.1074/jbc.M609695200.Use

114. Hamdan FF, Percherancier Y, Breton B, Bouvier M. Monitoring Protein-Protein Interactions in Living Cells by Bioluminescence Resonance Energy Transfer (BRET) . *Curr Protoc Neurosci*. 2006;34(1):1-20. doi:10.1002/0471142301.ns0523s34

115. Griesbeck O, Baird GS, Campbell RE, Zacharias DA, Tsien RY. Reducing the environmental sensitivity of yellow fluorescent protein. Mechanism and applications. *J Biol Chem*. 2001;276(31):29188-29194. doi:10.1074/jbc.M102815200

116. Hamdan FF, Audet M, Garneau P, Pelletier J, Bouvier M. High-throughput screening of G protein-coupled receptor antagonists using a bioluminescence resonance energy transfer 1-based β-arrestin2 recruitment assay. *J Biomol Screen*. 2005;10(5):463-475. doi:10.1177/1087057105275344

117. Nguyen AW, Daugherty PS. Evolutionary optimization of fluorescent proteins for intracellular FRET. *Nat Biotechnol*. 2005;23(3):355-360. doi:10.1038/nbt1066

118. You X, Nguyen AW, Jabaiah A, Sheff MA, Thorn KS, Daugherty PS. Intracellular protein interaction mapping with FRET hybrids. *Proc Natl Acad Sci U S A*. 2006;103(49):18458-18463. doi:10.1073/pnas.0605422103

119. Bertrand L, Parent S, Caron M, et al. The BRET2/arrestin assay in stable recombinant cells: A platform to screen for compounds that interact with g protein-coupled receptors (GPCRS). *J Recept Signal Transduct*. 2002;22(1-4):533-541. doi:10.1081/RRS-120014619

120. Fujii H, Noda K, Asami Y, Kuroda A, Sakata M, Tokida A. Increase in bioluminescence intensity of firefly luciferase using genetic modification. *Anal Biochem*. 2007;366(2):131-136. doi:10.1016/j.ab.2007.04.018

121. Kricka LJ, Leach FR. In memoriam Dr Marlene Deluca. *J Biolumin Chemilumin*. 1989;3(1):1-5. doi:10.1002/bio.1170030102

122. DeLuca M, McElroy WD. Two kinetically distinguishable ATP sites in firefly luciferase. *Biochem Biophys Res Commun*. 1984;123(2):764-770. doi:10.1016/0006-291X(84)90295-X

123. Arai R, Nakagawa H, Kitayama A, Ueda H, Nagamune T. Detection of protein-protein interaction by bioluminescence resonance energy transfer from firefly luciferase to red fluorescent protein. *J Biosci Bioeng*. 2002;94(4):362-364. doi:10.1263/jbb.94.362

124. Yamakawa Y, Veda H, Kitayama A, Nagamune T. Rapid homogeneous immunoassay of peptides based on bioluminescence resonance energy transfer from firefly luciferase. *J Biosci Bioeng*. 2002;93(6):537-542. doi:10.1016/S1389-1723(02)80234-1

125. Chan WCW, Maxwell DJ, Gao X, Bailey RE, Han M, Nie S. Luminescent quantum dots for multiplexed biological detection and imaging. *Curr Opin Biotechnol*. 2002;13(1):40-46. doi:10.1016/S0958-1669(02)00282-3

126. Inouye S, Watanabe K, Nakamura H, Shimomura O. Secretional luciferase of the luminous shrimp Oplophorus gracilirostris: cDNA cloning of a novel imidazopyrazinone luciferase. *FEBS Lett*. 2000;481(1):19-25. doi:10.1016/S0014-5793(00)01963-3

127. Kim J, Grailhe R. Nanoluciferase signal brightness using furimazine substrates opens bioluminescence resonance energy transfer to widefield microscopy. *Cytom Part A*. 2016;89(8):742-746. doi:10.1002/cyto.a.22870

128. Machleidt T, Woodroofe CC, Schwinn MK, et al. NanoBRET A Novel BRET Platform for the Analysis of Protein−Protein Interactions. *ACS Chem Biol*. 2015.

129. Schaub FX, Reza MS, Flaveny CA, et al. Fluorophore-NanoLuc BRET Reporters Enable Sensitive In Vivo Optical Imaging and Flow Cytometry for Monitoring Tumorigenesis. *Cancer Res*. 2015;75(23):5023-5033. doi:10.1158/0008-5472.CAN-14-3538.Fluorophore-NanoLuc

130. Boute N, Lowe P, Berger S, Malissard M, Robert A, Tesar M. NanoLuc Luciferase - A multifunctional tool for high throughput antibody screening. *Front Pharmacol*. 2016;7(FEB):1-11. doi:10.3389/fphar.2016.00027

131. Hall MP, Unch J, Binkowski BF, et al. Engineered luciferase reporter from a deep sea shrimp utilizing a novel imidazopyrazinone substrate. *ACS Chem Biol*. 2012;7(11):1848-1857. doi:10.1021/cb3002478

132. Khardori N, Stevaux C, Ripley K. Antibiotics: From the Beginning to the Future: Part 1. *Indian J Pediatr*. 2020;87(1):43-47. doi:10.1007/s12098-019-03113-0

133. Davies J. Origins and evolution of antibiotic resistance. *Microbiologia*. 1996;12(1):9-16. doi:10.1128/mmbr.00016-10

134. Lancini, G., Parenti F, Gualaberto G. *Antibiotics: A Multidisciplinary Approach*. New York: Plenum Pless; 1995.

135. Greenwood D. *Antimicrobial Chemoterapy*. New York: Oxford University Press; 1995.

136. O'Grady, H. P. Lambert RGF and D, Greenwood. *Antibiotic and Chemotherapy: Anti-Infective Agents and Their Use in Therapy*. 7th editio.; 1997.

137. Capasso L. 5300 years ago, the Ice Man used natural laxatives and antibiotics [12]. *Lancet*. 1998;352(9143):1864. doi:10.1016/S0140-6736(05)79939-6

138. Khardori N. Antibiotics-Past, Present, and Future. *Med Clin North Am*. 2006;90(6):1049-1076. doi:10.1016/j.mcna.2006.06.007

139. Gould K. Antibiotics: From prehistory to the present day. *J Antimicrob Chemother*. 2016;71(3):572-575. doi:10.1093/jac/dkv484

140. Porter R. *The Greatest Benefit to Mankind: A Medical History of Humanity*. (Publishers H, ed.).; 1999.

141. Saga T, Yamaguchi K. History of antimicrobial agents and resistant bacteria. *Japan Med Assoc J*. 2009;52(2):103-108.

142. US News World Rep. *Alexander Fleming - medicine's accidental hero*. 1998:58-63.

143. Levine DP. Vancomycin : A History. 2006;42(Suppl 1):5-12.

144. Yadav S, Kapley A. Antibiotic resistance: Global health crisis and metagenomics. *Biotechnol Reports*. 2021;29:e00604. doi:10.1016/j.btre.2021.e00604

145. U. H. The cost of antimicrobial resistance. *Nat Rev Microbiol*. 2019;17:3.

146. O' Neil J. Review on Antibiotic resisitance. Antimicrobial Resistance : Tackling a crisis for the health and wealth of nations. *Heal Wealth Nations*. 2014;(December):1-16. https://amr-review.org/sites/default/files/AMR Review Paper - Tackling a crisis for the health and wealth of nations_1.pdf.

147. Abraham EP, Chain E. An Enzyme from Bacteria able to. *Nature*. 1940;146:837.

148. W. M. M. K. Extraction of a highly potent penicillin inactivator from penicillin resistant staphylococci. *Science (80-)*. 1944;99(2579):452-453.

149. Kathleen Keyes, Margie D. Lee JJM. Antibiotics: mode of action and mechanisms of resistance, and tranfer. In: *Microbial Food Safety in Animal Agriculture: Current Topics*. Vol 25. ; 2003:49-55. doi:10.7748/ns.25.42.49.s52

150. Funnel, B. E. and Phillips GJ, ed. *Plasmid Biology*. ASM Press, Whashington, DC.; 2004. doi:10.1128/9781555817732

151. Helinski DR. Introduction to plasmids: a selective view of their history. In: Funnel, B. E. and Phillips GJ, ed. *Plasmid Biology*. ASM Press, Whashington, DC.; 2004:1-21.

152. Liu Y, Tong Z, Shi J, Li R, Upton M, Wang Z. Drug repurposing for next-generation combination therapies against multidrug-resistant bacteria. *Theranostics*. 2021;11(10):4910-4928. doi:10.7150/thno.56205

153. Liu Y, Ding S, Shen J, Zhu K. Nonribosomal antibacterial peptides that target multidrug-resistant bacteria. *Nat Prod Rep*. 2019;36(4):573-592. doi:10.1039/c8np00031j

154. Wright GD, Sutherland AD. New strategies for combating multidrug-resistant bacteria. *Trends Mol Med*. 2007;13(6):260-267. doi:10.1016/j.molmed.2007.04.004

155. Zhang W, Fisher JF, Mobashery S. The bifunctional enzymes of antibiotic resistance. 2009:505-511. doi:10.1016/j.mib.2009.06.013

156. Wright GD. Aminoglycoside-modifying enzymes. 1999:499-503.

157. Ramirez MS, Tolmasky ME. NIH Public Access. 2011;13(6):151-171. doi:10.1016/j.drup.2010.08.003.Aminoglycoside

158. Long KS, Poehlsgaard J, Kehrenberg C, Schwarz S, Vester B. The Cfr rRNA Methyltransferase Confers Resistance to Phenicols , Lincosamides , Oxazolidinones , Pleuromutilins , and Streptogramin A Antibiotics. 2006;50(7):2500-2505. doi:10.1128/AAC.00131-06

159. Vester B. Research in Microbiology The cfr and cfr-like multiple resistance genes. *Res Microbiol*. 2018;169(2):61-66. doi:10.1016/j.resmic.2017.12.003

160. Zhang W, Xu X, Schwarz S, et al. Characterization of the IncA / C plasmid pSCEC2 from Escherichia coli of swine origin that harbours the multiresistance gene cfr. 2014;(September 2013):385-389. doi:10.1093/jac/dkt355

161. Liu Y, Wang Y, Walsh TR, et al. Emergence of plasmid-mediated colistin resistance mechanism MCR-1 in animals and human beings in China : a microbiological and molecular biological study. *Lancet Infect Dis*. 2015;3099(15):1-8. doi:10.1016/S1473-3099(15)00424-7

162. Villagra A, Undabarrena A, Wozniak A, et al. Porin alterations present in non-carbapenemase- producing Enterobacteriaceae with high and intermediate levels of carbapenem resistance in Chile. 2012:1270-1279. doi:10.1099/jmm.0.045799-0

163. Tigecycline I. crossm Emergence of a Plasmid-Encoded Resistance-Nodulation- Division Efflux Pump Conferring Resistance to Multiple Drugs ,. 2020;11(2):1-15.

164. Oakley AJ. A structural view of bacterial DNA replication. *Protein Sci*. 2019;28(6):990-1004. doi:10.1002/pro.3615

165. Lee H, Popodi E, Tang H, Foster PL. Rate and molecular spectrum of spontaneous mutations in the bacterium Escherichia coli as determined by whole-genome sequencing. *Proc Natl Acad Sci U S A*. 2012;109(41). doi:10.1073/pnas.1210309109

166. Lewis JS, Jergic S, Dixon NE. *The E. Coli DNA Replication Fork*. Vol 39. 1st ed. Elsevier Inc.; 2016. doi:10.1016/bs.enz.2016.04.001

167. Chodavarapu S, Kaguni JM. *Replication Initiation in Bacteria*. Vol 39. 1st ed. Elsevier Inc.; 2016. doi:10.1016/bs.enz.2016.03.001

168. Nancy L Craig; Orna Cohen-Fix; Rachel Green; Carol W Greider; Gisela Storz; Cynthia Wolberger; et al. *Molecular Biology : Principles of Genome Function*. Second edi. Oxford : Oxford University Press; 2014.

169. Xu ZQ, Dixon NE. Bacterial replisomes. *Curr Opin Struct Biol*. 2018;53:159-168. doi:10.1016/j.sbi.2018.09.006

170. Robinson A, J. Causer R, E. Dixon N. Architecture and Conservation of the Bacterial DNA Replication Machinery, an Underexploited Drug Target. *Curr Drug Targets*. 2012;13(3):352-372. doi:10.2174/138945012799424598

171. Jergic S, Horan NP, Elshenawy MM, et al. A direct proofreader-clamp interaction stabilizes the Pol III replicase in the polymerization mode. *EMBO J*. 2013;32(9):1322-1333.

doi:10.1038/emboj.2012.347

172. Neylon C, Kralicek A V., Hill TM, Dixon NE. Replication Termination in Escherichia coli : Structure and Antihelicase Activity of the Tus- Ter Complex . *Microbiol Mol Biol Rev*. 2005;69(3):501-526. doi:10.1128/mmbr.69.3.501-526.2005

173. Black MT, Coleman K. New inhibitors of bacterial topoisomerase GyrA/ParC subunits. *Curr Opin Investig Drugs*. 2009;10(8):804-810.

174. Ostrowska K. Coumarin-piperazine derivatives as biologically active compounds. *Saudi Pharm J*. 2020;28(2):220-232. doi:10.1016/j.jsps.2019.11.025

175. Hu CF, Zhang PL, Sui YF, et al. Ethylenic conjugated coumarin thiazolidinediones as new efficient antimicrobial modulators against clinical methicillin-resistant Staphylococcus aureus. *Bioorg Chem*. 2020;94:103434. doi:10.1016/j.bioorg.2019.103434

176. Dongxu F, Zhang A, Yang Y, Yang P. Coumarin-containing hybrids and their antibacterial activities.pdf. 2020. doi:10.1002/ardp.201900380

177. Bryskier A, Klich M. Coumarin Antibiotics: Novobiocin, Coumermycin, and Clorobiocin. In: André Bryskier M.D., ed. *Antimicrobial Agents: Antibacterials and Antifungals*. ; 2005. doi:10.1128/9781555815929.ch29

178. Hane MW, Wood TH. Escherichia coli K-12 mutants resistant to nalidixic acid: genetic mapping and dominance studies. *J Bacteriol*. 1969;99(1):238-241. doi:10.1128/jb.99.1.238-241.1969

179. Nakamura S, Nakamura M, Kojima T, Yoshida H. gyrA and gyrB mutations in quinolone-resistant strains of Escherichia coli. *Antimicrob Agents Chemother*. 1989;33(2):254-255. doi:10.1128/AAC.33.2.254

180. Kato J ichi, Nishimura Y, Imamura R, Niki H, Hiraga S, Suzuki H. New topoisomerase essential for chromosome segregation in E. coli. *Cell*. 1990;63(2):393-404. doi:10.1016/0092-8674(90)90172-B

181. Ferrero L, Cameron B, Crouzet J. Analysis of gyrA and grlA mutations in stepwise-selected ciprofloxacin- resistant mutants of Staphylococcus aureus. *Antimicrob Agents Chemother*. 1995;39(7):1554-1558. doi:10.1128/AAC.39.7.1554

182. Ng EY, Trucksis M, Hooper DC. Quinolone resistance mutations in topoisomerase IV: Relationship to the flqA locus and genetic evidence that topoisomerase IV is the primary target and DNA gyrase is the secondary target of fluoroquinolones in Staphylococcus aureus. *Antimicrob Agents Chemother*. 1996;40(8):1881-1888. doi:10.1128/aac.40.8.1881

183. Khodursky AB, Zechiedrich EL, Cozzarelli NR. Topoisomerase IV is a target of quinolones in Escherichia coli. *Proc Natl Acad Sci U S A*. 1995;92(25):11801-11805. doi:10.1073/pnas.92.25.11801

184. Breines DM, Ouabdesselam S, Ng EY, et al. Quinolone resistance locus nfxD of Escherichia coli is a mutant allele of the parE gene encoding a subunit of topoisomerase IV. *Antimicrob Agents Chemother*. 1997;41(1):175-179. doi:10.1128/aac.41.1.175

185. Soussy CJ, Wolfson JS, Ng EY, Hooper DC. Limitations of plasmid complementation test for determination of quinolone resistance due to changes in the gyrase A protein and identification of conditional quinolone resistance locus. *Antimicrob Agents Chemother*.

1993;37(12):2588-2592. doi:10.1128/AAC.37.12.2588

186. Hooper DC. Mechanisms of action of antimicrobials: Focus on fluoroquinolones. *Clin Infect Dis*. 2001;32(SUPPL. 1):9-15. doi:10.1086/319370

187. Kaguni JM. The macromolecular machines that duplicate the escherichia coli chromosome as targets for drug discovery. *Antibiotics*. 2018;7(1):1-28. doi:10.3390/antibiotics7010023

188. Weigel C, Messer W. Secondary Structure Predictions for 104 DnaA Protein Sequences . *Structure*. 2001.

189. Abe Y, Jo T, Matsuda Y, Matsunaga C, Katayama T, Ueda T. Structure and function of DnaA N-terminal domains: Specific sites and mechanisms in inter-DnaA interaction and in DnaB helicase loading on oriC. *J Biol Chem*. 2007;282(24):17816-17827. doi:10.1074/jbc.M701841200

190. Chodavarapu S, Gomez R, Vicente M, Kaguni JM. Escherichia coli Dps interacts with DnaA protein to impede initiation: A model of adaptive mutation. *Mol Microbiol*. 2008;67(6):1331-1346. doi:10.1111/j.1365-2958.2008.06127.x

191. Marszalek J, Kaguni JM. DnaA protein directs the binding of DnaB protein in initiation of DNA replication in Escherichia coli. *J Biol Chem*. 1994;269(7):4883-4890. doi:10.1016/s0021-9258(17)37627-5

192. Sutton MD, Carr KM, Vicente M, Kaguni JM. Escherichia coli DnaA protein. The N-terminal domain and loading of DnaB helicase at the E. coli chromosomal origin. *J Biol Chem*. 1998;273(51):34255-34262. doi:10.1074/jbc.273.51.34255

193. Seitz H, Weigel C, Messer W, Genetik ÈM. The interaction of domains of the DnaA and DnaB replication proteins of E.coli_Mol.Microbiol._2000.pdf. 2000;37:1270-1279.

194. Ishida T, Akimitsu N, Kashioka T, et al. DiaA, a novel DnaA-binding protein, ensures the timely initiation of Escherichia coli chromosome replication. *J Biol Chem*. 2004;279(44):45546-45555. doi:10.1074/jbc.M402762200

195. Keyamura K, Abe Y, Higashi M, Ueda T, Katayama T. DiaA dynamics are coupled with changes in initial origin complexes leading to helicase loading. *J Biol Chem*. 2009;284(37):25038-25050. doi:10.1074/jbc.M109.002717

196. Natrajan G, Noirot-Gros MF, Zawilak-Pawlik A, Kapp U, Terradot L. The structure of a DnaA/HobA complex from Helicobacter pylori provides insight into regulation of DNA replication in bacteria. *Proc Natl Acad Sci U S A*. 2009;106(50):21115-21120. doi:10.1073/pnas.0908966106

197. Chodavarapu S, Felczak MM, Yaniv JR, Kaguni JM. Escherichia coli DnaA interacts with HU in initiation at the E. coli replication origin. *Mol Microbiol*. 2008;67(4):781-792. doi:10.1111/j.1365-2958.2007.06094.x

198. Chodavarapu S, Felczak MM, Kaguni JM. Two forms of ribosomal protein L2 of Escherichia coli that inhibit DnaA in DNA replication. *Nucleic Acids Res*. 2011;39(10):4180-4191. doi:10.1093/nar/gkq1203

199. Weigel C, Schmidt A, Seitz H, Tüngler D, Welzeck M, Messer W. The N-terminus promotes oligomerization of the Escherichia coli initiator protein DnaA. *Mol Microbiol*.

1999;34(1):53-66. doi:10.1046/j.1365-2958.1999.01568.x

200. Simmons LA, Felczak M, Kaguni JM. DnaA Protein of Escherichia coli: Oligomerization at the E. coli chromosomal origin is required for initiation and involves specific N-terminal amino acids. *Mol Microbiol*. 2003;49(3):849-858. doi:10.1046/j.1365-2958.2003.03603.x

201. Felczak MM, Simmonst LA, Kaguni JM. An essential tryptophan of Escherichia coli DnaA protein functions in oligomerization at the E. coli replication origin. *J Biol Chem*. 2005;280(26):24627-24633. doi:10.1074/jbc.M503684200

202. Koonin E V. A superfamily of ATPases with diverse functions containing either classical or deviant ATP-binding motif. *J Mol Biol*. 1993;229(4):1165-1174. doi:10.1006/jmbi.1993.1115

203. Neuwald AF, Aravind L, Spouge JL, Koonin E V. AAA+: A class of chaperone-like ATPases associated with the assembly, operation, and disassembly of protein complexes. *Genome Res*. 1999;9(1):27-43. doi:10.1101/gr.9.1.27

204. Katayama T. Roles for the AAA+ motifs of DnaA in the initiation of DNA replication. *Biochem Soc Trans*. 2008;36(1):78-82. doi:10.1042/BST0360078

205. Erzberger JP, Pirruccello MM, Berger JM. The structure of bacterial DnaA: Implications for general mechanisms underlying DNA replication initiation. *EMBO J*. 2002;21(18):4763-4773. doi:10.1093/emboj/cdf496

206. Felczak MM, Kaguni JM. The box VII motif of Escherichia coli DnaA protein is required for DnaA oligomerization at the E. coli replication origin. *J Biol Chem*. 2004;279(49):51156-51162. doi:10.1074/jbc.M409695200

207. Roth A, Messer W. The DNA-binding domain of the initiator protein DnaA. *Trends Genet*. 1995;11(7):262-262. doi:10.1016/0168-9525(95)90557-x

208. Sutton MD, Kagnni JM. Threonine 435 of Escherichia coli DnaA protein confers sequence-specific DNA binding activity. *J Biol Chem*. 1997;272(37):23017-23024. doi:10.1074/jbc.272.37.23017

209. Blaesing F, Weigel C, Welzeck M, Messer W. Analysis of the DNA-binding domain of Escherichia coli DnaA protein. *Mol Microbiol*. 2000;36(3):557-569. doi:10.1046/j.1365-2958.2000.01881.x

210. Fujikawa N, Kurumizaka H, Nureki O, et al. Structural basis of replication origin recognition by the DnaA protein. *Nucleic Acids Res*. 2003;31(8):2077-2086. doi:10.1093/nar/gkg309

211. Mizushima T, Sasaki S, Ohishi H, et al. Molecular design of inhibitors of in vitro oriC DNA replication based on the potential to block the ATP binding of DnaA protein. *J Biol Chem*. 1996;271(41):25178-25183. doi:10.1074/jbc.271.41.25178

212. Leipe DD, Aravind L, Grishin N V., Koonin E V. The bacterial replicative helicase DnaB evolved from a RecA duplication. *Genome Res*. 2000;10(1):5-16. doi:10.1101/gr.10.1.5

213. Jezewska MJ, Rajendran S, Bujalowska D, Bujalowski W. Does single-stranded DNA pass through the inner channel of the protein hexamer in the complex with the Escherichia coli DnaB helicase? Fluorescence energy transfer studies. *J Biol Chem*. 1998;273(17):10515-10529. doi:10.1074/jbc.273.17.10515

214. San Martin C, Radermacher M, Wolpensinger B, et al. Three-dimensional reconstructions from cryoelectron microscopy images reveal an intimate complex between helicase DnaB and its loading partner DnaC. *Structure*. 1998;6(4):501-509. doi:10.1016/s0969-2126(98)00051-3

215. Wickner S, Wright M, Hurwitz J. Association of DNA dependent and independent ribonucleoside triphosphatase activities with dnaB gene product of Escherichia coli. *Proc Natl Acad Sci U S A*. 1974;71(3):783-787. doi:10.1073/pnas.71.3.783

216. LeBowitz JH, McMacken R. The Escherichia coli dnaB replication protein is a DNA helicase. *J Biol Chem*. 1986;261(10):4738-4748. doi:10.1016/s0021-9258(17)38564-2

217. Reha-Krantz LJ, Hurwitz J. The dnaB gene product of Escherichia coli. II. Single stranded DNA-dependent ribonucleoside triphosphatase activity. *J Biol Chem*. 1978;253(11):4051-4057. doi:10.1016/s0021-9258(17)34797-x

218. Jezewska MJ, Rajendran S, Bujalowski W. Strand specificity in the interactions of Escherichia coli primary replicative helicase DnaB protein with a replication fork. *Biochemistry*. 1997;36(33):10320-10326. doi:10.1021/bi970712a

219. Jezewska MJ, Rajendran S, Bujalowski W. Complex of Escherichia coli primary replicative helicase DnaB protein with a replication fork: Recognition and structure. *Biochemistry*. 1998;37(9):3116-3136. doi:10.1021/bi972564u

220. Kaplan DL. The 3'-tail of a forked-duplex sterically determines whether one or two DNA strands pass through the central channel of a replication-fork helicase. *J Mol Biol*. 2000;301(2):285-299. doi:10.1006/jmbi.2000.3965

221. Galletto R, Jezewska MJ, Bujalowski W. Unzipping mechanism of the double-stranded DNA unwinding by a hexameric helicase: The effect of the 3' arm and the stability of the dsDNA on the unwinding activity of the Escherichia coli DnaB helicase. *J Mol Biol*. 2004;343(1):101-114. doi:10.1016/j.jmb.2004.07.056

222. Itsathitphaisarn O, Wing RA, Eliason WK, Wang J, Steitz TA. The hexameric helicase DnaB adopts a nonplanar conformation during translocation. *Cell*. 2012;151(2):267-277. doi:10.1016/j.cell.2012.09.014

223. Carney SM, Gomathinayagam S, Leuba SH, Trakselis MA. Bacterial DnaB helicase interacts with the excluded strand to regulate unwinding. *J Biol Chem*. 2017;292(46):19001-19012. doi:10.1074/jbc.M117.814178

224. Kim S, Dallmann HG, McHenry CS, Marians KJ. Coupling of a replicative polymerase and helicase: A τ-DnaB interaction mediates rapid replication fork movement. *Cell*. 1996;84(4):643-650. doi:10.1016/S0092-8674(00)81039-9

225. Graham JE, Marians KJ, Kowalczykowski SC. Independent and Stochastic Action of DNA Polymerases in the Replisome. *Cell*. 2017;169(7):1201-1213.e17. doi:10.1016/j.cell.2017.05.041

226. Griep MA, Blood S, Larson MA, Koepsell SA, Hinrichs SH. Myricetin inhibits Escherichia coli DnaB helicase but not primase. *Bioorganic Med Chem*. 2007;15(22):7203-7208. doi:10.1016/j.bmc.2007.07.057

227. Lin HH, Huang CY. Characterization of flavonol inhibition of DnaB helicase: Real-time monitoring, structural modeling, and proposed mechanism. *J Biomed Biotechnol*.

2012;2012. doi:10.1155/2012/735368

228. Tougu K, Marians KJ. The extreme C terminus of primase is required for interaction with DnaB at the replication fork. *J Biol Chem*. 1996;271(35):21391-21397. doi:10.1074/jbc.271.35.21391

229. Chang P, Marians KJ. Identification of a region of Escherichia coli DnaB required for functional interaction with DnaG at the replication fork. *J Biol Chem*. 2000;275(34):26187-26195. doi:10.1074/jbc.M001800200

230. Bailey S, Eliason WK, Thomas A. Steitz. Structure of hexameric DnaB. *Science (80-)*. 2007;318(5849):459-464.

231. Soultanas P. The Bacterial Helicase-Primase Interaction.pdf. 2004;13(6):839-844. doi:10.1016/j.str.2005.04.006.The

232. Bird LE, Pan H, Soultanas P, Wigley DB. Mapping Protein – Protein Interactions within a Stable Complex of DNA Primase and DnaB Helicase from Bacillus. 2011;39(1):171-182.

233. Pan H, Wigley DB. Structure of the zinc-binding domain of Bacillus stearothermophilus DNA primase. *Structure*. 2000;8(3):231-239. doi:10.1016/S0969-2126(00)00101-5

234. Zhou Y, Luo H, Liu Z, et al. Structural Insight into the Specific DNA Template Binding to DnaG primase in Bacteria. *Sci Rep*. 2017;7(1):1-8. doi:10.1038/s41598-017-00767-8

235. Mitkova A V., Khopde SM, Biswas SB. Mechanism and Stoichiometry of Interaction of DnaG Primase with DnaB Helicase of Escherichia coli in RNA Primer Synthesis. *J Biol Chem*. 2003;278(52):52253-52261. doi:10.1074/jbc.M308956200

236. Hegde VR, Pu H, Patel M, et al. Two new bacterial DNA primase inhibitors from the plant Polygonum cuspidatum. *Bioorganic Med Chem Lett*. 2004;14(9):2275-2277. doi:10.1016/j.bmcl.2004.02.006

237. Agarwal A, Louise-May S, Thanassi JA, et al. Small molecule inhibitors of E. coli primase, a novel bacterial target. *Bioorganic Med Chem Lett*. 2007;17(10):2807-2810. doi:10.1016/j.bmcl.2007.02.056

238. Tarantino PM, Zhi C, Gambino JJ, Wright GE, Brown NC. 6-anilinouracil-based inhibitors of bacillus subtilis DNA polymerase III: Antipolymerase and antimicrobial structure-activity relationships based on substitution at uracil N3. *J Med Chem*. 1999;42(11):2035-2040. doi:10.1021/jm980693i

239. Dervyn E, Suski C, Daniel R, et al. Two essential DNA polymerases at the bacterial replication fork. *Science (80-)*. 2001;294(5547):1716-1719. doi:10.1126/science.1066351

240. Sanders GM, Dallmann HG, McHenry CS. Reconstitution of the B. subtilis Replisome with 13 Proteins Including Two Distinct Replicases. *Mol Cell*. 2010;37(2):273-281. doi:10.1016/j.molcel.2009.12.025

241. McHenry CS. Breaking the rules: Bacteria that use several DNA polymerase IIIs. *EMBO Rep*. 2011;12(5):408-414. doi:10.1038/embor.2011.51

242. Johansson E, Dixon N. Replicative DNA polymerases. *Cold Spring Harb Perspect Biol*. 2013;5(6):1-14. doi:10.1101/cshperspect.a012799

243. Liao Y, Li Y, Schroeder JW, Simmons LA, Biteen JS. Single-Molecule DNA Polymerase

Dynamics at a Bacterial Replisome in Live Cells. *Biophys J*. 2016;111(12):2562-2569. doi:10.1016/j.bpj.2016.11.006

244. Jameson KH, Wilkinson AJ. Control of initiation of DNA replication in Bacillus subtilis and Escherichia coli. *Genes (Basel)*. 2017;8(1). doi:10.3390/genes8010022

245. Indiani C, O'Donnell M. The replication clamp-loading machine at work in the three domains of life. *Nat Rev Mol Cell Biol*. 2006;7(10):751-761. doi:10.1038/nrm2022

246. O'Donnell M, Kuriyan J. Clamp loaders and replication initiation. *Curr Opin Struct Biol*. 2006;16(1):35-41. doi:10.1016/j.sbi.2005.12.004

247. Hedglin M, Kumar R, Benkovic SJ. Replication clamps and clamp loaders. *Cold Spring Harb Perspect Biol*. 2013;5(4):1-19. doi:10.1101/cshperspect.a010165

248. Erzberger JP, Berger JM. Evolutionary relationships and structural mechanisms of AAA+ proteins. *Annu Rev Biophys Biomol Struct*. 2006;35:93-114. doi:10.1146/annurev.biophys.35.040405.101933

249. Davey MJ, Jeruzalmi D, Kuriyan J, O'Donnell M. Motors and switches: AAA+ machines within the replisome. *Nat Rev Mol Cell Biol*. 2002;3(11):826-835. doi:10.1038/nrm949

250. Gao D, McHenry CS. τ binds and organizes Escherichia coli replication proteins Through distinct domains. Partial proteolysis of terminally tagged τ to determine candidate domains and to assign domain V as the α binding domain. *J Biol Chem*. 2001;276(6):4433-4440. doi:10.1074/jbc.M009828200

251. Mok M, Marians KJ. The Escherichia coli preprimosome and DNA B helicase can form replication forks that move at the same rate. *J Biol Chem*. 1987;262(34):16644-16654. doi:10.1016/s0021-9258(18)49304-0

252. Mok M, Marians KJ. Formation of rolling-circle molecules during phi X174 complementary strand DNA replication. *J Biol Chem*. 1987;262(5):2304-2309. doi:10.1016/s0021-9258(18)61654-0

253. Glover BP, McHenry CS. The χψ subunits of DNA polymerase III holoenzyme bind to single- stranded DNA-binding protein (SSB) and facilitate replication of an SSB- coated template. *J Biol Chem*. 1998;273(36):23476-23484. doi:10.1074/jbc.273.36.23476

254. Kelman Z, Yuzhakov A, Andjelkovic J, O'Donnell M. Devoted to the lagging strand - The χ subunit of DNA polymerase III holoenzyme contacts SSB to promote processive elongation and sliding clamp assembly. *EMBO J*. 1998;17(8):2436-2449. doi:10.1093/emboj/17.8.2436

255. Ali A, Aster SD, Graham DW, et al. Design and synthesis of novel antibacterial agents with inhibitory activity against DNA polymerase III. *Bioorganic Med Chem Lett*. 2001;11(16):2185-2188. doi:10.1016/S0960-894X(01)00407-3

256. Daly JS, Giehl TJ, Brown NC, Zhi C, Wright GE, Ellison RT. In vitro antimicrobial activities of novel anilinouracils which selectively inhibit DNA polymerase III of gram-positive bacteria. *Antimicrob Agents Chemother*. 2000;44(8):2217-2221. doi:10.1128/AAC.44.8.2217-2221.2000

257. Zhi C, Long ZY, Gambino J, et al. Synthesis of substituted 6-anilinouracils and their inhibition of DNA polymerase IIIC and gram-positive bacterial growth. *J Med Chem*.

2003;46(13):2731-2739. doi:10.1021/jm020591z

258. Guiles J, Sun X, Critchley IA, et al. Quinazolin-2-ylamino-quinazolin-4-ols as novel non-nucleoside inhibitors of bacterial DNA polymerase III. *Bioorganic Med Chem Lett*. 2009;19(3):800-802. doi:10.1016/j.bmcl.2008.12.038

259. Brötz-Oesterhelt H, Knezevic I, Bartel S, et al. Specific and potent inhibition of NAD+-dependent DNA ligase by pyridochromanones. *J Biol Chem*. 2003;278(41):39435-39442. doi:10.1074/jbc.M306479200

260. Miesel L, Kravec C, Xin AT, et al. A high-throughput assay for the adenylation reaction of bacterial DNA ligase. *Anal Biochem*. 2007;366(1):9-17. doi:10.1016/j.ab.2007.03.028

261. Srivastava SK, Dube D, Tewari N, Dwivedi N, Tripathi RP, Ramachandran R. Mycobacterium tuberculosis NAD+-dependent DNA ligase is selectively inhibited by glycosylamines compared with human DNA ligase I. *Nucleic Acids Res*. 2005;33(22):7090-7101. doi:10.1093/nar/gki1006

262. Meier TI, Yan D, Peery RB, et al. Identification and characterization of an inhibitor specific to bacterial NAD+-dependent DNA ligases. *FEBS J*. 2008;275(21):5258-5271. doi:10.1111/j.1742-4658.2008.06652.x

263. Ciarrocchi G, Macphee DG, Deady LW, Tilley L. Specific inhibition of the eubacterial DNA ligase by arylamino compounds. *Antimicrob Agents Chemother*. 1999;43(11):2766-2772. doi:10.1128/aac.43.11.2766

264. Dwivedi N, Dube D, Pandey J, Singh B, Kukshal V, Ramachandran, Ravishankar Tripathi RP. NAD+-Dependent DNA Ligase: ANovelTargetWaiting for the Right Inhibitor Namrata. *Med Res Rev*. 2008;28(6):545-568.

265. Srivastava, Sandeep Kumar Dube D, Kukshal V, Jha AK, Hajela J, Ramachandran R. NAD+-dependent DNA ligase (Rv3014c) from Mycobacterium tuberculosis: Novel structure-function relationship and identification of a specific inhibitor. *Proteins*. 2007.

266. Howard S, Amin N, Benowitz AB, et al. Fragment-based discovery of 6-azaindazoles as inhibitors of bacterial DNA ligase. *ACS Med Chem Lett*. 2013;4(12):1208-1212. doi:10.1021/ml4003277

267. Mills SD, Eakin AE, Buurman ET, et al. Novel bacterial NAD+-dependent DNA ligase inhibitors with broad-spectrum activity and antibacterial efficacy in vivo. *Antimicrob Agents Chemother*. 2011;55(3):1088-1096. doi:10.1128/AAC.01181-10

268. Stokes SS, Huynh H, Gowravaram M, et al. Discovery of bacterial NAD+-dependent DNA ligase inhibitors: Optimization of antibacterial activity. *Bioorganic Med Chem Lett*. 2011;21(15):4556-4560. doi:10.1016/j.bmcl.2011.05.128

269. Smith KT, Dawes IW. The preferential inhibition of. 1989:251-257.

270. Cossar PJ, Lewis PJ, McCluskey A. Protein-protein interactions as antibiotic targets: A medicinal chemistry perspective. *Med Res Rev*. 2020;40(2):469-494. doi:10.1002/med.21519

271. Robinson A, Brzoska AJ, Turner KM, et al. Essential Biological Processes of an Emerging Pathogen: DNA Replication, Transcription, and Cell Division in Acinetobacter spp. *Microbiol Mol Biol Rev*. 2010;74(2):273-297. doi:10.1128/mmbr.00048-09

272. Shereda RD, Kozlov AG, Lohman TM, Cox MM, Keck JL. SSB as an organizer/mobilizer of genome maintenance complexes. *Crit Rev Biochem Mol Biol*. 2008;43(5):289-318. doi:10.1080/10409230802341296

273. Bianco PR. The tale of SSB. *Prog Biophys Mol Biol*. 2017;127(1):111-118. doi:10.1016/j.pbiomolbio.2016.11.001.The

274. Butland G, Peregrin-Alvarez JM, Li J, et al. Interaction network containing conserved and essential protein complexes in Escherichia coli. *Nature*. 2005;433(7025):531-537. doi:10.1038/nature03239

275. Yuzhakov A, Kelman Z, O'Donnell M. Trading places on DNA-A three-point switch underlies primer handoff from primase to the replicative DNA polymerase. *Cell*. 1999;96(1):153-163. doi:10.1016/S0092-8674(00)80968-X

276. Witte G, Urbanke C, Curth U. DNA polymerase III χ subunit ties single-stranded DNA binding protein to the bacterial replication machinery. *Nucleic Acids Res*. 2003;31(15):4434-4440. doi:10.1093/nar/gkg498

277. Marceau AH, Bahng S, Massoni SC, et al. Structure of the SSB-DNA polymerase III interface and its role in DNA replication. *EMBO J*. 2011;30(20):4236-4247. doi:10.1038/emboj.2011.305

278. Costes A, Lecointe F, McGovern S, Quevillon-Cheruel S, Polard P. The C-terminal domain of the bacterial SSB protein acts as a DNA maintenance hub at active chromosome replication forks. *PLoS Genet*. 2010;6(12):1-15. doi:10.1371/journal.pgen.1001238

279. Kozlov AG, Jezewska MJ, Bujalowski W, Lohman TM. Binding specificity of escherichia coli single-stranded DNA binding protein for the χ subunit of DNA pol III holoenzyme and PriA helicase. *Biochemistry*. 2010;49(17):3555-3566. doi:10.1021/bi100069s

280. Naue N, Fedorov R, Pich A, Manstein DJ, Curth U. Site-directed mutagenesis of the χ subunit of DNA polymerase III and single-stranded DNA-binding protein of E. coli reveals key residues for their interaction. *Nucleic Acids Res*. 2011;39(4):1398-1407. doi:10.1093/nar/gkq988

281. Molineux IJ, Gefter ML. Properties of the Escherichia coli DNA binding (unwinding) protein: interaction with DNA polymerase and DNA. *Proc Natl Acad Sci U S A*. 1974;71(10):3858-3862. doi:10.1073/pnas.71.10.3858

282. Furukohri A, Nishikawa Y, Tatsumi Akiyama M, Maki H. Interaction between Escherichia coli DNA polymerase IV and single-stranded DNA-binding protein is required for DNA synthesis on SSB-coated DNA. *Nucleic Acids Res*. 2012;40(13):6039-6048. doi:10.1093/nar/gks264

283. Arad G, Hendel A, Urbanke C, Curth U, Livneh Z. Single-stranded DNA-binding protein recruits DNA polymerase V to primer termini on RecA-coated DNA. *J Biol Chem*. 2008;283(13):8274-8282. doi:10.1074/jbc.M710290200

284. Lu D, Bernstein DA, Satyshur KA, Keck JL. Small-molecule tools for dissecting the roles of SSB/protein interactions in genome maintenance. *Proc Natl Acad Sci U S A*. 2010;107(2):633-638. doi:10.1073/pnas.0909191107

285. Cadman CJ, McGlynn P. PriA helicase and SSB interact physically and functionally. *Nucleic Acids Res*. 2004;32(21):6378-6387. doi:10.1093/nar/gkh980

286. Huang YH, Lin MJ, Huang CY. Yeast two-hybrid analysis of prib-interacting proteins in replication restart primosome: A proposed PriB-SSB interaction model. *Protein J*. 2013;32(6):477-483. doi:10.1007/s10930-013-9509-y

287. Wessel SR, Marceau AH, Massoni SC, et al. PriC-mediated DNA replication restart requires PriC complex formation with the single-stranded DNA-binding protein. *J Biol Chem*. 2013;288(24):17569-17578. doi:10.1074/jbc.M113.478156

288. Naue N, Beerbaum M, Bogutzki A, Schmieder P, Curth U. The helicase-binding domain of Escherichia coli DnaG primase interacts with the highly conserved C-terminal region of single-stranded DNA-binding protein. *Nucleic Acids Res*. 2013;41(8):4507-4517. doi:10.1093/nar/gkt107

289. Zechner EL, Wu CA, Marians KJ. Coordinated leading- and lagging-strand synthesis at the Escherichia coli DNA replication fork. III. A polymerase-primase interaction governs primer size. *J Biol Chem*. 1992;267(6):4054-4063. doi:10.1016/s0021-9258(19)50630-5

290. Tougu K, Peng H, Marians KJ. Identification of a domain of Escherichia coli primase required for functional interaction with the DnaB helicase at the replication fork. *J Biol Chem*. 1994;269(6):4675-4682. doi:10.1016/s0021-9258(17)41829-1

291. Thirlway J, Turner IJ, Gibson CT, et al. DnaG interacts with a linker region that joins the N- and C-domains of DnaB and induces the formation of 3-fold symmetric rings. *Nucleic Acids Res*. 2004;32(10):2977-2986. doi:10.1093/nar/gkh628

292. Oakley AJ, Loscha K V., Schaeffer PM, et al. Crystal and solution structures of the helicase-binding domain of Escherichia coli primase. *J Biol Chem*. 2005;280(12):11495-11504. doi:10.1074/jbc.M412645200

293. Soultanas P, Bolt E. Replicative DNA helicases and primases. In: Wells RD, Bond JS, Klinman J, Masters BSS, Bell E, eds. *Molecular Life Sciences*. Springer: New York, NY, USA, 2014; 2014.

294. Lu Y Bin, Ratnakar PVAL, Mohanty BK, Bastia D. Direct physical interaction between DnaG primase and DnaB helicase of Escherichia coli is necessary for optimal synthesis of primer RNA. *Proc Natl Acad Sci U S A*. 1996;93(23):12902-12907. doi:10.1073/pnas.93.23.12902

295. Pokhrel N, Origanti S, Davenport EP, et al. Monitoring Replication Protein A (RPA) dynamics in homologous recombination through site-specific incorporation of non-canonical amino acids. *Nucleic Acids Res*. 2017;45(16):9413-9426. doi:10.1093/nar/gkx598

296. Carro L. Protein-protein interactions in bacteria: A promising and challenging avenue towards the discovery of new antibiotics. *Beilstein J Org Chem*. 2018;14:2881-2896. doi:10.3762/bjoc.14.267

297. Marceau AH, Bernstein DA, Walsh BW, Shapiro W, Simmons LA, Keck JL. Protein Interactions in Genome Maintenance as Novel Antibacterial Targets. *PLoS One*. 2013;8(3). doi:10.1371/journal.pone.0058765

298. Voter AF, Killoran MP, Ananiev GE, Wildman SA, Hoffmann FM, Keck JL. A High-Throughput Screening Strategy to Identify Inhibitors of SSB Protein–Protein Interactions in an Academic Screening Facility. *SLAS Discov*. 2018;23(1):94-101. doi:10.1177/2472555217712001

299. Chilingaryan Z, Headey SJ, Lo ATY, et al. Fragment-based discovery of inhibitors of the

bacterial DnaG-SSB interaction. *Antibiotics*. 2018;7(1):1-12. doi:10.3390/antibiotics7010014

300. Fang J, Engen JR, Beuning PJ. Escherichia coli processivity clamp β from DNA polymerase III is dynamic in solution. *Biochemistry*. 2011;50(26):5958-5968. doi:10.1021/bi200580b

301. Fay PJ, Johanson KO, McHenry CS, Bambara RA. Size classes of products synthesized processively by DNA polymerase III and DNA polymerase III holoenzyme of Escherichia coli. *J Biol Chem*. 1981;256(2):976-983. doi:10.1016/s0021-9258(19)70075-1

302. Yao NY, Georgescu RE, Finkelstein J, O'Donnell ME. Single-molecule analysis reveals that the lagging strand increases replisome processivity but slows replication fork progression. *Proc Natl Acad Sci U S A*. 2009;106(32):13236-13241. doi:10.1073/pnas.0906157106

303. Maki S, Kornberg A. DNA polymerase III holoenzyme of Escherichia coli. II. A novel complex including the γ subunit essential for processive synthesis. *J Biol Chem*. 1988;263(14):6555-6560. doi:10.1016/s0021-9258(18)68677-6

304. Maki H, Kornberg A. The polymerase subunit of DNA polymerase III of Escherichia coli. II. Purification of the α subunit, devoid of nuclease activities. *J Biol Chem*. 1985;260(24):12987-12992. doi:10.1016/s0021-9258(17)38825-7

305. Koleva BN, Gokcan H, Rizzo AA, et al. Dynamics of the E. coli β-Clamp Dimer Interface and Its Influence on DNA Loading. *Biophys J*. 2019;117(3):587-601. doi:10.1016/j.bpj.2019.06.035

306. Oakley AJ, Prosselkov P, Wijffels G, Beck JL, Wilce MCJ, Dixon NE. Flexibility revealed by the 1.85 Å crystal structure of the β sliding-clamp subunit of Escherichia coli DNA polymerase III. *Acta Crystallogr - Sect D Biol Crystallogr*. 2003;59(7):1192-1199. doi:10.1107/S0907444903009958

307. Kong XP, Onrust R, O'Donnell M, Kuriyan J. Three-dimensional structure of the β subunit of E. coli DNA polymerase III holoenzyme: A sliding DNA clamp. *Cell*. 1992;69(3):425-437. doi:10.1016/0092-8674(92)90445-I

308. Johnson A, O'Donnell M. Cellular DNA replicases: Components and dynamics at the replication fork. *Annu Rev Biochem*. 2005;74:283-315. doi:10.1146/annurev.biochem.73.011303.073859

309. Zhuang Z, Ai Y. Processivity factor of DNA polymerase and its expanding role in normal and translesion DNA synthesis. *Biochim Biophys Acta - Proteins Proteomics*. 2010;1804(5):1081-1093. doi:10.1016/j.bbapap.2009.06.018

310. Neuwald AF. Evolutionary clues to DNA polymerase III β clamp structural mechanisms. *Nucleic Acids Res*. 2003;31(15):4503-4516. doi:10.1093/nar/gkg486

311. Kazmirski SL, Zhao Y, Bowman GD, O'Donnell M, Kuriyan J. Out-of-plane motions in open sliding clamps: Molecular dynamics simulations of eukaryotic and archaeal proliferating cell nuclear antigen. *Proc Natl Acad Sci U S A*. 2005;102(39):13801-13806. doi:10.1073/pnas.0506430102

312. López de Saro FJ, O'Donnell M. Interaction of the β sliding clamp with MutS, ligase, and DNA polymerase I. *Proc Natl Acad Sci U S A*. 2001;98(15):8376-8380. doi:10.1073/pnas.121009498

313. Hughes AJ, Bryan SK, Chen H, Moses RE, McHenry CS. Escherichia coli DNA polymerase II

is stimulated by DNA polymerase III holoenzyme auxiliary subunits. *J Biol Chem*. 1991;266(7):4568-4573. doi:10.1016/s0021-9258(20)64360-5

314. Wagner J, Fujii S, Gruz P, Nohmi T, Fuchs RPP. The β clamp targets DNA polymerase IV to DNA and strongly increases its processivity. *EMBO Rep*. 2000;1(6):484-488. doi:10.1093/embo-reports/kvd109

315. Bonner CA, Stukenberg PT, Rajagopalan M, et al. Processive DNA synthesis by DNA polymerase II mediated by DNA polymerase III accessory proteins. *J Biol Chem*. 1992;267(16):11431-11438. doi:10.1016/s0021-9258(19)49928-6

316. Dalrymple BP, Kongsuwan K, Wijffels G, Dixon NE, Jennings PA. A universal protein-protein interaction motif in the eubacterial DNA replication and repair systems. *Proc Natl Acad Sci U S A*. 2001;98(20):11627-11632. doi:10.1073/pnas.191384398

317. Stukenberg PT, Studwell-Vaughan PS, O'Donnell M. Mechanism of the sliding β-clamp of DNA polymerase III holoenzyme. *J Biol Chem*. 1991;266(17):11328-11334. doi:10.1016/s0021-9258(18)99166-0

318. Naktinis V, Turner J, O'Donnell M. A molecular switch in a replication machine defined by an internal competition for protein rings. *Cell*. 1996;84(1):137-145. doi:10.1016/S0092-8674(00)81000-4

319. Lenne-Samuel N, Wagner J, Etienne H, Fuchs RPP. The processivity factor β controls DNA polymerase IV traffic during spontaneous mutagenesis and translesion synthesis in vivo. *EMBO Rep*. 2002;3(1):45-49. doi:10.1093/embo-reports/kvf007

320. Tang M, Pham P, Shen X, et al. Roles of E. coli DNA polymerases IV and V in lesion-targeted and untargeted SOS mutagenesis. *Nature*. 2000;404(6781):1014-1018. doi:10.1038/35010020

321. Tang M, Shen X, Frank EG, O'Donnell M, Woodgate R, Goodman MF. UmuD'2C is an error-prone DNA polymerase, Escherichia coli pol V. *Proc Natl Acad Sci U S A*. 1999;96(16):8919-8924. doi:10.1073/pnas.96.16.8919

322. Bunting KA, Roe SM, Pearl LH. Structural basis for recruitment of translesion DNA polymerase Pol IV/DinB to the β-clamp. *EMBO J*. 2003;22(21):5883-5892. doi:10.1093/emboj/cdg568

323. Katayama T, Kubota T, Kurokawa K, Crooke E, Sekimizu K. The initiator function of DnaA protein is negatively regulated by the sliding clamp of the E. coli Chromosomal replicase. *Cell*. 1998;94(1):61-71. doi:10.1016/S0092-8674(00)81222-2

324. Kurz M, Dalrymple B, Wijffels G, Kongsuwan K. Interaction of the sliding clamp β-subunit and Hda, a DnaA-related protein. *J Bacteriol*. 2004;186(11):3508-3515. doi:10.1128/JB.186.11.3508-3515.2004

325. Naktinis V, Onrust R, Fang L, O'Donnell M. Assembly of a chromosomal replication machine: Two DNA polymerases, a clamp loader, and sliding clamps in one holoenzyme particle. II. Intermediate complex between the clamp loader and its clamp. *J Biol Chem*. 1995;270(22):13358-13365. doi:10.1074/jbc.270.22.13358

326. Bruck I, O'Donnell M. The DNA replication machine of a Gram-positive organism. *J Biol Chem*. 2000;275(37):28971-28983. doi:10.1074/jbc.M003565200

327. Dohrmann PR, McHenry CS. A bipartite polymerase-processivity factor interaction: Only

the internal β binding site of the α subunit is required for processive replication by the DNA polymerase III holoenzyme. *J Mol Biol*. 2005;350(2):228-239. doi:10.1016/j.jmb.2005.04.065

328. Yin Z, Kelso MJ, Beck JL, Oakley AJ. Structural and thermodynamic dissection of linear motif recognition by the E. Coli sliding clamp. *J Med Chem*. 2013;56(21):8665-8673. doi:10.1021/jm401118f

329. Burnouf DY, Olieric V, Wagner J, et al. Structural and Biochemical Analysis of Sliding Clamp/Ligand Interactions Suggest a Competition between Replicative and Translesion DNA Polymerases. *J Mol Biol*. 2004;335(5):1187-1197. doi:10.1016/j.jmb.2003.11.049

330. Georgescu RE, Yurieva O, Kim SS, Kuriyan J, Kong XP, O'Donnell M. Structure of a small-molecule inhibitor of a DNA polymerase sliding clamp. *Proc Natl Acad Sci U S A*. 2008;105(32):11116-11121. doi:10.1073/pnas.0804754105

331. Wijffels G, Johnson WM, Oakley AJ, et al. Binding inhibitors of the bacterial sliding clamp by design. *J Med Chem*. 2011;54(13):4831-4838. doi:10.1021/jm2004333

332. Yin Z, Whittell LR, Wang Y, et al. Discovery of lead compounds targeting the bacterial sliding clamp using a fragment-based approach. *J Med Chem*. 2014;57(6):2799-2806. doi:10.1021/jm500122r

333. Yin Z, Whittell LR, Wang Y, et al. Bacterial Sliding Clamp Inhibitors that Mimic the Sequential Binding Mechanism of Endogenous Linear Motifs. *J Med Chem*. 2015;58(11):4693-4702. doi:10.1021/acs.jmedchem.5b00232

334. Yin Z, Wang Y, Whittell LR, et al. DNA replication is the target for the antibacterial effects of nonsteroidal anti-inflammatory drugs. *Chem Biol*. 2014;21(4):481-487. doi:10.1016/j.chembiol.2014.02.009

335. Kjelstrup S, Hansen PMP, Thomsen LE, Hansen PR, Løbner-Olesen A. Cyclic Peptide Inhibitors of the β-Sliding Clamp in Staphylococcus aureus. *PLoS One*. 2013;8(9). doi:10.1371/journal.pone.0072273

336. Kling A, Lukat P, Almeida D V., et al. Targeting DnaN for tuberculosis therapy using novel griselimycins. *Science (80-)*. 2015;348(6239):1106-1112. doi:10.1126/science.aaa4690

337. Pandey P, Verma V, Dhar SK, Gourinath S. Screening of E. coli β-clamp Inhibitors revealed that few inhibit Helicobacter pylori more effectively: structural and functional characterization. *Antibiotics*. 2018.

338. Sartini S, Levati E, Maccesi M, et al. New Antimicrobials Targeting Bacterial RNA Polymerase Holoenzyme Assembly Identified with an in Vivo BRET-Based Discovery Platform. *ACS Chem Biol*. 2019;14(8):1727-1736. doi:10.1021/acschembio.9b00178

339. Wijffels G, Dalrymple BP, Prosselkov P, et al. Inhibition of Protein Interactions with the β2 Sliding Clamp of Escherichia coli DNA Polymerase III by Peptides from β 2-Binding Proteins. *Biochemistry*. 2004;43(19):5661-5671. doi:10.1021/bi036229j

340. André C, Martiel I, Wolff P, et al. Interaction of a Model Peptide on Gram Negative and Gram Positive Bacterial Sliding Clamps. *ACS Infect Dis*. 2019;5(6):1022-1034. doi:10.1021/acsinfecdis.9b00089

341. Lamers MH, Georgescu RE, Lee SG, O'Donnell M, Kuriyan J. Crystal Structure of the Catalytic α Subunit of E. coli Replicative DNA Polymerase III. *Cell*. 2006;126(5):881-892.

doi:10.1016/j.cell.2006.07.028

342. Wolff P, Oliéric V, Briand JP, et al. Structure-based design of short peptide ligands binding onto the E. coli processivity ring. *J Med Chem*. 2011;54(13):4627-4637. doi:10.1021/jm200311m

343. Niesen FH, Berglund H, Vedadi M. The use of differential scanning fluorimetry to detect ligand interactions that promote protein stability. *Nat Protoc*. 2007;2(9):2212-2221. doi:10.1038/nprot.2007.321

344. Luan C, Light SH, Dunne SF, Anderson WF. Ligand Screening Using Fluorescence Thermal Shift Analysis (FTS). In: *Structural Genomics and Drug Discovery: Methods and Protocols*. Vol 1140. ; 2014:263-289. doi:10.1007/978-1-4939-0354-2

345. Mumberg D, Müller R, Funk M. Yeast vectors for the controlled expression of heterologous proteins in different genetic backgrounds. *Gene*. 1995;156(1):119-122. doi:10.1016/0378-1119(95)00037-7